Hydrodynamic effects on soiled surfaces : an experimental study and theoretical analysis

Thesis

David Ward, B. Sc. Hons

Hydrodynamic Effects on Soiled Surfaces

- An Experimental Study and Theoretical Analysis -

PhD

Department of Environmental and Mechanical Engineering

The Open University

United Kingdom

July 2000

.....To my mother and father

.....To my wife Licia and children Brian and Scott

..... and the loveliest family in the world

..... To be what we are, and to become what we are capable of being, is the only end of life.

R. L. Stevenson, *Familiar Studies of Man and Books*

Acknowledgements

There is no doubt in my mind that my acknowledgements should start with Fred Stave, a very rare species of man, who not only master minded the Mass Transfer project at Whirlpool but inspired and indirectly coached me towards my PhD. He has left a tough role model that I will endeavour to emulate to the best of my ability. I will be indebted to Fred for the rest of my life.

Claudio Danelli facilitated matters by joining forces with Fred and allowing me to start my research while under his charge at Whirlpool. This noble act was carried on by Marco Poma, whom I am not only grateful for sharing a common vision in personal development but who has revealed numerous other features that who knows how long it will take me to truly understand and apply. Of equal standing is my present boss, Adriano Scaburri, who understood that I was walking a tight rope by combining academic expectations and job milestones, especially in my final year, and let me get on with the job.

A big thank you to Alex, a long standing friend and he who refereed my original application to the OU at the beginning of 1997, an academic I will strive to match and exceed.

And how could I repay the work of Daniele, Marco and Elio?, three undergraduate students who will no doubt make their mark as time goes by. Daniele laid the foundation stone for the early part of the research and has been justly rewarded with the opportunity to do research himself. Good luck.

Marco, continued this excellent early work, not an easy task by all means, and provided me not only with the fuel to persist and attempt the unfeasible but co-generated the sphere idea. I still remember the day this idea was born, a wonderful sensation, full of risk but so rich in potential that we just couldn't resist the temptation. Marco was also my first stager and provided me with a unique mix of tutorship and friendship, may this last forever.

And what may I say about Elio? not only was he propelled into the most difficult of tasks, the testing of the sphere, but was a true example of patience. He followed my guidelines and advice through thick and thin, and transformed the sphere idea into reality.

Dan, the "big" man, must figure along side Mark as being the drill behind the M.T. project and to whom my most sincere "all the best" is consigned for the future. Maybe we haven't re-invented the wheel but our work will make things easier for future researchers.

Marco, Giovanni, Samuele and Domenico, all dear colleagues from the model shop along with Massimo, Sig. Milani and Sig. Colombo at the Politecnico, were the men behind the scenes. These were the people that made the experimentation particularly gratifying and fruitful. And what may I say about Ivano and Patrizia?, two people grossly undervalued yet always willing to help me, whatever the price. To all these associates may God help me to repay the immense arrears I have with them.

So on to Bill. There have been a lot of 'first times', 'ifs', 'buts' in my research so Bill must have been quite perplexed when I called him to speak about my plans to do a PhD way back in 1997. From that simple phone call all of what is in my thesis was born. Bill has always been there to listen, providing me with simple but fundamental advice. The OU should be proud of Bill, a shining example and typical of the OU.

So here I am with the most difficult of closures, thanking Giovanni from start to finish for his backing and involvement in my research that is not only mandatory but above all, a pleasure. Thank you also for believing in me and making my path easier. Perhaps it is too unpretentious but my immediate thoughts are to wish Giovanni the very best for the future and hope that my academic contribution has given him the same satisfaction and proudness that it has given me.

List of Contents

Hydrodynamic Effects on Soiled Surfaces

- An Experimental Study and Theoretical Analysis -

This thesis presents the findings of an investigation aimed at understanding the effects of hydrodynamic shear stress on soil removal from textile surfaces both inside the washing machine and in closely controlled laboratory conditions.

The research has involved developing a technique for the indirect measurement of shear stress based on pressure recordings and small block probes that provide both an indication of shear stress magnitude and direction. The probes have been investigated and calibrated in a purpose-built, rectangular-section, water tunnel in which tests were also carried out on specially prepared soiled cotton textile samples. This has allowed the correlation between shear stress and soil removal efficiency for $15k \leq Re \leq 155k$. A more general investigation involving the washing machine has also been carried out so as to quantify and compare the effects of detergency, water temperature, time, abrasion, warping and tangential shear force.

The hydrodynamic conditions inside the washing machine were investigated providing insight into flow conditions both on the inside and outside of the wash load. This was achieved through the use of a wireless device in the form of a sphere with an on-board pressure-flow sensor and radio transmitter for remote monitoring via radio. This remote data acquisition system was designed, developed and patented by the author. A model of the wash load motion has also been developed and high speed filming techniques employed to qualify and quantify the wash load dynamics.

The main outcome of the research may be summarised as follows:

- Hydrodynamic shear stress up to 7.7Pa circa ($15k \leq Re \leq 155k$) is inadequate to remove soil from the standard EMPA textile surfaces.
- Only 10-15% of the soil removed in the washing machines can be attributed to abrasion, warping (due to churning) and hydrodynamic shear stress, the rest is attributed to detergency and heat transfer.
- There are at least two different flow domains within a horizontal-axis washing machine, one on the inside of the wash load and one on the outside.
- Flow conditions on both the inside and outside are turbulent and velocities up to several meters per second have been recorded.

List of Symbols

English and Greek Symbols

β = Angular coefficient for small block probe

β^* = Angular coefficient for small block probe

$\overline{p_d}$ = Average dynamic pressure (Pa)

$\bar{u}$ = Average local flow velocity (ms^{-1})

$\overline{U}$ = Average main stream flow velocity e.g. tunnel (ms^{-1})

$\bar{a}$ = Average particle acceleration (ms^{-2})

$\overline{\tau_w}$ = Average wall shear stress (Pa or Nm^{-2})

K_t = Calibration coefficient for Pitot tube

C_f = Coefficient (used in Clauser's graph)

C_v = Coefficient of variance

d_t = Diameter of tubing (m)

d_t = Diameter of tubing (m)

ΔP_θ = Differential pressure at angle θ (Pa)

ΔP_O = Differential pressure at zero angle of incidence (Pa)

ΔP^o = Differential pressure measurement according to Gaudet et al. data (Pa)

x^* = Dimensionless pressure difference

y^* = Dimensionless shear stress

Δr = Distance travelled by particle (m)

P_D = Dynamic pressure e.g. sphere probe (Pa)

μ = Dynamic viscosity (Pa s)

σ = Fluctuating component of local velocity (general)

σ_u = Fluctuating component of local velocity (refers to u)

u' = Fluctuating component of u

$\overline{\tau_w'}$ = Fluctuations (average) shear stress (Pa)

ρ = Fluid density (kgm^{-3})

u^* = Friction velocity (ms^{-1})

υ = Kinematic viscosity (m^2s^{-1})

P_o = Local (dynamic) pressure (Pa)

p_m = Measured pressure (Pa)

$\tan\theta$ = Particle release angle (°)

Δr = Particle vector increment

v = Particle velocity (ms^{-1})

π = Pi

Δ = Pressure gradient factor

C_{vp} = Pressure transducer response coefficient (m^3bar^{-1})

α = Probe angle alpha (°)

θ = Probe angle theta (°)

ΔP = Probe differential pressure (Pa)

h = Probe height (m)

Y^+ = Ratio of σ_u to u

y^+ = Ratio of σ_u to u

p_i = Real pressure (Pa)

d_t^+ = Reynolds friction number

Re_S = Reynolds number according to Schmidt

Re_W = Reynolds number according to Ward

τ = Time constant (s)

P_W = Wall (static) pressure (Pa)

θ = Weir notch angle (°)

ω = Angular drum speed (rad s^{-1})

ρ = Fluid (water) density (kgm^{-3})

μ = Fluid (water) dynamic viscosity (Nsm^{-2})

υ = Fluid (water) kinematic viscosity (m^2s^{-1})

ρ_a = Added mass density (kgm^{-3})

ω_D = Angular drum speed (rad s^{-1})

ρ_{Fp} = Fabric plug density (kgm^{-3})

ΔP_h = Pressure head (Pa)

ΔP_k = Pressure drop (Pa)

ΔR_h = Difference between inner and outer radially filling radii (m)

ρ_t = Specific weight of wash load textile (m^3kg^{-1})

α = Angle due to water level height (°)

a = Acceleration (plug, drum etc.) (ms^{-2})

a = major axis length (m)

A^*_D = Internal drum surface area (m^2)

A^*_h = Total surface area of wash load: dry conditions (m^2)

A_c = Centripetal acceleration (ms^{-2})

a_D = Acceleration of drum or model (ms^{-2})

A_D = Cross-sectional area of drum (m^2)

a_D = Drum acceleration (ms^{-2})

A_h = Cross-sectional area of transverse filling of drum: dry conditions (m^2)

a_p = Acceleration of fabric plug or prototype (ms^{-2})

a_p = Fabric plug acceleration (ms^{-2})

a_{pm} = Fabric plug acceleration to drum acceleration ratio (or factor)

a_{pm} = Ratio of accelerations e.g. plug to drum, prototype to model etc.

C = Drum circumference (m)

c = Impact penetration width (m)

C_a = Added mass coefficient

C_D = Drag coefficient

C_r = Resistance coefficient of drum perforation

D = Drum diameter (m)

D, d = Fibre (nominal) diameter (m)

DP = Differential pressure (Pa)

dP = Pressure drop e.g. along tunnel (Pam^{-1})

e = Drum surface finish (m)

F = Force (N)

F_D = Drag force (N)

F_n = Fluid force due to impact (N)

g = Acceleration due to gravity (ms^{-2})

g = acceleration due to gravity (ms^{-2})

H = Fibre height (m)

h = water level height: static conditions (m)

H = Weir pressure head (m or cm)

h_o = Fabric plug position height in m at critical angle position

h_w = Water level head (m)

h_x = Horizontal distance travelled by fabric plug (m)

h_y = Vertical distance travelled by fabric plug: undershoot - below release datum (m)

J_{mod} = Dimensionless pressure drop

K = Angular coefficient for small block probe

k = Pressure loss factor for drum perforation

K = Weir constant (m^{-1})

K_e = Kinetic energy (J)

k_f = Dry laundry filling factor

K_g = Force field strength factor

K_h = Ratio of drum filling height to radius factor

K_L = Drum length to radius ratio factor

K_n = Fluid kinetic energy due to impact (J)

K_p = Wetted drum perforations to total drum perforations ratio (or factor)

K_{rf} = Radial filling factor

L = Length of tubing (m)

L = Textile thickness (m)

L_D = Drum length (m)

m = Mass (kg)

M* = Effective mass (kg)

m_p = Fabric plug mass (kg)

m_{wl} = Mass of wash load (kg)

N = Drum speed (rad s^{-1}) or Number of perforations per drum

n_p = Number of wetted perforations

N_p = Perforations per unit drum area

p = Single pressure (Pa)

p = Wetted drum perimeter (m)

P' = Total perimeter of drum water (m)

pn = Differential pressure readings (e.g. p1, p2, p3) w. r. t. local (probe) static pressure tapping (Pa)

PN = Differential pressure readings (e.g. P1, P2, P3) w. r. t. remote static pressure tapping (Pa)

p_{rif} = Reference pressure (Pa)

Q = Tunnel flow rate (m^3s^{-1})

R = Drum radius (m)

r = Particle position vector

r = Radius of sphere (for added mass concept) or wheel rolling radius (m)

R = Remote static pressure reference e.g. P1R, P2R etc.

R = Soil particle radius (m)

R_D = Drum radius (m)

Re = Reynolds number

Re_D = Reynolds number based on mixing vessel model or thread or fibre diameter

r_f = Final particle position vector

R_h = Inner radius of radially filled drum (m)

r_i = Initial particle position vector

R_p = Radius of fabric plug or prototype (m)

R_{pm} = Ratio of fabric plug radius to drum radius

R_{pm} = Ratio of radii e.g. plug to drum, prototype to model etc.

t = Fabric plug travel time or time to reach greatest height -after release (s)

t = Time increment (s)

t_D = Drum perforation length: drum thickness (m)

t_l = Fabric plug travel (for y_p=0) time (s)

U = Average tunnel velocity (ms^{-1})

U, u = Average fluid speed (ms^{-1})

U, $\overline{U}_h$ = Average drum perforation flow velocity (ms^{-1})

u, $\overline{u}$ = Average flow velocity (ms^{-1})

u_t = Tangential flow speed (ms^{-1})

V_a = Added mass volume (m^3)

V_D = Drum speed (ms^{-1})

V_D = Tangential velocity of drum or model (ms^{-1})

V_{Fp} = Fabric plug volume (m^3)

V_{max} = Maximum tangential velocity of fabric plug (ms^{-1})

V_p = Fabric plug speed (ms^{-1})

V_p = Tangential velocity of fabric plug or prototype (ms^{-1})

V_{pm} = Ratio of fabric plug speed to drum speed

V_{pm} = Ratio of tangential velocities e.g. plug to drum, prototype to model etc.

V_t = Fabric plug tangential velocity (ms^{-1})

V_{term} = Fabric plug terminal velocity (ms^{-1})

V_{wl} = Volume of wash load (m^3)

W_L = Wash load water level (m)

x = Linear length applied to Reynolds number

X* = Dimensionless wall coefficient

Y = Distance from centreline of tunnel (mm)

y = Vertical distance from wall (m)

Y* = Dimensionless wall coefficient

y_p = Vertical distance travelled by fabric plug in m (overshoot - above release datum)

z = Impact penetration depth (m)

Abbreviations

3D (or 2D)	- Three dimensional (or two dimensional)
3DP	- 3D Printing
ANOVA	- Analysis of Variance
ANSYS	- Finite element simulation software
Av	- average
BPM	- Ballistic Particle Manufacturing
CAD	- Computed Aided Design
Carbon Black	- Carbon black and mineral oil
CB	- Carbon Black (and mineral oil soil)
CFD	- Computational Fluid Dynamics
Ch	- Chocolate (and milk) or chapter
CL	- Centre line
DA	- Data Acquisition (system)
Daewoo	- Korean washing machine manufacturer
DAQCARD	- National Instrument PCMCIA data acquisition card
DMT	- Derjaguin, Muller, and Toporov (adhesion theory)
DOE	- Design of Experiments
DVLO	- Derjaguin, Landau, Verwey and Overbeek (adhesion theory)
EMPA	- Swiss Federal Laboratories for Materials Testing and Research

FDM	- Fused Deposition Modelling
FLUENT	- CFD software package
FMT	- Free Moving Textile (EMPA stripe)
FPS	- Frames per second
F-V	- Frequency to Voltage (converter)
GAMBIT	- CFD software meshing tool for FLUENT
GOST	- Russian Washing Machine Performance Standard
HW	- Hardware
IEC	- International standard (No.60456 for domestic appliances)
JKR	- Johnson, Kendall and Roberts (adhesion theory)
LABVIEW	- National Instruments symbolic data acquisition programming environment and language
LOM	- Laminated Object Manufacturing
MINITAB	- Statistical Software
MT	- Mass Transfer project
NA	- Not Applicable
NI	- National Instruments
N-S	- Navier-Stokes equations
OFAT	- One Factor At a Time
PB	- Pigs Blood (soil)
PCB	- Printed Circuit Board
PCMCIA	- Personal Computer Memory Card International Association (PC card system)
Pro-E	- Professional Engineer - a professional 3D solid modeller software package
PSU	- Power Supply Unit
R.H.	- Right hand (L.H. - left hand)
RP	- Rapid Prototyping
RPM	- Revolutions per minute
RSM	- Reynolds stress model
S & T	- Soak and Twist
S	- Sphere

SEM - Scanning Electronic Microscope

SGC - Solid Ground Curing

Sigma Scan - Image analysis software

SLA - Stereolithography Apparatus

SLS - Selective Laser Sintering

SMD - Surface Mounted Device

SNR - Signal to Noise Ratio

STL - Stereolithography file

SW - Software

T - Tunnel (water)

TTM - Time to Market

UNS - Unstructured

UV - Ultra Violet

V-F - Voltage to Frequency (converter)

VR - Virtual Reality

W - Red Wine (soil)

Wh - White (soil reference)

Subscripts

θ - Incidence angle

a - Added mass

c - Centripetal

D - Drum or drag (coefficient)

d - Dynamic

e - Energy (kinetic)

f - Friction coefficient for drum perforation or particle trajectory finish point

Fp - Fabric plug

g - Gravity

h - Drum filling or wash load or machine parameter

i - Real or initial particle trajectory starting point

k	- Kinetic or kinematic
L	- Drum length
m	- Drum or model or measured
max	- Maximum
med	- Average (dimensionless pressure drop)
n, N	- Pressure readings reference or normal, impact
o	- Local
p	- Fabric plug, drum perforation(s)
pm	- Prototype or plug model
r	- Resistance
rf	- Radial filling
rif	- Reference e.g. pressure
s	- Schmidt (e.g. Re_s)
t	- Tangential
t	- Tubing, Pitot tube
term	- Terminal (e.g. velocity)
u	- Velocity (fluctuations)
v	- Variance
vp	- Transducer coefficient
w	- Modified Schmidt number according to Ward (e.g. Re_w)
w	- Wall, static pressure ref.
wl	- Water line or wash load
x,y,z	- Cartesian coordinates

Superscripts

+	- Law-of-the-wall variable, friction number
*	- Dimensionless variable, effective mass
'	- Fluctuating component (e.g. of u), total perimeter
°	- Experimental pressure data according to Gaudet
-	- Average or time mean

Chapter 1 – Introduction

List of Contents

List of Figures

List of References

1. Desmond K., The Harwin Chronology of Inventions, Innovations, Discoveries, Constable, London, 1986.
2. Strasser S., "Never Done", Panetheon Books, New York, 1982.
3. Ward D., Whirlpool internal report project definition and Monthly report, March 1997.
4. Van den Brekel L. D. M., Hydrodynamic and Mass Transfer in Domestic Drum-type Fabric Washing Machines, PhD thesis, pp. 145-154, Delft University of Technology, NL, 1987.
5. Cutler W. G. and Davis R. C., Detergency Theory and Test Methods part 1: a). pp.98-100, Marcel Decker, N. York, 1972.
6. Ward D., Whirlpool internal monthly report, Washing R & D group, Oct. 1997.
7. Evaluating Domestic Washing Machine Performance, IEC standard 60456, third edition, 1998.
8. EMPA report, Evaluation of Detergents and Washing Process with Artificially Soiled Fabrics, CH, 1999.
9. Ward D., Modelling of a Horizontal-Axis Domestic Washing Machine, J. Text. Inst., Vol. 91, Part 1, No. 2, 2000.
10. Ward D., High Speed Filming of Clothes and Fabric Plug Motion, Whirlpool Internal Report, Sept. 1999.

11. Schmidt H., Washebewegung in Trommelwashmachinen, Washereitechnik unde chemie, vols.10, pp. 500-504 (1957), 11, pp. 224-232 (1958) and 12, pp. 549-554 (1959).
12. Ward D. et al, Microelectronic Sensor for the Measurement of Shear Stress within a Domestic Washing Machine Drum, IMAPs99, Milan, July 1999.
13. Ward D., Evaluation of Soil removal, Whirlpool internal report, Aug. 1999.
14. Ward D., Boundary Layer Theory, Shear Stress Measurement and the Washing machine-Tunnel investigation, pp. 80-119, ch.4, issue 2, Whirlpool Internal Report, Dec. 1999.
15. Bocchiola D., Una Metodologia per la Misura Puntuale dell'Attritto di Parete in Correnti Cilindriche *("A Method for Measuring Local Skin Friction in Cylindrical flows")*, Engineering degree thesis, No. 611090, Politecnico di Milano, Italy, 1998.
16. Viterbo M, Sonde di Strato Limite per la misura dello Sforzo d'attritto – Studio Sperimentale ed Analisi Teorica *("Boundary Layer Probes used for the Measurement of Wall Shear Stress and Skin Friction – Experimental Investigation and Theoretical Analysis")*, Engineering degree thesis No. 599289, Politecnico di Milano, Italy, 1999.

Introduction and Research Background

The domestic washing machine is a prime example of an empirically designed man-made household appliance, which, despite all the efforts, still basically remains the same since its conception during the early part of the last century [ref. 1.1]. In fact the milestones of major machine innovation essentially concern: the introduction of an electric motor to assist clothes motion (1907), spin-dry feature (1924), a stainless steel drum (1965), plastic drum (1980), microprocessors (1985), use of synthetic detergents (from 1913) and elaborate washing algorithms (cycles), all of which either automate and/or amplify the process of washing by hand. Over the last century two scenarios have slowly taken the stage these being categorised according to the orientation of the washing drum axis i.e. horizontal and vertical [ref. 1.2]. The horizontal-axis machine (sometimes termed 'front loader') is favoured in Europe and Western countries while the vertical-axis machine ('top loader') is preferred especially in North America and Asia. Both machines are very different not just in terms of size but also in design, build and features. However, the goal is common i.e. to remove soil in the most efficient and effective way. Ironically both machines are plagued with one common, and may I add dramatic, shortcoming and that is machine design is still by 'trial and error' and remains immune to radical innovation.

The reason for this lack of breakthrough and consequent stalemate in fabric care advancement lies in the scarcity of fundamental soil removal knowledge. In other words while there is ample evidence of profound knowledge concerning fields such as detergents, electronics, thermodynamics, machine dynamics, textiles, colloidal science, adhesion etc. virtually nothing is known about their interaction in the washing machine.

The gap between these scientific fields is large and therefore perhaps not surprisingly consolidated information and models that help the washing machine design engineer are very

thin on the ground and the basic approach is (still) empiricism.

To bridge this gap in knowledge the Mass Transfer project was started within the R & D group of Whirlpool Corporation in 1995. A global team was set-up and areas of knowledge insufficiency discussed, listed and ranked. The overall outcome [ref. 1.3] was that it was essential for Whirlpool to scrap all previous semi-empirical attempts and forge a pure research approach to understand the fundamentals behind washing. The team also recognised that the project would probably be open-ended and require a consistent company commitment, tenacity and long-term resources allocation.

Setting the Scene

The reader may ask "why has this empiricism survived for so long and why is soil removal surrounded by so much mystery".

The fundamental reason is that the washing machine is an extremely complex mix of physical-chemical phenomena with an apparently distinct stochastic signature and behaviour [ref. 1.4].

Hence the design engineer is not confronted with a singular event or a sequence of phenomena such as abrasion, detergency, water temperature, hydrodynamics, twisting and churning etc. but simultaneously with a multitude of factors that enter or exit the scene continuously during the washing process.

The engineer also has to deal with equally important parameters such as consumer trends (e.g. modern fashion uses more delicate fibres), less energy and water consumption, international washing performance standards, origin of the fibre, weave patterns and many more.

An example of a part of this very complex jigsaw is shown next:

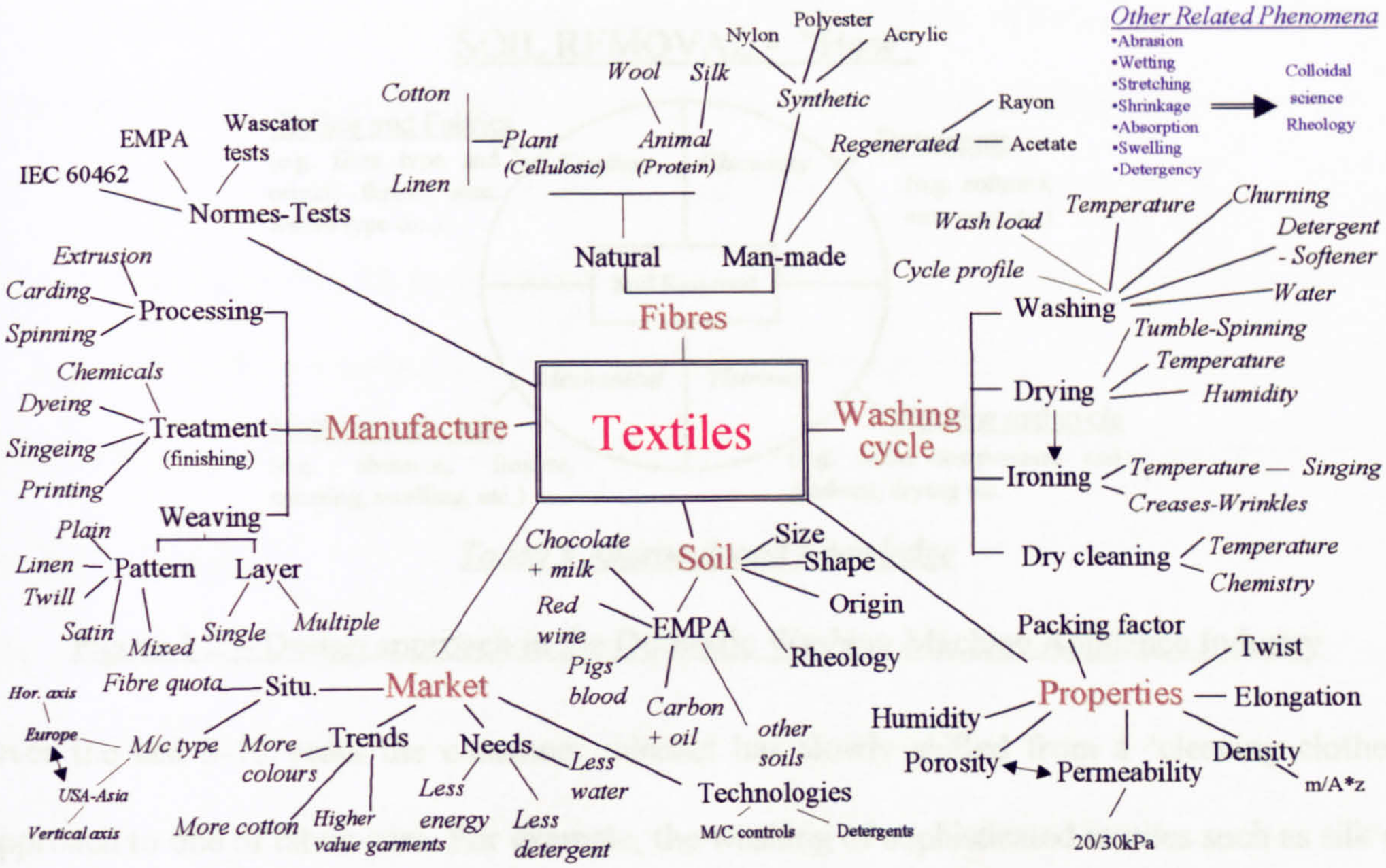

Figure 1.1 – Example of the complexity behind Fabric Care

It was this fuzzy situation that spurred the author to initially set out to analyse today's overall macro-approach i.e. how is machine design tackled by the industry today.

The conclusion was that the industry mainly focuses on four areas: 1.Clothes and fabric, 2.Detergents, 3.Machine and cycle (i.e. mechanical aspects such as soaking, abrasion, load motion etc.) 4. Machine and cycle (i.e. heat and mass transfer aspects such as water heating, water spraying, pumping etc). Hence the emphasis today is "how" can these factors be optimised so as to produce the most efficient and effective cleaning result without damaging the clothes while satisfying performance criteria.

This 'how' approach is depicted in the following figure.

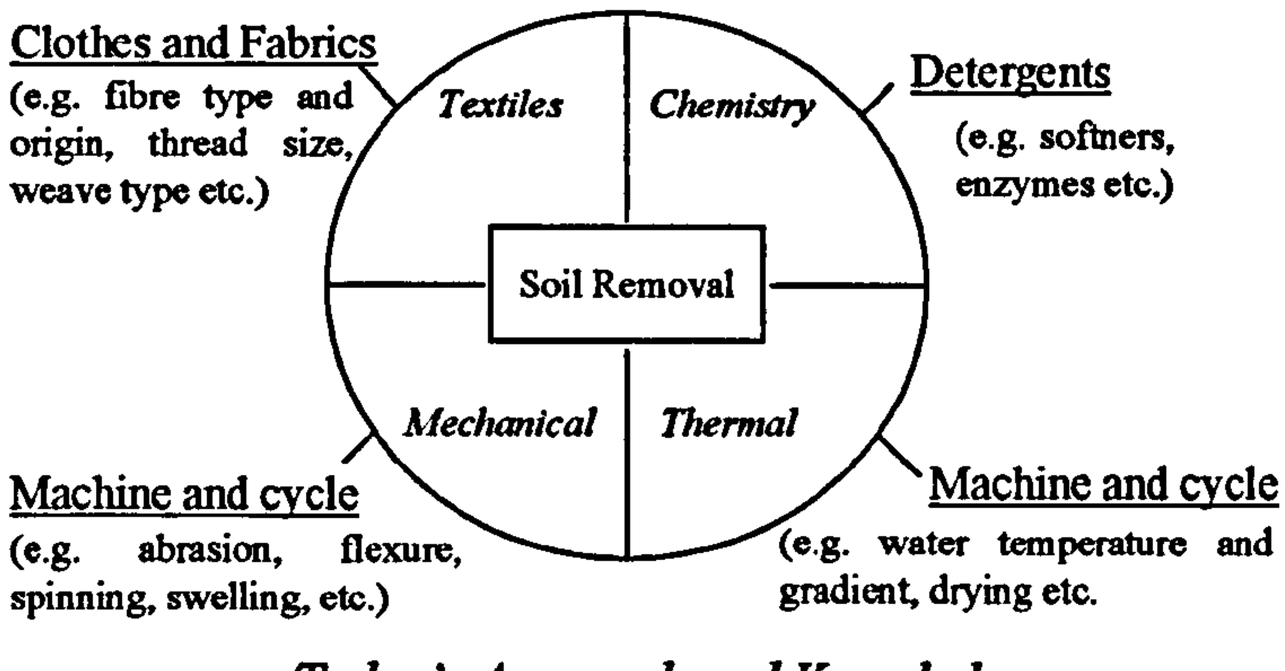

Figure 1.2 – Design approach in the Domestic Washing Machine Appliance Industry

Over the last 5-10 years the consumer mindset has slowly shifted from a 'cleaning clothes' approach to one of fabric care. For example, the washing of sophisticated textiles such as silk or cashmere and the rise in consumer fashion conscientiousness is no longer considered a latent need but a declared need[1].

This intrinsically implies using a different design approach and shifting from 'how' to 'why and how'. In other words there is a need for much more focus on detail and the gap in (missing) fundamental knowledge cannot be satisfied simply by adding electronics, programs and features to the machine. An example of missing knowledge is shown below:

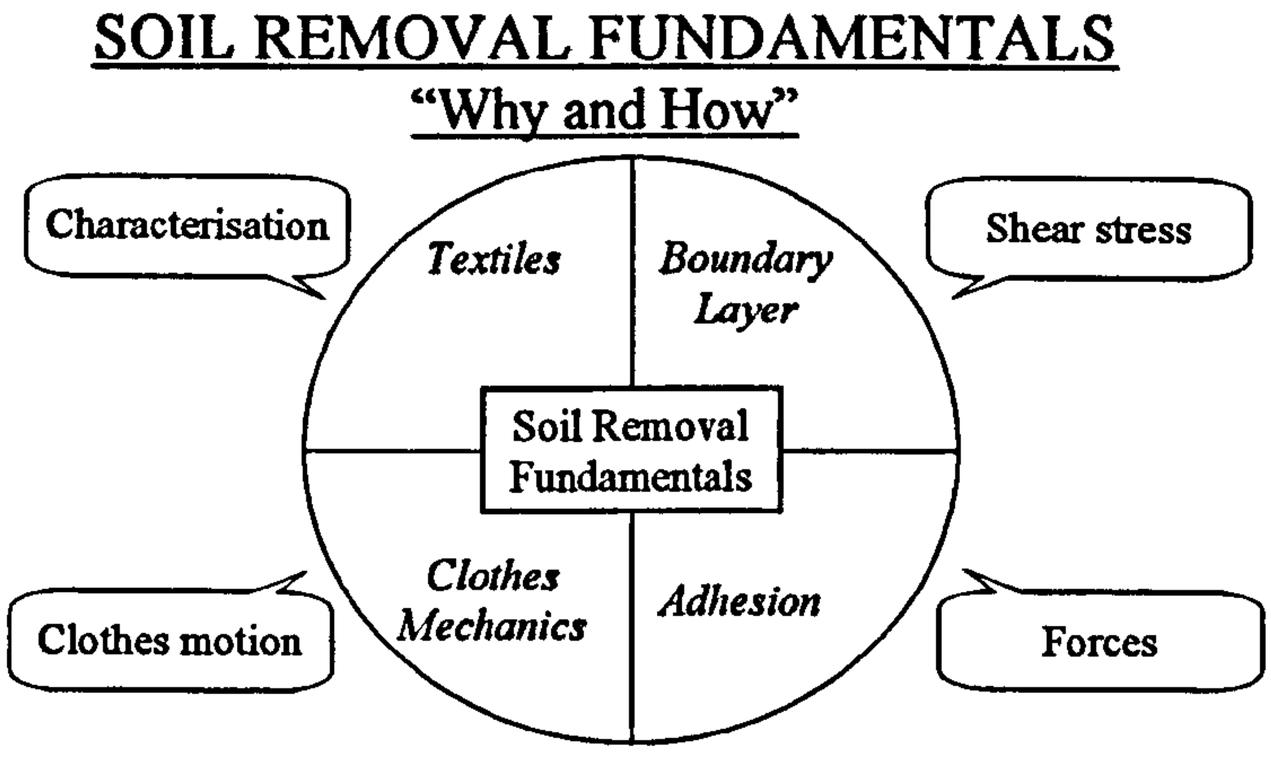

Figure 1.3 – Examples of Missing Knowledge

[1] Recent US market data indicates a typical wash load value of 300-500US$.

Using mapping techniques of this sort, the team identified three immediate areas of interest, which subsequently became the backbone of the team's research, these being:

- ❖ Adhesion mechanisms between soil and fibre
- ❖ Dry and Wet Abrasion mechanisms
- ❖ Boundary layer and hydrodynamics near the weave surface.

This ultimate research topic was assigned to me and is the subject of this thesis and research.

Research History

The research started in March 1997 and has involved Dr W. Kennedy (my internal supervisor from The Open University, UK), Prof. G. Menduni (my external supervisor from the Politecnico di Milano, Italy) as my tutor and Dr Dan Conrad, the Mass Transfer Project leader, who is based at Whirlpool Corporation, Benton Harbor, USA and three undergraduate students for whom I was their co-tutor. The research focuses on understanding and characterising the hydrodynamics near a (soiled) surface and the effects it has on the removal of soil.

The research consisted of emulating the washing machine hydrodynamic conditions in a purpose-built water tunnel as well as experimentation in the washing machine itself.

Particular attention has been given to the hydrodynamic shear stress in the boundary layer, relative boundary layer shear stress theory and its measurement in turbulent flow conditions. This is because the hydrodynamics are considered a fundamental feature of soil removal [ref. 1.5] and turbulent flow is known to provide the highest surface shear stresses and drag forces. Thus a sizeable part of the research was dedicated to determining how the shear stress near the soiled surface could be evaluated and establishing just how important it is for soil removal [ref. 1.6]. To achieve this goal the research was split into 5 steps, these being:

1. Quantification of the magnitude of hydrodynamic shear stress in a turbulent boundary layer by developing and testing two types of small block shear stress probe suitable for water

flows. This work involved designing, building and calibrating a purpose-built water tunnel.

2. Continuation and extension of step 1 but with emphasis on quantifying also the direction of hydrodynamic shear stress in a turbulent boundary layer.
3. Establishing the effects of hydrodynamic shear stress on the removal of soil from standard EMPA samples.
4. Determining flow conditions on the outside of the wash load using the same small block probes developed in steps 1 and 2. This step also involved modelling of the wash load motion and high speed filming of the wash water.
5. Determining the flow conditions on the inside of the wash load using a purpose-built remote data acquisition and sensor system based on the same small block probes developed in steps 1 and 2. The whole system was housed in a plastic sphere with one triangular shaped probe mounted on the outside surface of the sphere. This step also involved evaluating other factors involved in soil removal e.g. abrasion, detergency etc, modelling and high speed filming of the wash load.

An overview of the complete research is given in the next figure.

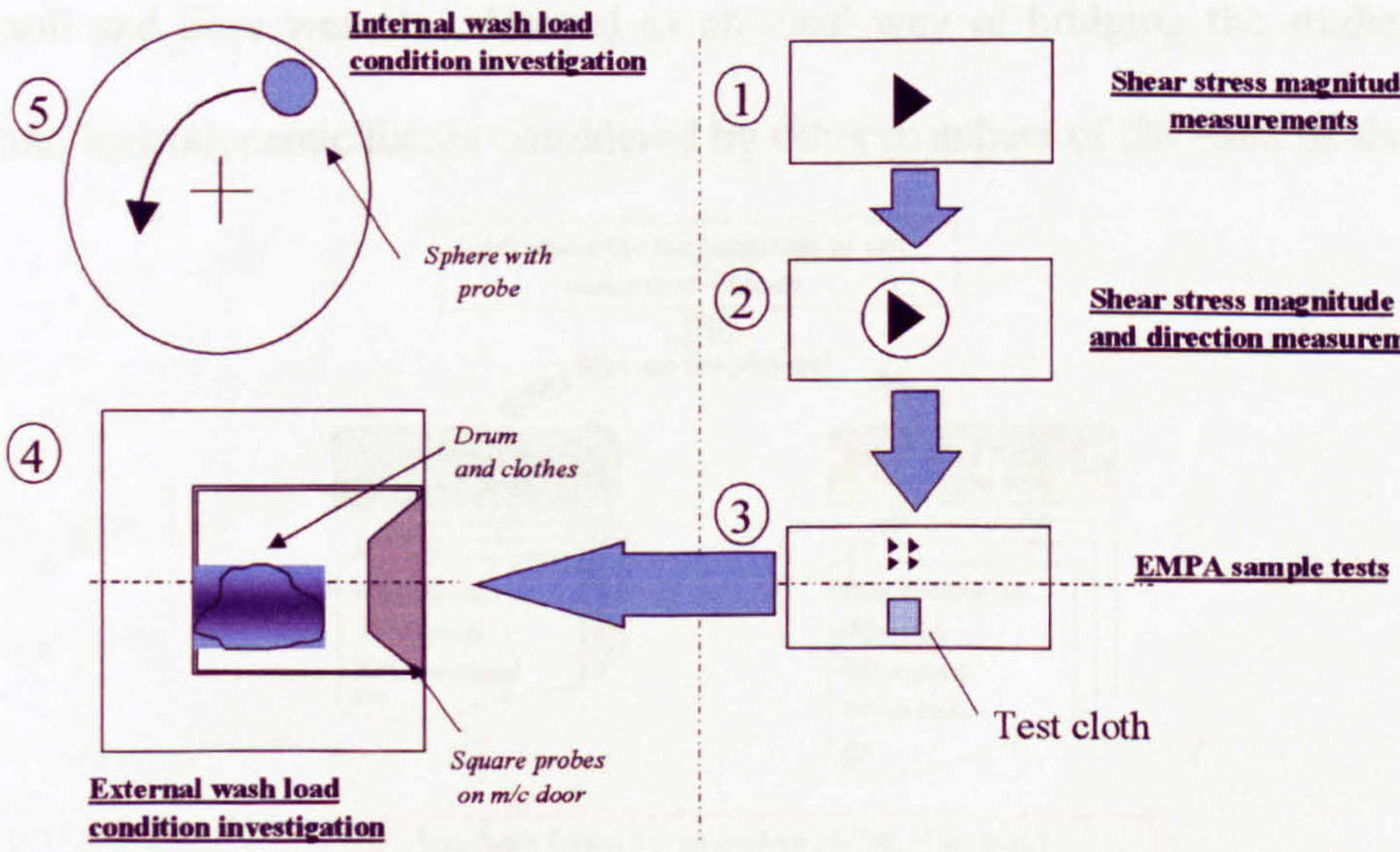

Figure 1.4 – Overview of Research

Originally the idea was to determine the flow conditions in the washing machine and then emulate them in a closely controlled environment (the water tunnel).

However, this approach was abandoned early in the project because it was thought that it would focus too much attention on today's machine rather than the fundamentals of soil removal. In other words there was concern that the 'machine first' approach would narrow down the team's vision and again concentrate on 'how'. Consequently the water tunnel was built first followed by shear stress measurement and experimentation of the small block probes (steps 1-2). Once this work was completed the EMPA [refs. 1.7 and 1.8] samples were tested (step 3) and the first link between hydrodynamic forces and soil removal determined and quantified.

The research then moved to the washing machine where the focus was the determination of the flow conditions inside the drum (steps 4 and 5). This included modelling the motion of the wash load, and developing methods of measuring the flow velocity both inside and outside it.

Hence one of the keys to correlating tunnel and washing machine conditions was to understand the hydrodynamic conditions, especially (soil detachment) hydrodynamic forces inside the washing machine. Moreover, the prospect of associating attraction and detachment forces between soil and fibre was also deemed as an ideal way of bridging the studies of adhesion, abrasion and hydrodynamic forces considered by other members of the team as shown below:

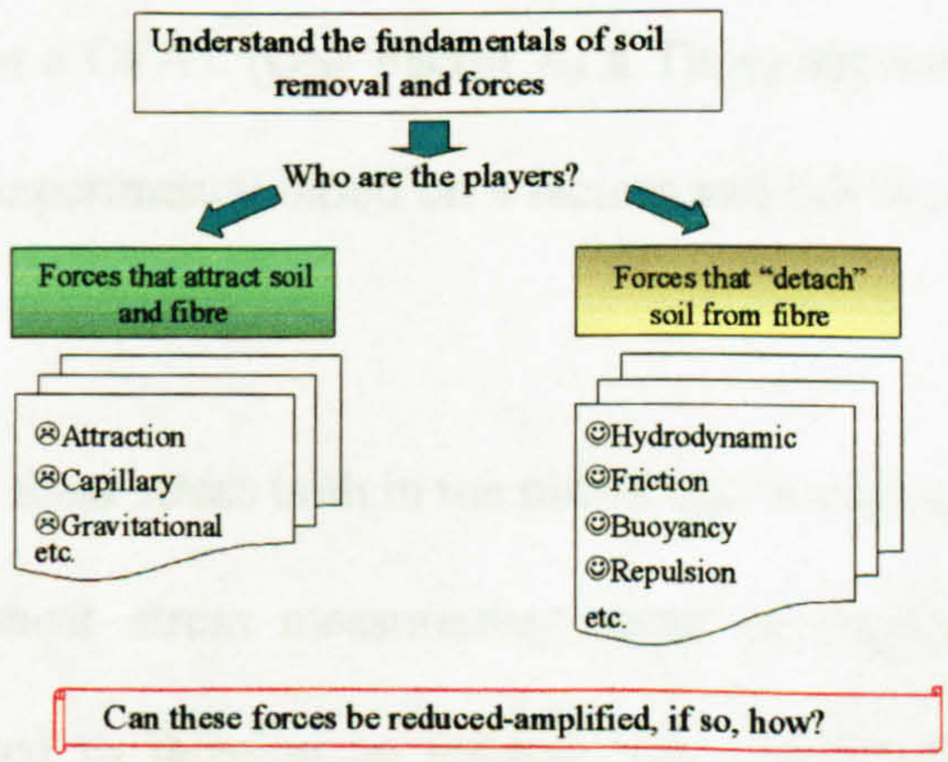

Figure 1.5 – Bridging Adhesion, Abrasion and Hydrodynamic force studies

Linking Tunnel and Washing Machine Hydrodynamic Conditions

One of the fundamental questions that arose during the research was how to ensure that the tunnel was emulating the same hydrodynamic shear stress conditions found normally in the washing machine.

This led to the whole issue of clothes and fluid motion in the washing machine, subsequent development of the fabric plug model [ref. 1.9] and relative validation using high-speed digital filming [ref. 1.10]. This latter activity also demonstrated that clothes motion was at least qualitatively predictable and two (or more) flow domains (e.g. inside and outside the wash load) were applicable. This work generated the idea of using a modified Reynolds number based on mixing vessel research, i.e. the washing machine was considered a mixing vessel [ref. 1.11]. It also brought out the idea of monitoring flow conditions inside the drum using a probe in the form of a sphere (step 5) equipped with the small block shear stress probes [ref. 1.12] experimented in steps 1 and 2.

One more piece was needed to generate overall confidence in the project results and that was establishing just how important shears stress was in the washing machine. Hence a further investigation (step 5) was carried out [ref. 1.13] in which 6 factors: detergency, water temperature, abrasion, warping (churning), shear stress and soaking, were compared. This investigation was based on a OFAT (One Factor At a Time) approach but was also supported by a 2^K DOE (Design of Experiments) based on 4 factors and full factorial design.

Shear Stress probes

Since the measurement of shear stress both in the tunnel and washing machine was a key project goal the techniques of shear stress measurement were investigated [ref. 1.14]. From this examination it was decided to develop an indirect measurement method based on pressure differential across a small obstacle (known as 'small block probes') placed in the fluid flow. The

objective was to measure both shear stress magnitude and direction and relate these conditions to those normally found on the textile surface.

Two probes were developed [refs. 1.15 and 1.16], the first was square shaped, which essentially measured magnitude, while the second was triangular shaped that added the necessary direction component of the shear stress: both probes were tested and calibrated in step 1.

The square probe was tested in step 4 by applying it to the inside surface of the washing machine door while only the triangular probe was experimented in steps 2 (angular calibration) and 5 (sphere tests). Both probes are illustrated below:

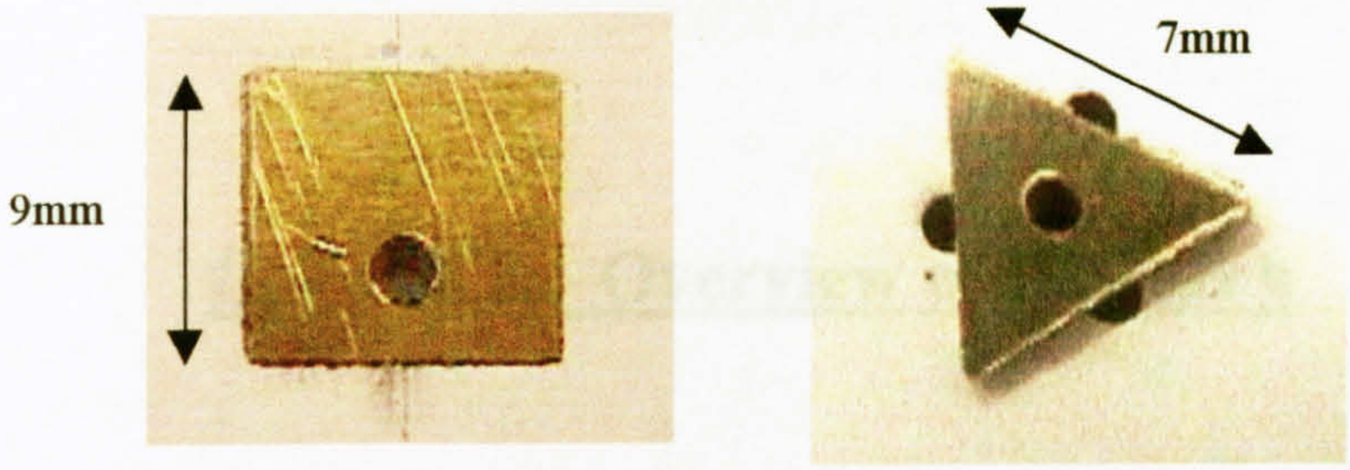

Figure 1.6 – Square and Triangular shaped small block probes

Chapter 2 – Overview of Research

List of Contents

List of Figures

List of References

1. Ward D., Project Charter and Definition, Whirlpool internal report, Monthly report, March, 1997.
2. Goldstein R. J., Fluid Mechanics Measurements, pp. 575-648, 2nd Edition, Taylor and Francis, 1998.
3. Owen F. K. and Bellhouse B. J., Skin Friction Measurements at Supersonic Speeds, AIAA J., vol. 8, pp. 1358-1360, 1970.
4. Bardelli et al., Ultrasonic Measurement of Shear Stress in Blood Streams, Ospedale di Cattinara, Trieste, Italy, 1998.
5. Bocchiola D., Una Metodologia per la Misura Puntuale dell'Attritto di Parete in Correnti Cilindriche *("A Method for Measuring Local Skin Friction in Cylindrical flows")*, Engineering degree thesis, No. 611090, Politecnico di Milano, Italy, 1998.
6. Dexter P., Evaluation of a Skin-friction Vector Measuring Instrument for use in 3-D Turbulent Incompressible Flow, Project Report, University of Southampton, Dept. of Astronautics and Aeronautics, UK, 1974.
7. Ward et al., Numerical Simulation of a Rectangular-section Water Duct equipped with Small Block Shear Stress Probes. CAPI'99, Politecnico di Milano, Italy, Nov., 1999.

8. Preston J. H., The Determination of Turbulent Skin Friction by Means of Pitot Tubes, J. R. Aeronaut. Soc., vol. 58, pp. 109-121, 1953.
9. Viterbo M, Sonde di Strato Limite per la misura dello Sforzo d'attritto – Studio Sperimentale ed Analisi Teorica *("Boundary Layer probes used for the measurement of wall shear stress and skin friction – Experimental investigation and Theoretical analysis")*, Engineering degree thesis, No. 599289, Politecnico di Milano, Italy, 1999.
10. Ward et al., Conditioning Effects of Hydrodynamic Shear Stress on Soil Removal, Whirlpool Internal report Nov., 1999.
11. Ward D., High Speed Filming of Clothes and Fabric Plug Motion, Whirlpool Internal Report, Sept., 1999.
12. Ward D., Introductory Evaluation of Soil Removal Conditions, Whirlpool Internal report, Aug., 1999.
13. Ward D. and Maritan M., Weave Model Construction using Stereolithography ....an example of Rapid-Prototyping and the advance use of Pro-E and Fluent, Whirlpool Internal Seminar, March, 1998.
14. Ward et al., Microelectronic Sensor for the Measurement of Shear Stress within a Domestic Washing Machine Drum, IMAPS'99, Milan, Italy, July 1999.
15. Ward et al., Remote Measurement and Monitoring of Critical Washing Process Data directly inside the Washing machine drum, IEEE Instrumentation and Measurement Technology Conference, USA, May, 2000.

Research Synopsis

In the previous chapter the five steps of the research were introduced and briefly outlined. In this chapter each step will be expanded further and discussed in greater detail.

The intent is to provide a summary of each of the five project steps, introduce the major tasks involved and then link them together.

Step 1 – Measurement of Shear Stress Magnitude and Tunnel Characterisation

The original idea behind studying the effects of hydrodynamic conditions on soil removal was to subject soiled textile to a pure tangential shear stress, although this presented several complications including:

- How can shear stress be measured in liquid flows?
- Is it possible to determine the washing machine hydrodynamic conditions so as to control and emulate them in a purpose built prototype?
- How does the textile surface interact with the flow conditions, such as the boundary layer?

Many more supplementary questions were raised but the initial core dilemma was centred around understanding the boundary layer [ref. 2.1] and in particular the measurement of shear stress. This led to a need to measure shear stress from which steps 1 and 2 were initiated.

Over the past century a great deal of effort has been dedicated to measuring the magnitude of hydrodynamic shear stress in turbulent boundary layers [ref. 2.2], mainly because of the practical consequences it has on our everyday life. In fact this research effort spans from understanding aeroplane wing performance [ref. 2.3] to correcting cardio-vascular defects such as partially blocked arteries with by-pass surgery [ref. 2.4]. However, very little information was available concerning hydrodynamic conditions, especially shear stress, in washing machines.

Step 1 was thus set-off with the intent to understand the boundary layer in general, establishing what hydrodynamic conditions we should expect in the washing machine and attempt to emulate them in a purpose built prototype.

The outcome was a water tunnel measuring about 12 meters in length in which two small shear stress probes (triangular and squared shaped) were installed and tested [ref. 2.5]. The scope of the probes was to be able to measure the shear stress during experimentation (especially step 3) and establish if it was possible to do the same in the washing machine (steps 4 and 5).

Two probes were developed and these were based on a probe originally developed by Dexter. Dexter [ref. 2.6] essentially developed a triangular shaped block probe in the form of a yawmeter for air-flows, while our designs were aimed at measuring shear stress in water flows. Essentially the concept behind the two 'new' probes was the same as for all small block probes but they were different in terms of scope and required a tailor-made water tunnel for calibration.

The design of the tunnel was based on the need to produce a fully developed turbulent flow, and regulate the flow between $20k \leq \mathrm{Re} \leq 160k$ in steady state conditions. How these conditions were established is explained later but for time being it will suffice to say that they are based on mixing vessel analysis.

Tunnel development also involved CFD simulation [ref. 2.7] including the effects of the triangular shaped version of the small block shear stress probe. This probe was initially used to measure the magnitude of the shear stress and characterise the tunnel

The characterisation of the tunnel implied measuring the shear stress in the area of the tunnel where subsequent experiments (steps 2 and 3) were planned.

Henceforth, step 1 involved developing a method of shear stress measurement, calibrating and testing it and then applying it to "map" or characterise the tunnel. The mapping of the tunnel consisted of two separate activities and techniques:

- Using a Preston tube [ref. 2.8] to measure the shear stress across half the upper wall of the tunnel.
- Using triangular and square shaped small block probes to measure shear stress across and along the tunnel.

An example of these mapping techniques is shown below:

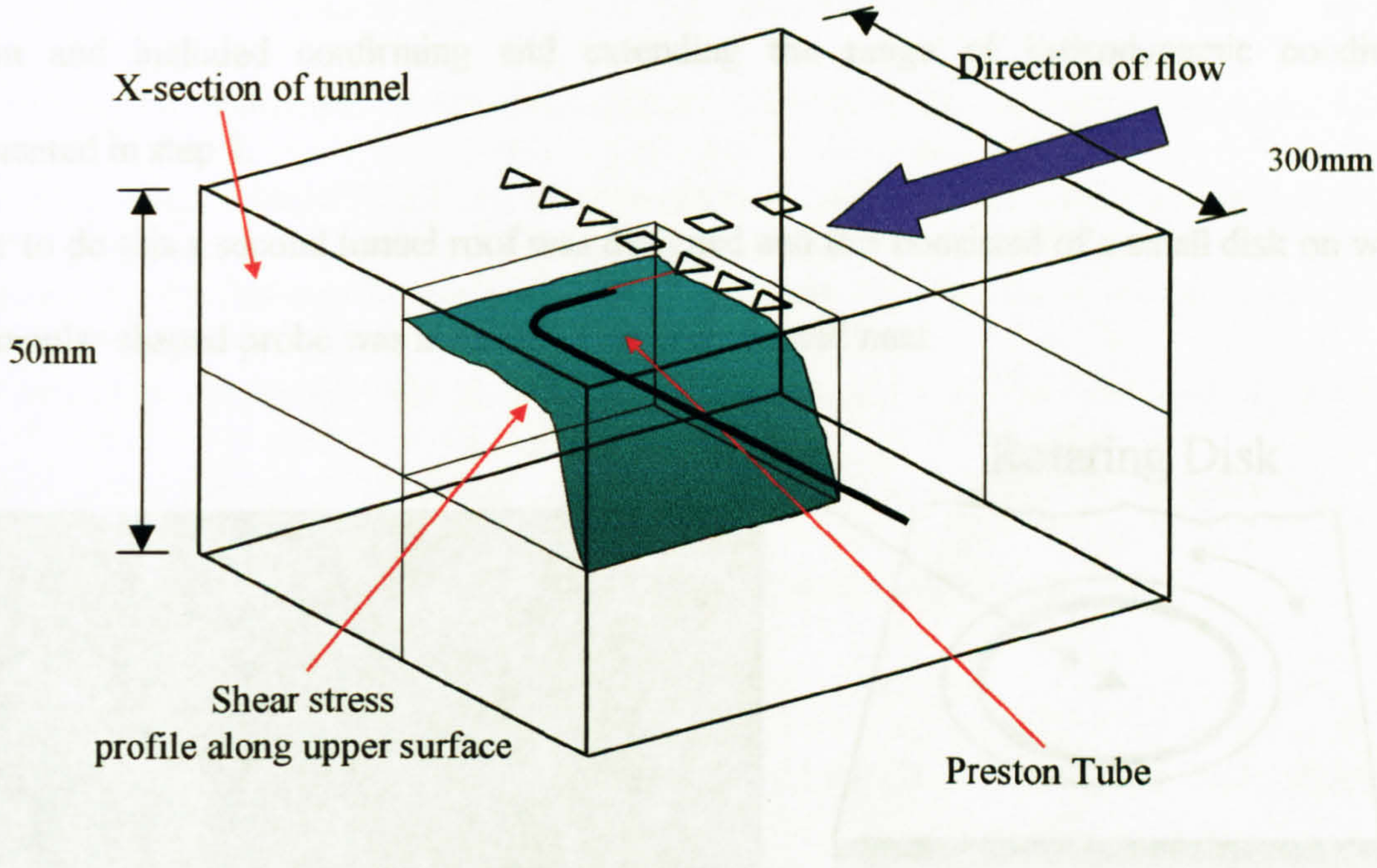

Figure 2.1 – Mapping of Tunnel Shear Stress

As can be seen above the characterisation of the tunnel essentially was aimed at obtaining the shear stress profile on the inner surface of the tunnels upper wall. This profile was essential to understand where the skin friction variation occurred and what was its magnitude. Once the tunnel was mapped and confidence was gained in the use of the small block probes the research moved to step 2.

Step 2 – Measurement of Shear Stress Direction and further Tunnel characterisation

In step 2 the emphasis was on determining both the magnitude and direction of the hydrodynamic shear stress [ref. 2.9]. This need stemmed from doubts about possible variation in shear across the area where the EMPA samples would be tested in step 3.

This meant focusing on the triangular shaped small block probe and extending the validity of its calibration to obtain a relationship between probe angle and measured pressures. The square shaped probe was therefore discarded in step 2 for it was unsuitable to provide both magnitude and direction of the shear stress.

Tests were carried out so as to simultaneously measure both shear stress magnitude and direction and included confirming and extending the range of hydrodynamic conditions experimented in step 1.

In order to do this a second tunnel roof was designed and this consisted of a small disk on which one triangular shaped probe was installed. This is illustrated next.

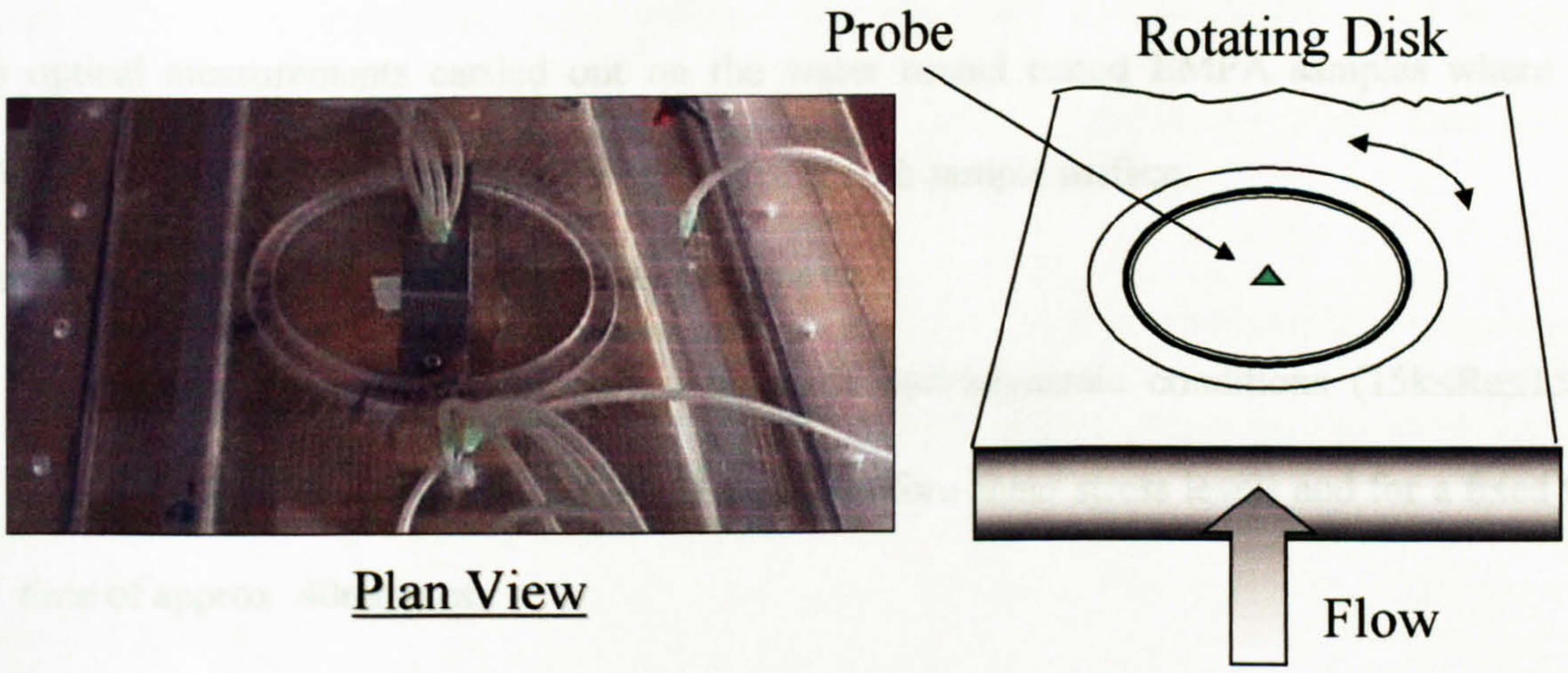

Figure 2.2 – Angular shear stress and the Disk

During experimentation the disk and probe were manually rotated, set at specific angles and pressures recorded. Since the probe was based on an equilateral triangular shape the disk and probe were rotated a total of only 60 degrees with 5 degree increments.

Measurements were taken between the static pressure tapping and each one of the probes three dynamic pressure tappings. The same procedure was repeated for another remote static pressure tapping located some distance away from the probe. In this way a set of differential pressures were recorded for a given set of disk angles, both locally and remotely.

Henceforth the experimentation provided not only a calibration curve but also a method of establishing the shear stress value and its direction simply by knowing the differential pressures of the probe.

Step 3 – Correlating Hydrodynamic Shear Stress and Soil Removal

At the end of step 2 it became apparent that the wall shear stress where the EMPA samples were going to be tested was acceptably constant. That is to say the area where the EMPA samples were going to be installed was an area where the shear stress profile was essentially flat (see figure 2.1). In this way it was reasonable to assume that the shear stress on the EMPA samples would be constant for the given hydrodynamic conditions. This was later confirmed by the optical measurements carried out on the water tunnel tested EMPA samples where the reflectance value was substantially constant across each sample surface.

Two experiments were conducted on the samples i.e.:

- Subjecting the EMPA samples to a range of hydrodynamic conditions ($15k \leq Re \leq 155k$, $0.2 \leq u \leq 1.97 ms^{-1}$ and $0.14 \leq \tau \leq 7.74 N/m^2$), and therefore shear stress levels and for a fixed test time of approx. 40minutes.
- Subjecting the EMPA samples to a fixed Reynolds number (Re=80000 circa) but varying the exposure time between 1 and 150 minutes circa. The intent was to observe the time dependency of the soil removal.

In order to carry out step 3 a third tunnel roof was built which consisted of mounting a flanged plug that allowed the accurate mounting of the EMPA samples. The plug was fitted with one sample at a time and located so that it did protrude excessively into the tunnel flow. During both tests the pressure drop was taken along the tunnel and the flow rate recorded.

In both instances all four standard EMPA soils (chocolate, pigs blood, red wine and carbon black) were optically tested to measure the amount of soil that had been removed during the

test. This optical measurement was realised with the same standard textile reflectance equipment used to measure washing machine performance and based on EMPA samples measuring 90 x 90mm.

The test time of 40 minutes was based on observation and the need to first understand the reaction of the sample to the hydrodynamic conditions. The tests were repeated 3 times for each sample and test condition (i.e. Reynolds number), while the optical measurements were based on an area of 30mm in diameter but repeated in five different areas across the sample. Hence the results were based on at least 15 observations for each soil and test condition.

Measurements confirmed that soil removal by shear stress alone [ref. 2.10] was only very marginal and no dominant Reynolds number was observed. It was thus decided to set an average Re=80k circa for the next set of tests where the time dependency of soil removal was investigated.

Exposure times were varied, ranging from every minute for the first 5 minutes to a maximum of 150mnutes:circa, this condition being defined as 'infinite'. With this test data in hand the time dependency of the soil removal could be plotted and the importance of hydrodynamic shear stress established.

<u>Step 4 – Measuring Flow Conditions on the Outside of the Wash Load</u>

The next task was to attempt to correlate the tunnel conditions with those found in the washing machine.

Several ideas came out of this analysis, including the need to model the wash load motion in the drum, but in step 4 it was decided to use the same square probes developed in step 1 to measure the flow conditions on the inside of the washing machine door. The assumption was that the external wash load conditions could be estimated by observing the water motion.

This observation could be done by high speed filming [ref. 2.11] or more simply by measuring the dynamic pressure using the small block probe.

Several square block probes were fitted to the door and pressure recordings taken. High speed filming was also carried out on the oscillation of the water line and clothes motion during drum rotation.

To address the motion of the clothes during drum rotation a mathematical model was developed in which the average flow velocities are estimated. The model assumes that the wash load can be represented by a concentrated mass in the form of a fabric plug or sphere. This concept proved to be the starting block for step 5 and its validity was confirmed both by the high speed filming and the evaluation of soil removal mechanisms in the drum (see DOE in step 5).

Step 5 – Measuring Flow Conditions on the Inside of the Wash Load

The testing of the EMPA samples in step 3 would be incomplete unless the water tunnel tests could be adequately weighted against other parameters in the washing machine. In other words comparing, for example, detergency, water temperature, abrasion, churning and soaking to hydrodynamic shear stress would allow an objective conclusion about the whole question of hydrodynamics.

It was decided to carry out a specific activity to look into these parameters and carry out a design-of-experiments accordingly [ref. 2.12]. The objective of the DOE was not only to determine which mechanisms were relevant but also to assign, where possible, a measure of importance using the previously mentioned optical methods.

The experimentation also involved comparing free moving textiles and the polystyrene spheres covered with the same, albeit smaller, EMPA samples. In this way it was possible to determine just how different the fabric plug behaved with respect to the wash load.

With this information available the second part of step 5 was initiated.

A special plastic, hollow, sphere (based on the fabric plug concept) was designed, built and tested so that flow information could be obtained during drum rotation. The main technologies to do this were essentially stereolithography (to make the sphere) and wireless electronics (to transmit and receive the data) and a data acquisition system to store and process the data [ref. 2.13 and 2.14].

Basically the flow conditions on the inside of the wash load were captured using the same small block probes developed in steps 1 and 2 and located on the surface of the sphere. To do this involved connecting a triangular shaped probe to a pressure transducer and then transmitting the data via a radio transmitter housed in the sphere as well. On the outside of the washing machine was located the receiver and data acquisition system [ref. 2.15].

Round-up

The overall research has been split into 5 steps (see also chapters 5a to 5e) and two domains, the first domain involving an ideal laboratory environment where the tunnel was the main prototype and the second, representing the real world, involving the washing machine.

There were substantially 3 principal original pieces of work or advances obtained from this part of the M.T. project, these being:

- The measurement of shear stress magnitude and direction in water flows with small block probes.
- Correlation of hydrodynamic shear stress effects on soil removal.
- The measurement of flow conditions inside the washing machine using a remote and wireless data acquisition system.

Chapter 3 – Development of Prototypes

List of Contents

List of Figures

List of Tables

List of Equations

List of References

1. EMPA report, Evaluation of Detergents and Washing Process with Artificially Soiled Fabrics, St. Gallen, Ch, 1999.
2. Preston J. H., The Determination of Turbulent Skin Friction by Means of Pitot Tubes, J. R. Aeronaut. Soc., vol. 58, pp.109–121, 1953.
3. Horton R. E., Weir Experiments, Coefficients and Formulae, Water–supply and Irrigation Paper No. 200, pp.46–47, United States Geographical Survey, Dept. of the Interior, 1907.
4. Nikarduse J., Strömungsgesetze in rauhen Rohen, Forsch. Arb. Ing.–Wes., no. 361, 1933.
5. Rechenberg I., The Measurement of Turbulent Wall Shear Stress, A. R. A. Translation No.11, Bedford, England, 1963.
6. Goldstein R. J., Fluid Mechanics Measurements, 2nd Ed., Taylor and Francis, 1996.
7. White F. W., Viscous Fluid Flow, pp.426–429, Mc Graw–Hill, 1991.
8. Dexter P., Evaluation of a Skin–friction Vector Measuring Instrument for use in 3–D Turbulent Incompressible Flow, Project Report, University of Southampton, Dept. of Astronautics and Aeronautics, UK, 1974.
9. Gaudet et al., Calibration and Use of a Triangular Yawmeter for Surface Shear Stress and Flow Direction Measurement, Proc. 2nd Intern. Conf. On Experimental Fluid Mechanics, Torino, 1994.
10. Ward D. et al., Numerical Simulation of a Rectangular–section Water Duct equipped with Small Block Shear Stress Probes. CAPI'99, University of Milan, Nov. 1999.
11. Ward D., Stereolithography, Whirlpool Internal Report, 1999.
12. Griffith M. and Lamancusa J. S., Rapid prototyping Technologies, 1998, Amazon book reference
13. Hilton P., Making the Leap to Rapid Tool Making, Mechanical Engineer Journal, July, 1995.
14. Chee Kai Chua, Leong Kah Fai, Chua Chee Kai, Kah Fai Leong, Rapid Prototyping: Principles & Applications in Manufacturing, Wiley & Sons, 1998.
15. Ashley S., From CAD Art to Rapid Metal Tools, Mechanical Engineering Journal, March 1997.
16. Jian Dong, Rapid Response Manufacturing – Contemporary methodologies, tools and technologies, Chapman & Hall, 1997.
17. Hartwig G., Rapid 3D Modelers, DE, March, 1997.
18. Ashley S., Rapid Prototyping is Coming of Age, Mechanical Engineering Journal, July 1995.

19. Medical applications, 3D System Corporation, http://www.3dsystems.com

20. Helisys Inc., http://www.helisys.com

21. Selective Laser Sintering, Accelerated Technologies Inc., http://www.acceltechinc.com

22. Fused Deposition Modelling, Stratasys Inc., http://www.stratasys.com

23. SOLIGEN Technologies, Direct Shell Production Casting, http://www.soligen.com

24. Sanders Prototype Inc., http://www.sanders–prototype.com.

25. MIT 3D printing, MIT Engineering library, http://libraries.mit.edu/barker/

26. Cotton Report, Institut für Textiltechnick der RWTH, Aachen, 1989.

27. Ward D., Literature review – First Interim Report, Whirlpool internal report, 1997.

28. Ward D., Weave model tests, Whirlpool Internal Report, 1999.

29. Ward D., SEM investigation, Whirlpool Internal Report, 1999.

30. Ward D., Modelling of a Horizontal–Axis Domestic Washing Machine, Journal of the Textile Institute, Vol. 91, Part 1, No. 2, 2000.

31. Ward D., Introductory Evaluation of Soil Removal Conditions, Whirlpool Internal report, Aug., 1999.

32. Sphere Patent, European Patent application, Sept., 2000.

33. Table Curve 2D manual, Jandel Software, California, USA, 1997.

34. Viterbo M, Sonde di Strato Limite per la misura dello Sforzo d'attritto – Studio Sperimentale ed Analisi Teorica *("Boundary Layer probes used for the measurement of wall shear stress and skin friction – Experimental investigation and Theoretical analysis")*, Engineering degree thesis No. 599289, Politecnico di Milano, Italy, 1999.

35. Druck Group Holdings PLC, http://www.druck.com.

36. National Instruments Inc., http://www.ni.com.

37. Henderson F.M., Open Channel Flow, ch.6, Macmillan Co.

38. Schoder E. W. and Turner K. B., Precise Weir Measurements, Trans. Am. Soc. Civil Engineers, p.1143, vol. 93, 1929.

39. Munson, Young, Okishi, Fundamentals of Fluid Mechanics, pp. 479–483, Wiley, 3rd edition, 1996.

40. Pezzotta E., Progetto e Realizzazione di un Sistema di Misure delle Condizioni Fluidodinamiche in una Lavatrice Domestica *("The Design and Development of a Measurement System for the Monitoring of*

Hydrodynamic Conditions in a Domestic Washing Machine"), Engineering degree thesis, No. 855766, Politecnico di Milano, Italy, 1999.

41. Bocchiola D., Una Metodologia per la Misura Puntuale dell'Attritto di Parete in Correnti Cilindriche *("A Method for Measuring Local Skin Friction in Cylindrical flows"*), Engineering degree thesis, No. 611090, Politecnico di Milano, Italy, 1998.
42. Ward D., Boundary Layer Theory, Shear Stress Measurement and the Washing machine-Tunnel investigation, Whirlpool Internal Report, issue 2, Dec. 1999.

Development of Prototypes and Tools

One of the key parts to the research has been the development and use of specific tools–prototypes. In this chapter the design and use of these tools–prototypes will be unveiled and discussed in detail, including the relative technologies involved to realise and use them. Emphasis will be on illustrating how and why these technologies were applied rather than explaining their theoretical background, which is tackled in later chapters.

Water Tunnel and EMPA Test Sample Jig

The water tunnel has been designed with two research activities in mind, these being:

1. To develop, test and calibrate the small block probes in water flows (steps 1 and 2.
2. To subject the EMPA samples [ref. 3.1] to specific hydrodynamic conditions (step 3).

The design of tunnel focused on satisfying the following essential criteria:

- To stabilise and render fully developed the flow in the test section of the tunnel where the probes and EMPA samples would be tested.
- To regulate the hydrodynamic conditions i.e. flow rate and pressure in the tunnel.
- To measure the flow rate using a Thomson weir.
- To measure the inlet pressure head, the pressure drop along the test section and probe differential pressure for all tested hydrodynamic conditions.
- To measure shear stress both along and across the test section including the use of a Preston tube [ref. 3.2].

The tunnel was split into three macro sections and 10 sub–sections, as shown next.

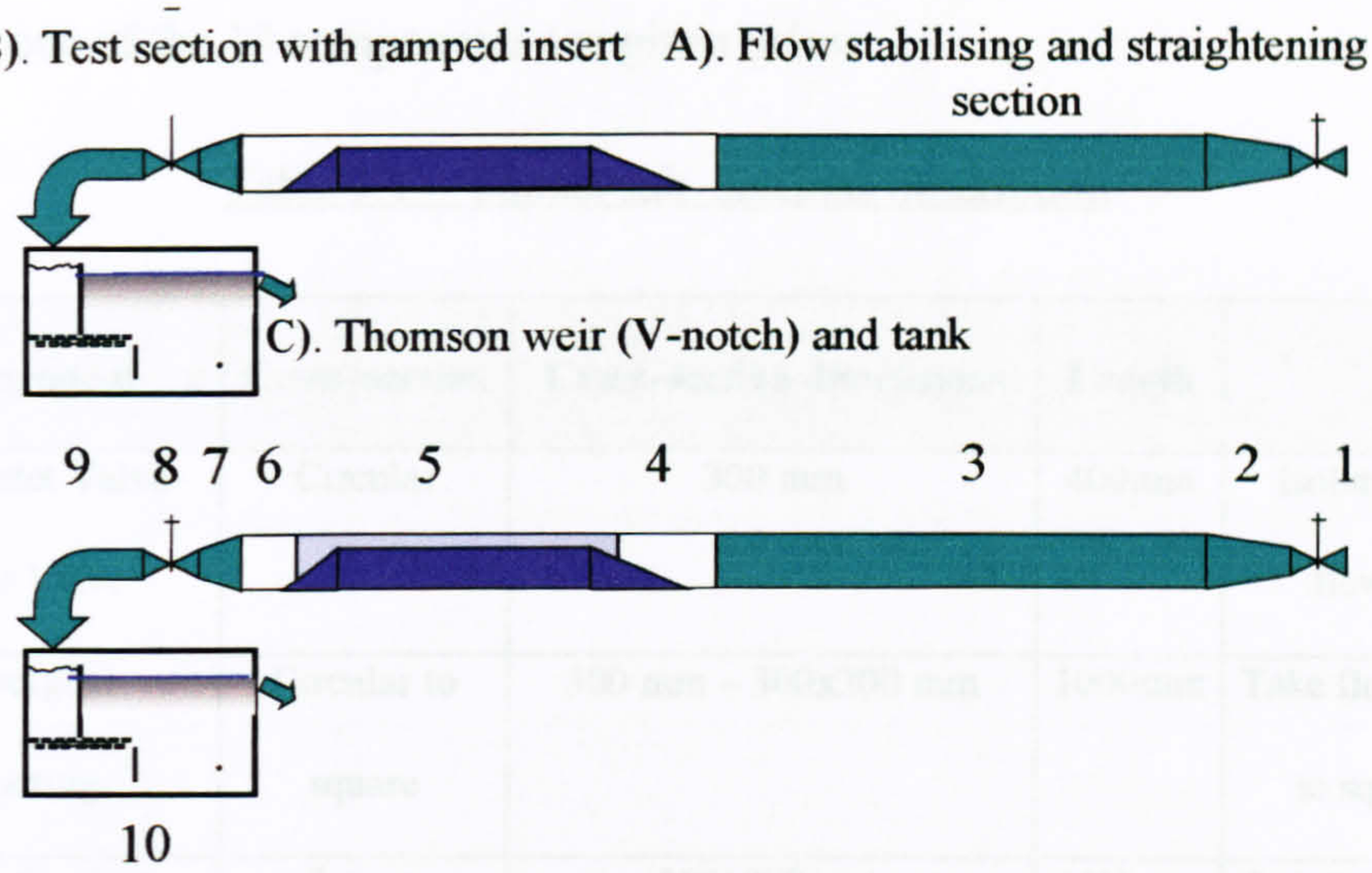

Figure 3.1 – Complete Tunnel

The scope of these three macro sections was:

Inlet section : To regulate and stabilise the water flow.

Test section : To stabilise and fully develop flow in the test section.

Outlet section : To regulate and take flow to the Thomson weir.

The basic design of the tunnel was based on a maximum flow rate of 70E–3 m^3s^{-1} measurable by the Thomson weir [ref. 3.3] and an inlet static pressure head of approx. 1m H_2O. These conditions were later fine tuned to $20000 \leq Re \leq 160000$, $15 \leq T \leq 22°C$, $0.2 \leq U \leq 2$ ms^{-1}, $0.003 \leq Q \leq 0.03$ m^3s^{-1}.

The test section was designed to accelerate the flow, provide sufficient pressure drop to be measured by the pressure measurement system and ensure fully developed flow. The test section length was determined to guarantee fully developed flow in the area where the probe and EMPA samples were to be tested. Nikarduse [ref. 3.4] suggested a length to hydraulic radius ratio of approx. 100 so the test section length was set to 2.154m. However, practical pressure measurements have shown that this could be safely reduced by at least 0.5m while subsequent CFD work indicated a theoretical length of only 1m.

Details of each one of the 10 components are given below:

Table 3.1 – Tunnel sub–sections description

Ref.	Component	Cross–section	Cross–section dimensions	Length	Role
1	Main Inlet Valve– Gate Valve	Circular	300 mm	400mm	Isolate and regulate flow conditions
2	Divergent Ducting	Circular to square	300 mm – 300x300 mm	1000mm	Take flow from circular to square ducting
3	Steel ducting	Square	300x300 mm	4500mm	Stabilise and straighten flow
4	Perspex Ducting	Square	300x300 mm	1500mm	Introduce flow to first ramp
5	Test section – Perspex ducting with removable Lexan roof	Square	300x300 mm without ramped insert 300x50mm with ramped insert	2150mm	Accelerate flow and carry out experimentation
6	Perspex Ducting	Square	300x300 mm	500mm	Guide flow after end ramp
7	Convergent Ducting	Square to circular	300*300mm to 200mm dia.	500mm	Take flow from square to circular piping
8	Main Outlet Valve – Gate valve	Circular	150 mm	200mm	Isolate and regulate flow conditions
9	Steel piping	Circular	150 mm	700mm	Take outlet flow to Thomson weir
10	Steel pipe bend & Thomson weir	Circular	150 mm	500mm	Take outlet flow to Thomson weir

The test section and triangular probe were also simulated using FLUENT and a mesh with 2 domains and up to 204k volumes. The final CFD model consisted of sub–sections 4 to 6 but

with only half the solid, wetted, tunnel boundaries being simulated. Part of the CFD activity is shown on the next page (see also chapter 6).

Both square and triangular probes were tested and calibrated in the tunnel (see below). In step 1 these were placed (fixed) both along and across the tunnel while in step 2 a triangular probe was mounted on a rotating disk to correlate shear stress magnitude and angular direction.

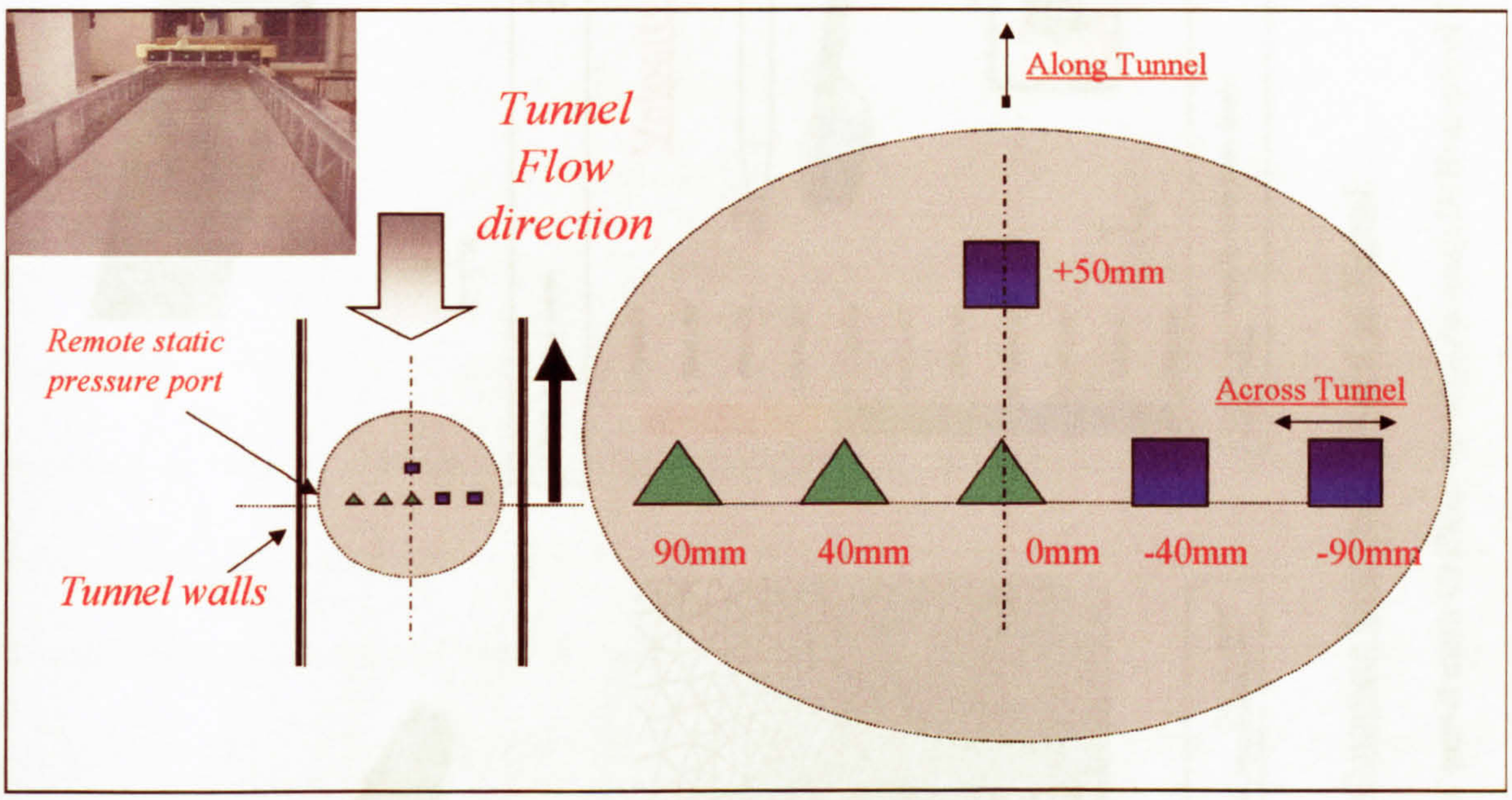

Figure 3.2 – Installation of Square and Triangular probes

(a picture of tunnel x–section without roof is shown in top L.H. corner)

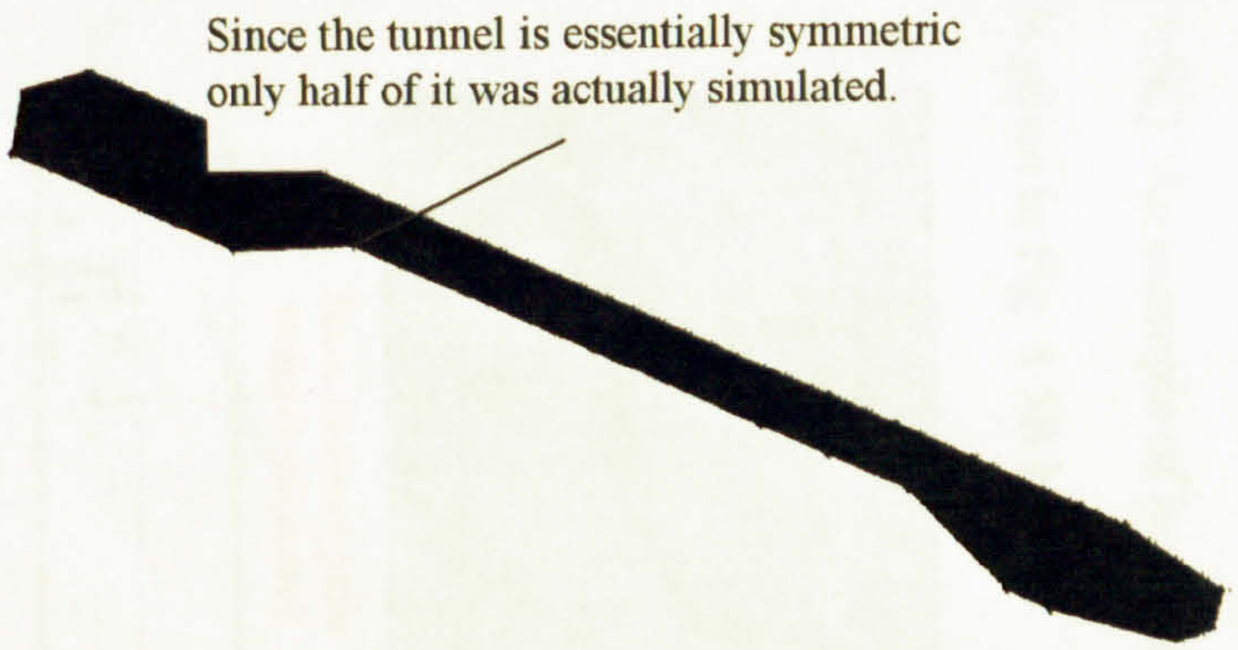

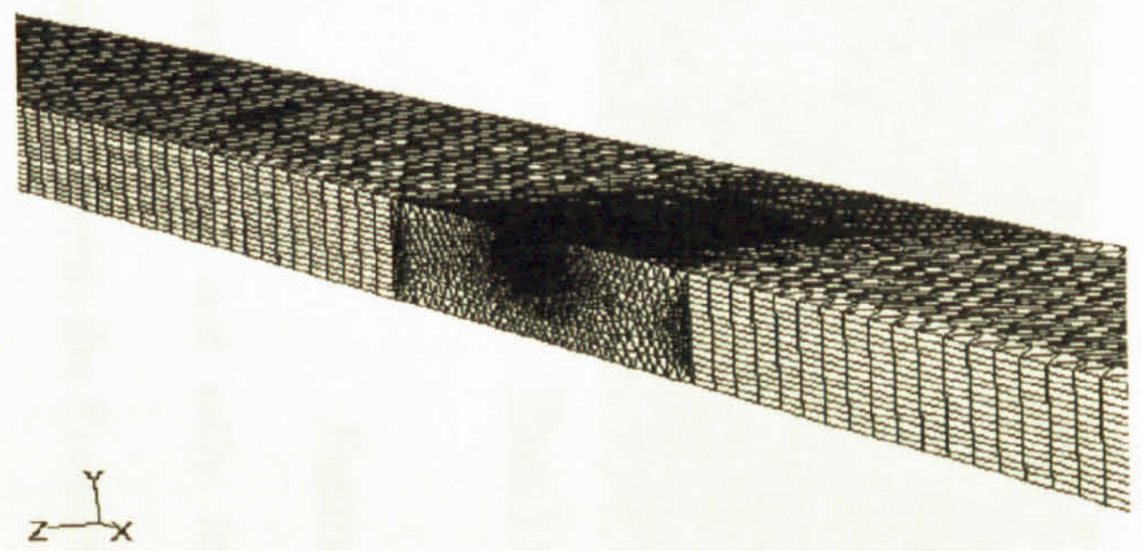

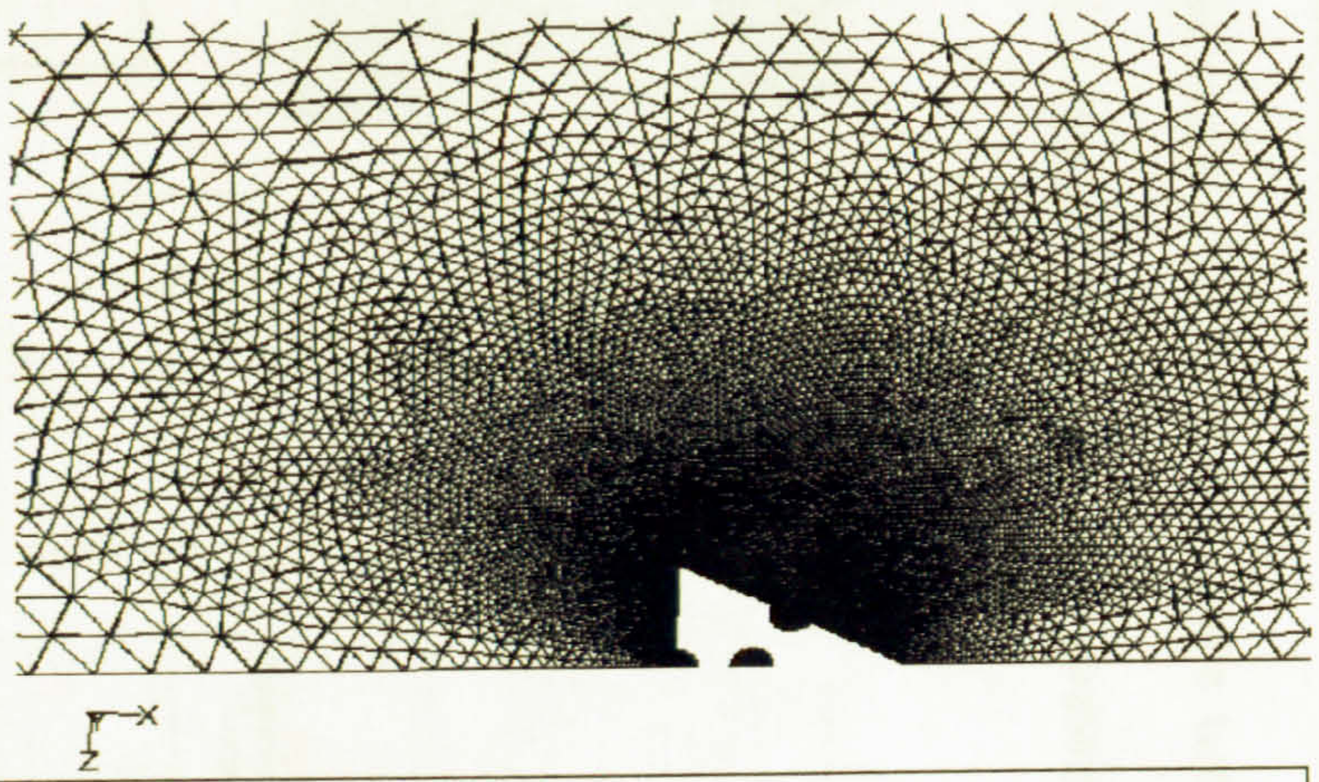

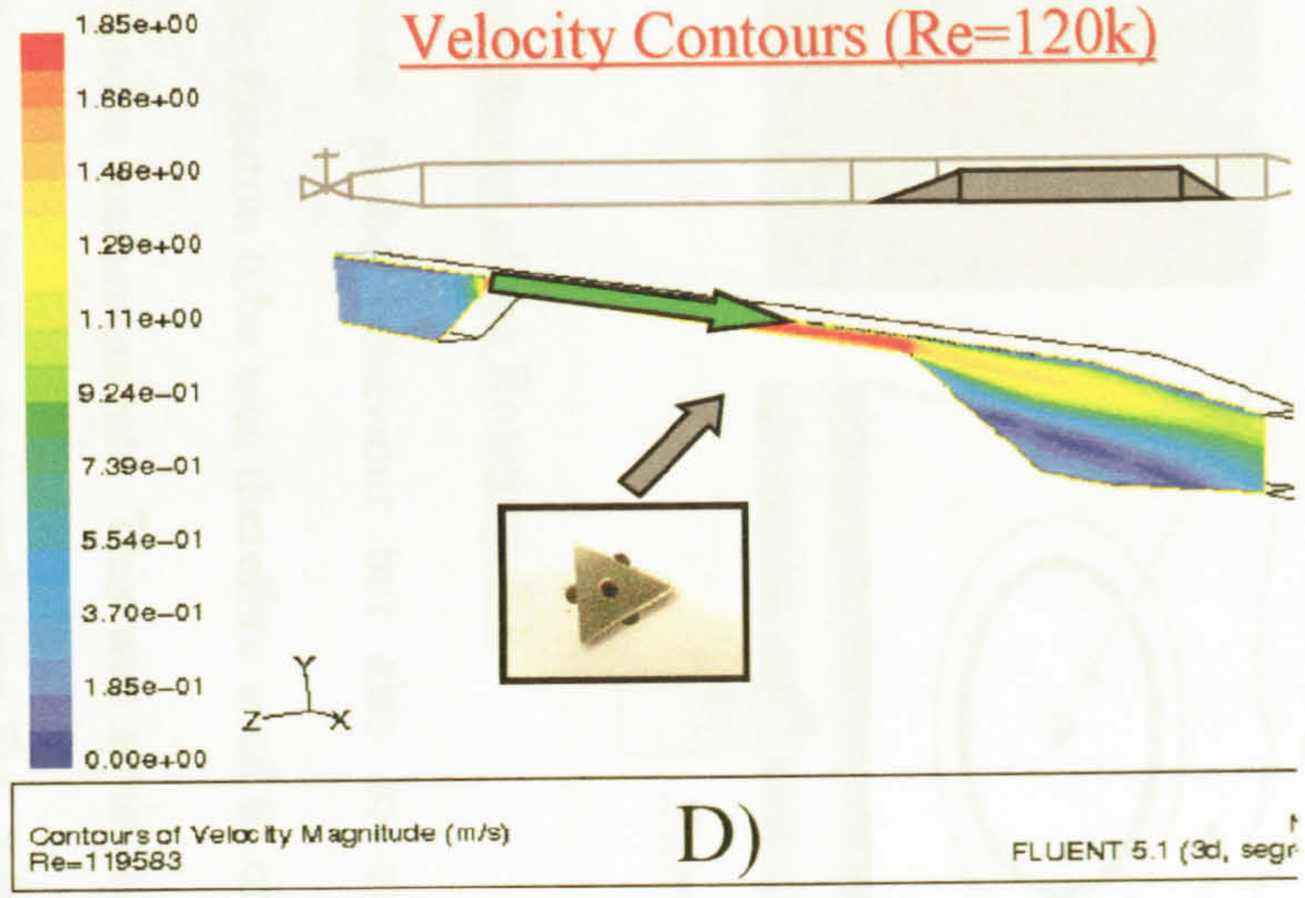

Figure 3.3 – Complete Geometric Model of Tunnel

A) Overall meshed model B) Close–up of tunnel mesh C) Close–up of probe mesh D) Example of CFD results

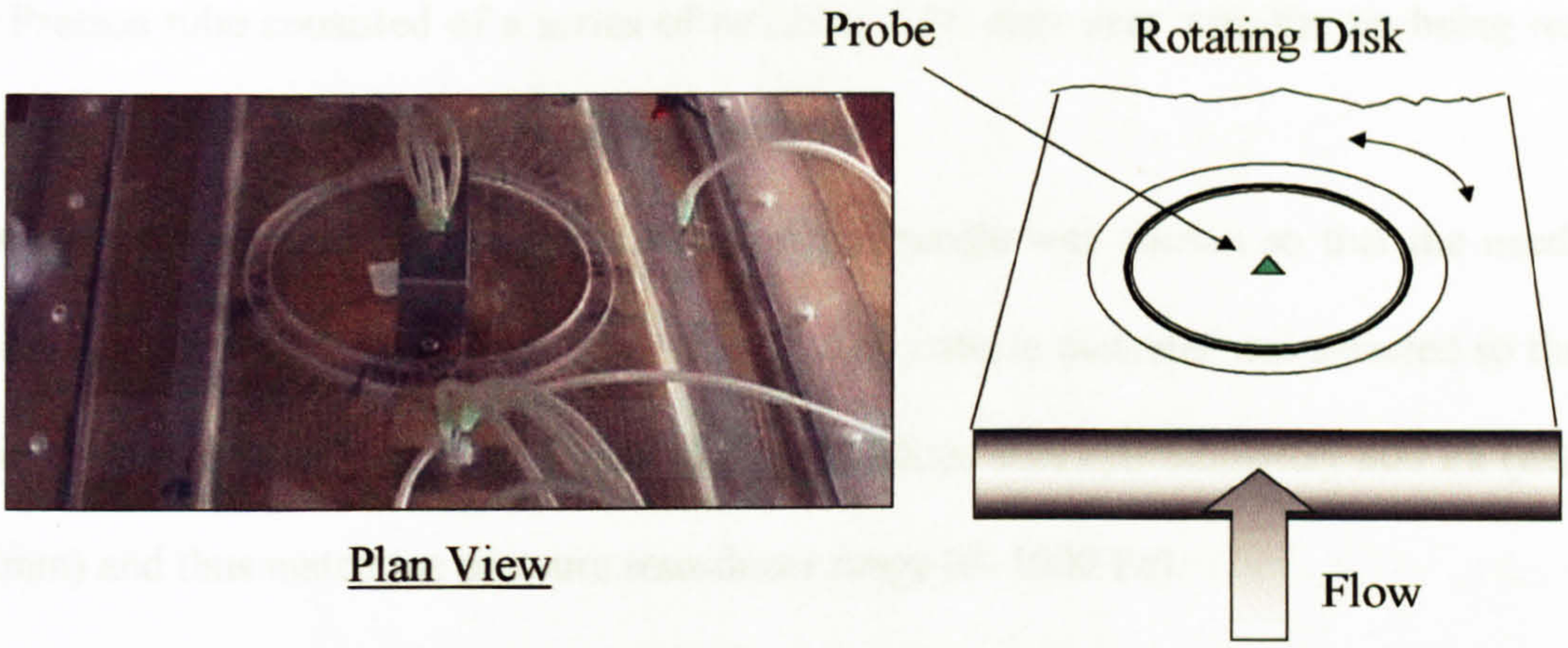

Plan View

Figure 3.4 – Installation of the Rotating disk

The scope was not only to understand probe behaviour but also to correlate these measurements with the Preston tube. The Preston tube was therefore used to characterise the shear stress across the flow and verify probe measurements. This was achieved by manually "scanning or wiping" the tube across the tunnel inner upper wall (see Fig. 3.5D) and taking measurements at 16 different points. Since the flow was symmetric and fully developed these measurements were realised only in the upper R.H. quadrant of the test section (see Fig. 3.5C). An example of how this was done to complete a typical shear stress profile at Re=119K is given in Fig. 3.5B below:

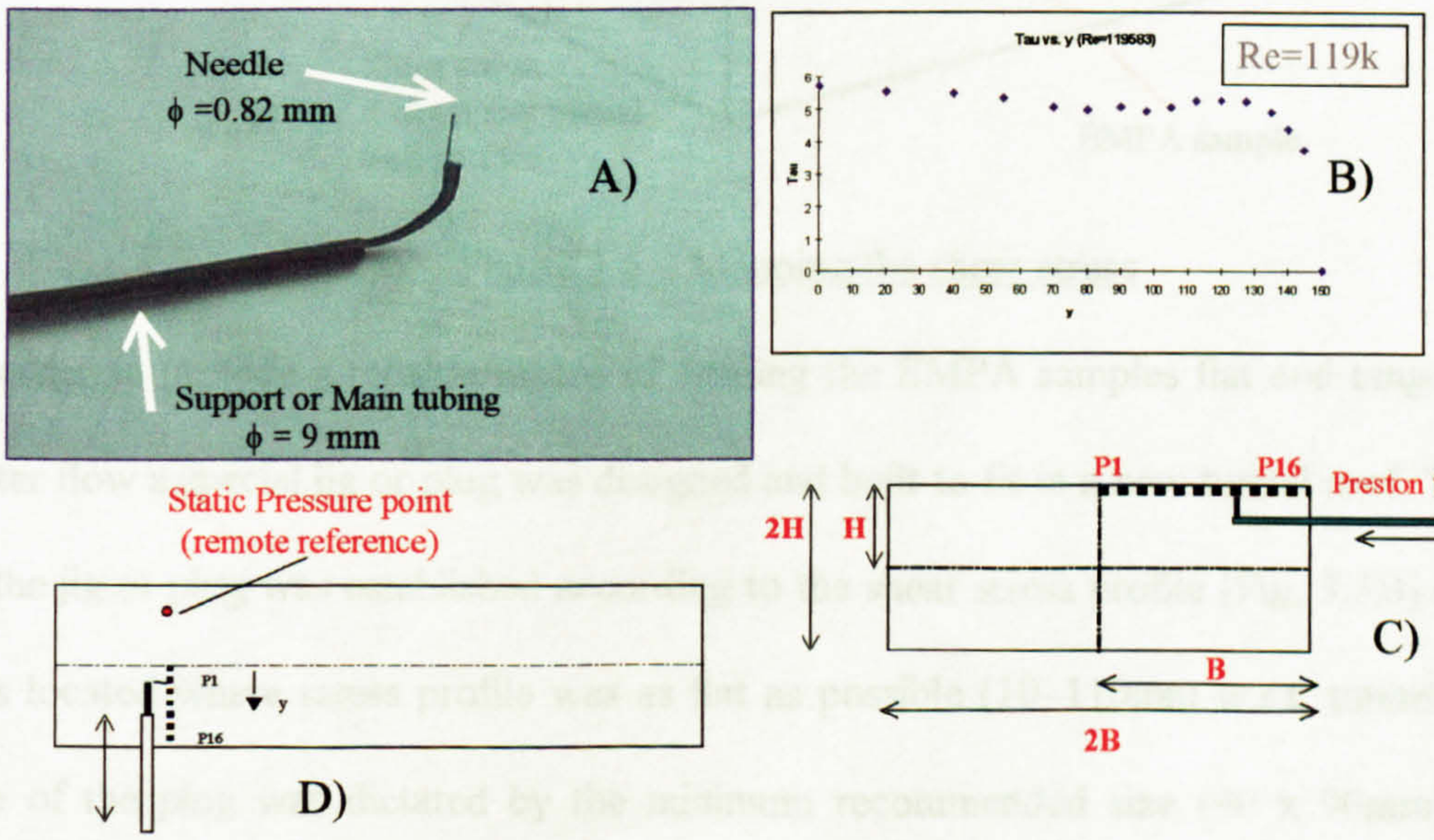

Figure 3.5 – Preston tube in use

The Preston tube consisted of a series of reducing tube diameters with the tip being realised with a simple, but very effective, medical needle.

To avoid unnecessary measurement correction the needle was chosen so that the needle tip inner and outer diameter ratio was 0.6 [ref. 3.5]. The outside diameter was selected so that the maximum pressure reading for the given flow conditions was approximately 800 Pa (ext. dia. 0.82mm) and thus match the pressure transducer range (0–1000 Pa).

By combining probe and Preston tube measurements it was therefore possible to obtain a map or profile of the shear in the area where the EMPA samples were going to be tested. This was needed to justify any eventual difference in soil removal efficiency that may have been noticed in step 3. An example of this concept is shown below:

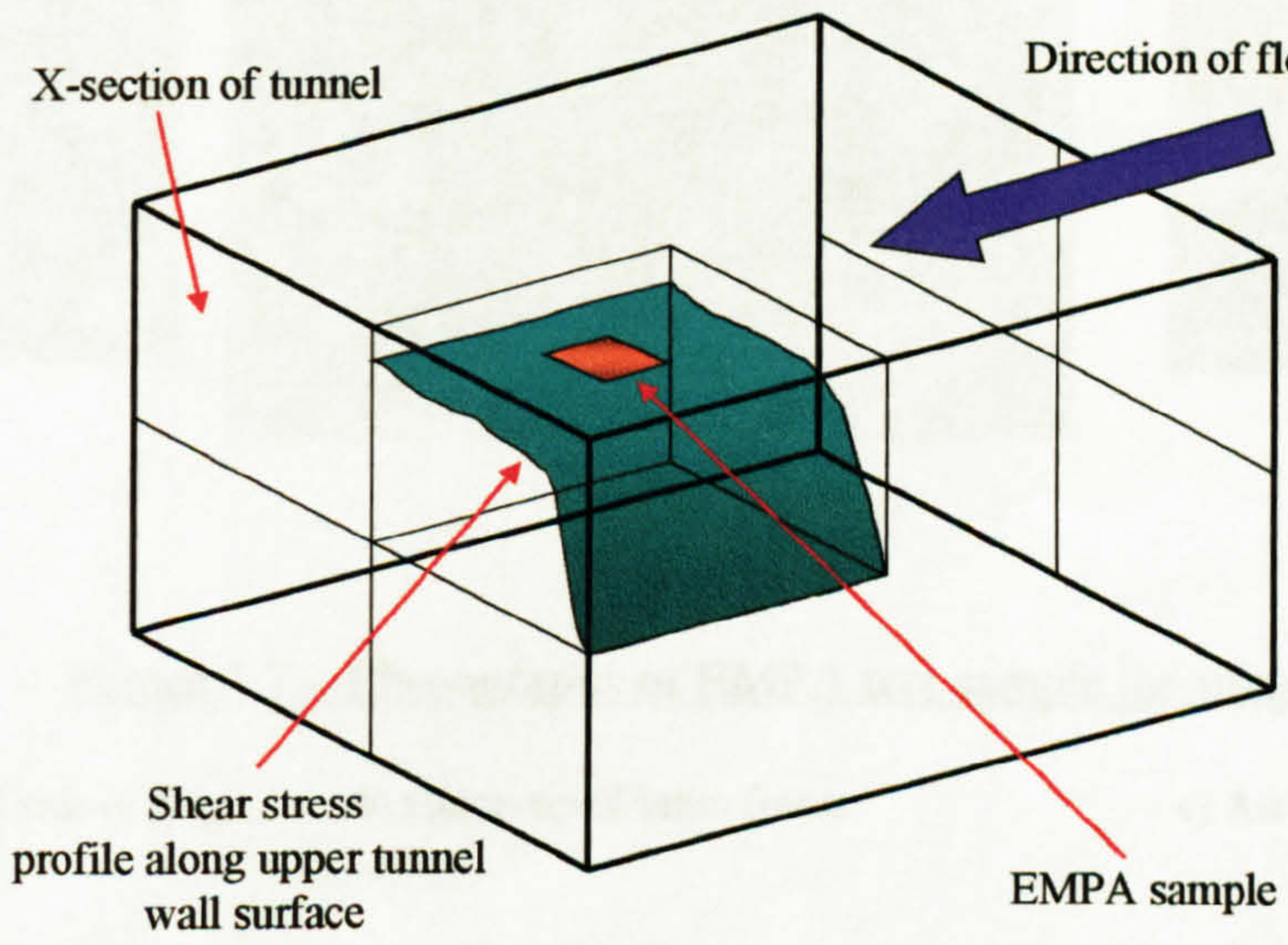

Figure 3.6 – Mapping the shear stress

In order to provide a reliable means of holding the EMPA samples flat and tangential to the water flow a special jig or plug was designed and built to fit in a new tunnel roof. The position of the jig or plug was established according to the shear stress profile (Fig. 3.5B) i.e. the plug was located where stress profile was as flat as possible (10–110mm w.r.t. tunnel C.L.). The size of the plug was dictated by the minimum recommended size (90 x 90mm) of EMPA sample that was to be used in step 3.

The plug was held in place by a series of bolts that also provided adequate regulation of the plug penetration depth in the flow through the compression of the plug seal. The plug design was also an easy method of test sample mounting and inspection.

The test (EMPA) sample was fixed (pressed not glued) to the plug by means of a brass frame that was locked in place by means of grub screws. To minimise flow disturbance the plug was mounted so that the test sample was always just protruding (≈0.2mm) into the boundary layer of the fluid flow. The jig or plug is shown in the next two figures.

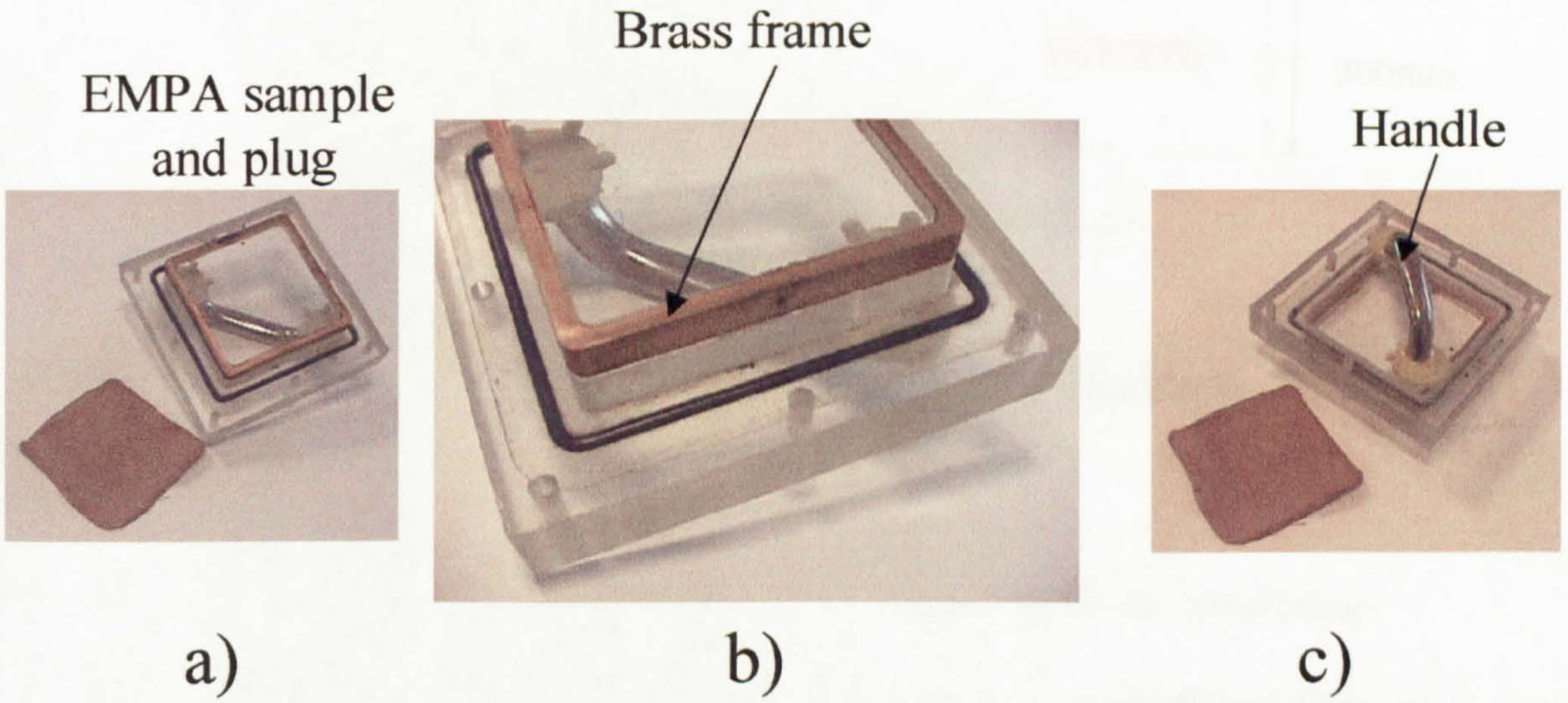

Figure 3.7 – Photographs of EMPA test sample jig–plug

a) Water (lower) side of plug b) Close–up of brass frame c) Air (upper) side of plug

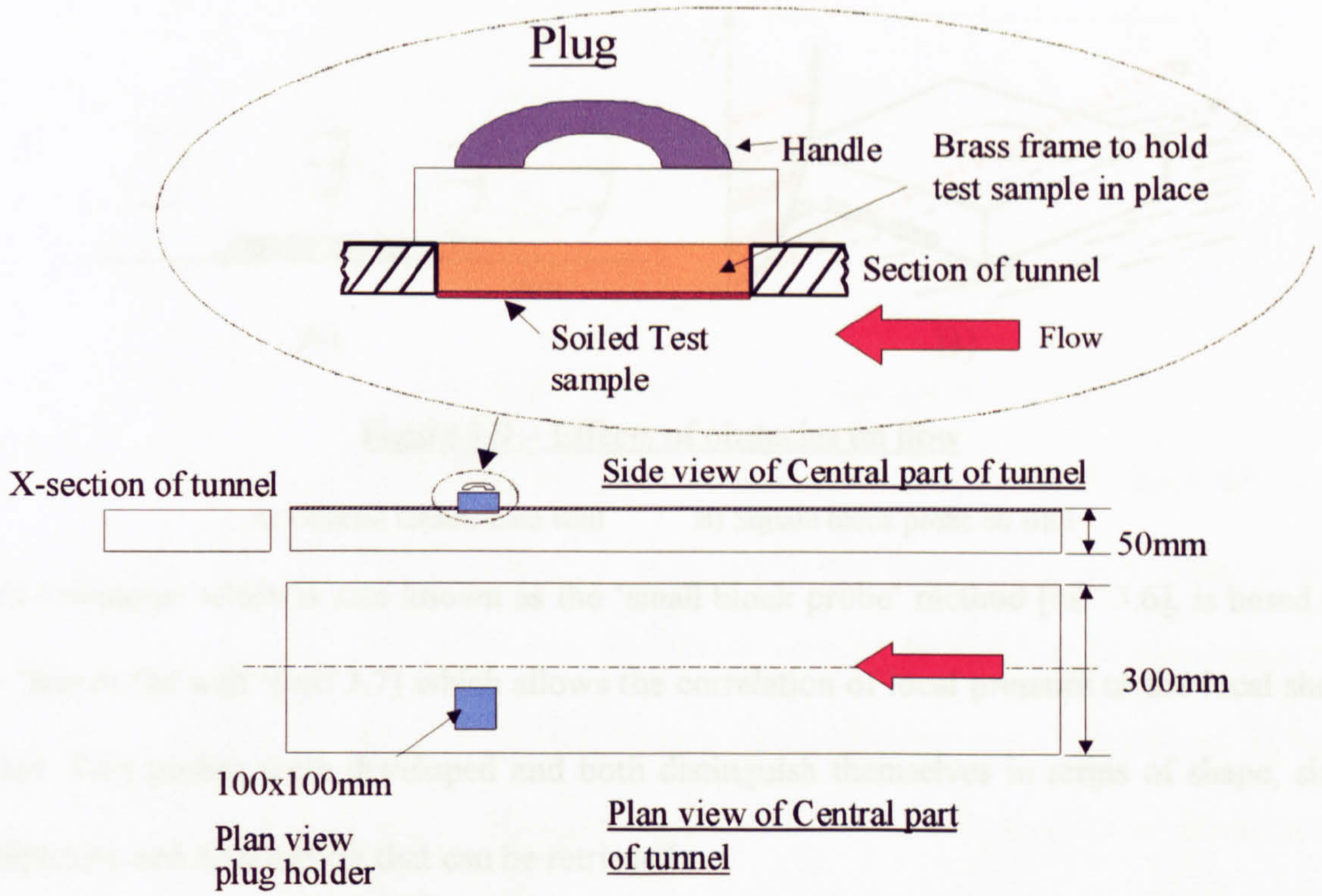

Figure 3.8 – EMPA test sample plug mounting details

Shear Stress Probes

The shear stress probes were designed to reach three main objectives, these being:

- Develop a technique for the measurement of shear stress magnitude and direction in water flows while minimising flow disturbance.
- Develop an accurate and economical method to produce the right shape and size of probe
- Develop an accurate and reliable method for the bonding of the probes to the tunnel wall

The basic probe design concept consisted of introducing a small obstruction in the flow so that a pressure differential could be measured across the obstacle.

This is illustrated next together with the velocity gradient starting from the wall:

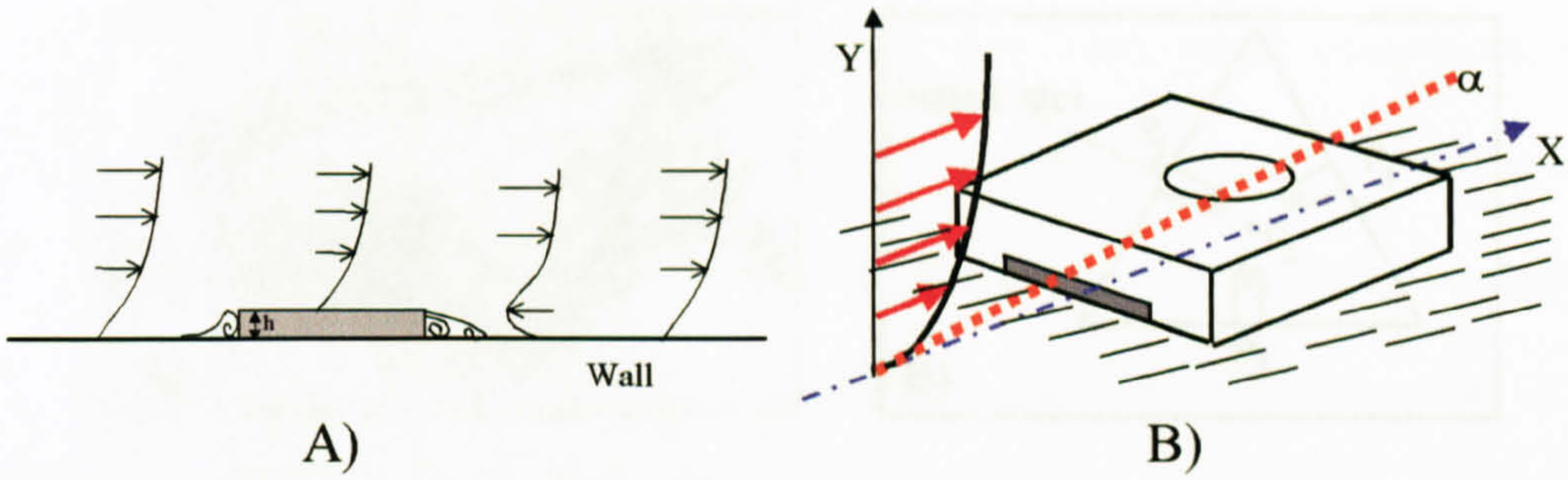

Figure 3.9 – Effects of obstacles on flow

A) General Obstacle on wall B) Square block probe on wall

This technique, which is also known as the 'small block probe' method [ref. 3.6], is based on the 'law of the wall' [ref. 3.7] which allows the correlation of local pressure to the local shear stress. Two probes were developed and both distinguish themselves in terms of shape, size, complexity and information that can be retrieved.

- SQUARE PROBE: This probe measured 9mmx9mmx0.35mm and was equipped with one dynamic pressure tapping located on one side and one static pressure tapping located towards the rear. This probe provides only an indication of the magnitude of the shear stress only. It is shown above with a skew angle alpha and again in figure 3.15.
- TRIANGULAR PROBE: This probe was based on a equilateral triangle (7mm per side and 0.35mm in height) and was equipped with one dynamic pressure tapping (1.6mm wide) for each of the three sides and one static pressure tapping located at the centre. This probe provides both an indication of the shear stress magnitude and direction and is shown in figure 3.14.

The square probe was a new design and thus no previous work had been done.

The concept of the triangular shaped probe was based on a design originally conceived by Dexter and developed further by Gaudet et al [refs. 3.8 and 9]. In both cases the scope was to develop a yawmeter for wing surfaces in air-flows. Both these probes are shown next:

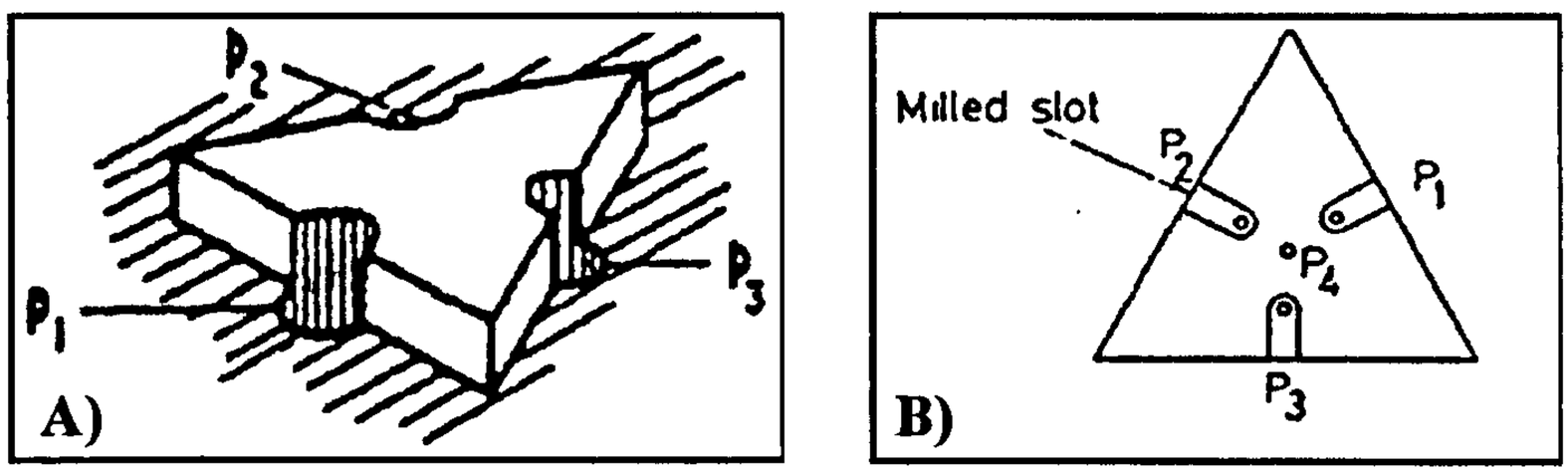

Figure 3.10 – A) Dexter probe B) Gaudet et al. probe

As can be seen in the above designs the dynamic pressure tappings (one for each side of the equilateral triangle) were not shielded or covered and probe construction was achieved using precision but expensive material removal processes such as NC milling or electro–erosion. They were also designed for air-flows and were at least twice the size of our probes. In terms of originality both our probe designs (see figs. 3.14 and 3.15) included substantially six features, improvements and/or modifications, these being:

a) Probe design and application was for water flows. In particular a steady state, fully developed 2D flow, was assumed in the tunnel. This assumption was later verified with the Preston tube and is illustrated later in the dissertation.

b) Both probes were based on a layer structure, which allowed the variation of probe height simply by adding layers or increasing layer height. In our case the probe was fitted with one lower and one upper layer.

c) The layers were obtained by punching directly from thin brass plate measuring up to approx. 0.4mm. The shape of the punch was dictated by the shape and size of the probe as well as the position and size of tappings. Punching the probe provided a very accurate (but economical) means of producing each layer and also an additional method of changing probe height simply by adopting thicker (or thinner) brass sheet for each layer (i.e. 0.1 or 0.15mm) before punching. Both probe and adhesive tape were punched together to provide a very accurate bonded laminar.

d) Probe bonding was achieved by using precision twin sided, water compatible, adhesive tape with a thickness of 50microns (3M Y9460). Hence probe bonding was achieved simply by peeling off the protective layer of the tape and positioning it on the wall surface. Previous techniques were based on liquid adhesives that are difficult to apply accurately and require longer (typ. 24hours) curing time.

e) The probes upper layer provided a means of covering the lower layer in order to obtain a fluid trap for the dynamic pressure. The same feature also provided partial protection for each dynamic pressure tapping. Previous designs (see Fig. 3.10) did not have this feature.

f) Probe design involved CFD simulation [ref. 3.10] to predict behaviour and included modelling of the water tunnel test section (see Fig. 3.11B) where the probes were later tested and calibrated. The scope of the CFD activity was also to uncover re-circulation and turbulence problems around the height tips and edges of the probe (see Fig. 3.11A) and any uneven pressure across the probe mouth.

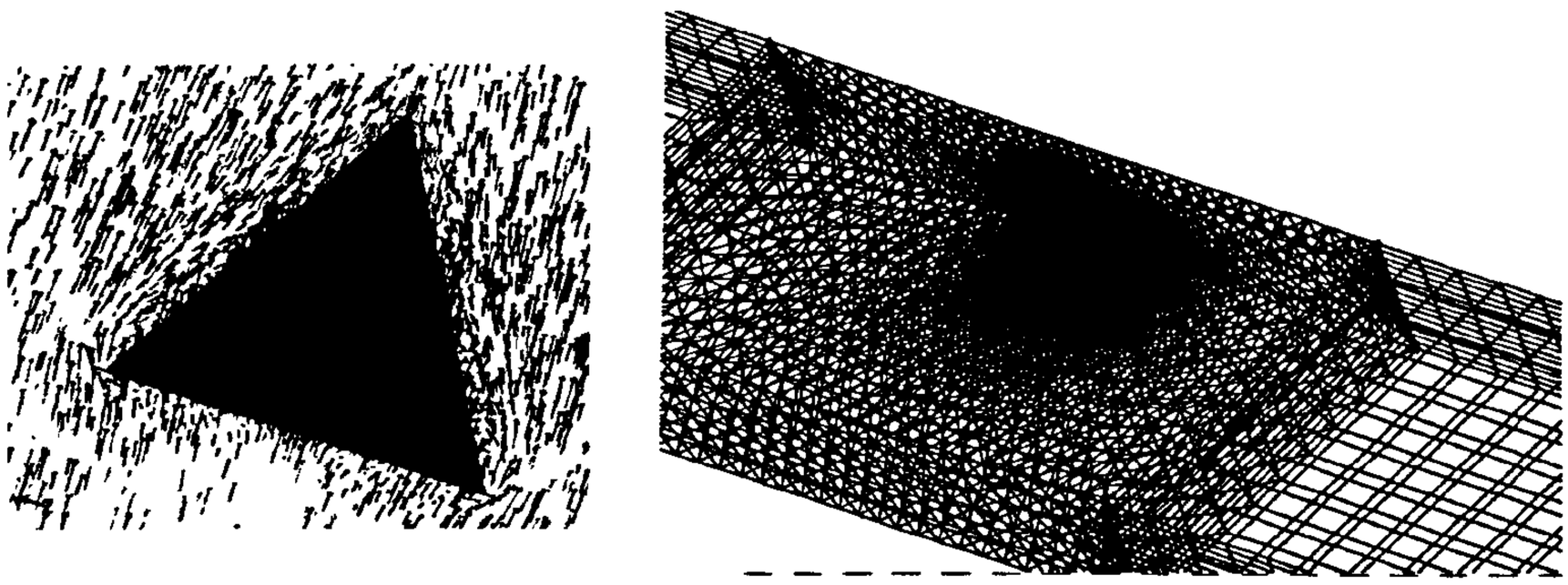

A) B)

Figure 3.11 – Velocity Vectors and Mesh around Triangular Probe

Both probe designs were designed so that the dynamic pressure tappings (≈0.9mm Ø) were placed at the rear of the probe 'mouth' with a capture height of 0.2mm (=0.15+0.05mm). This was determined to suit both the hydrodynamic conditions (Re, U and τ) and the EMPA sample roughness (see Fig. 3.13). The layer structure of the probes is shown next.

Example of triangular probe layer structure

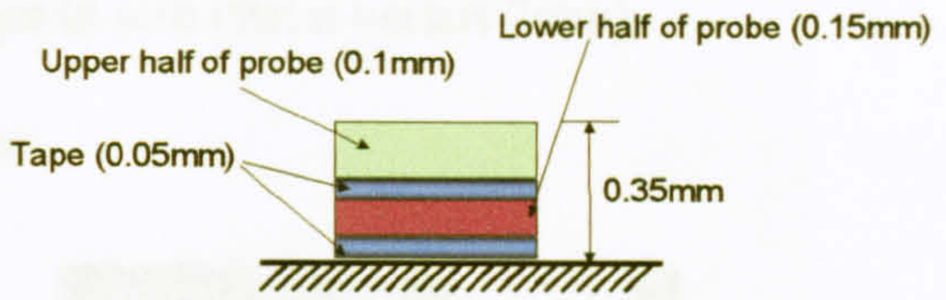

Cross-section for both probes

Figure 3.12 – Layer structure of probe

The tappings of the triangular shaped probe were only partially covered, i.e. half of each tapping protruded out of the probe, just as for the Dexter design in Fig. 3.10a. Although having now acquired punch design experience it is likely that the tappings could be incorporated under the upper layer (see square probe).

The diameter of the tappings was sized (0.9mm) to suit the tubing that was used to connect the probe to the pressure transducer. The tubing was realised with small medical needles to which silicone tubing was connected and lead to the transducer as shown below:

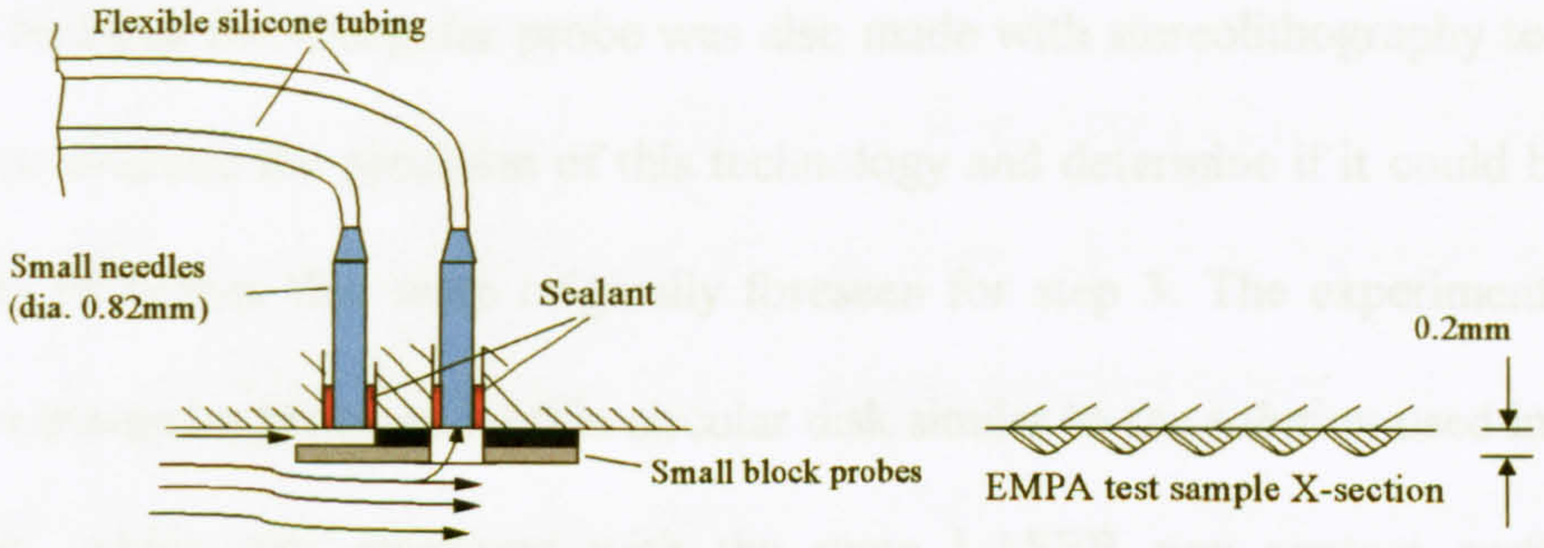

Figure 3.13 – Probe connections

A picture of the triangular shaped probe and relative assembly is shown next:

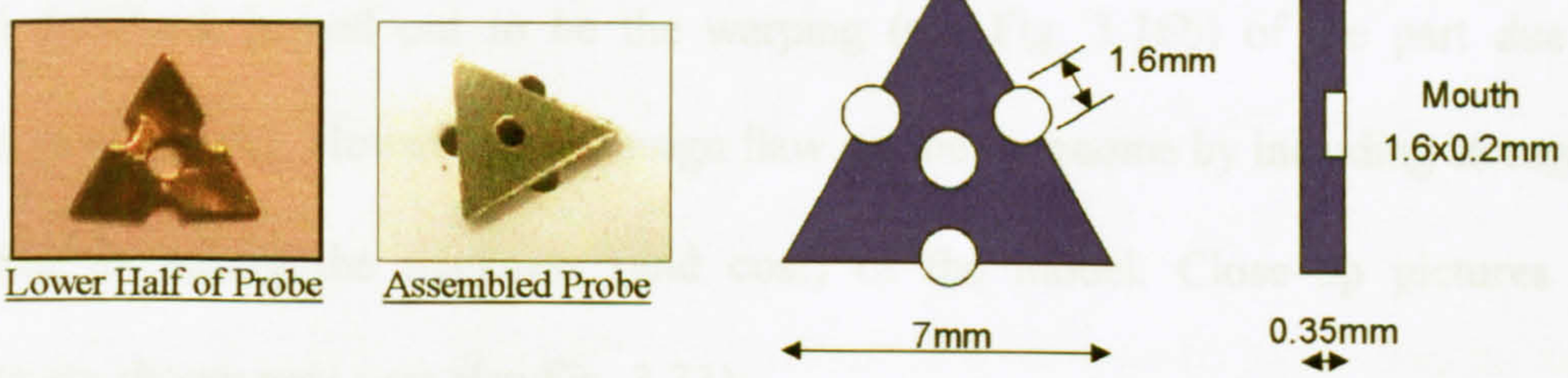

Figure 3.14 – Triangular shaped probe details

The square shaped probe had a very similar assembly except that the dynamic pressure tapping was entirely covered. It was also slightly larger in size (9mm versus 7mm).

Assembly of the square probe is shown below:

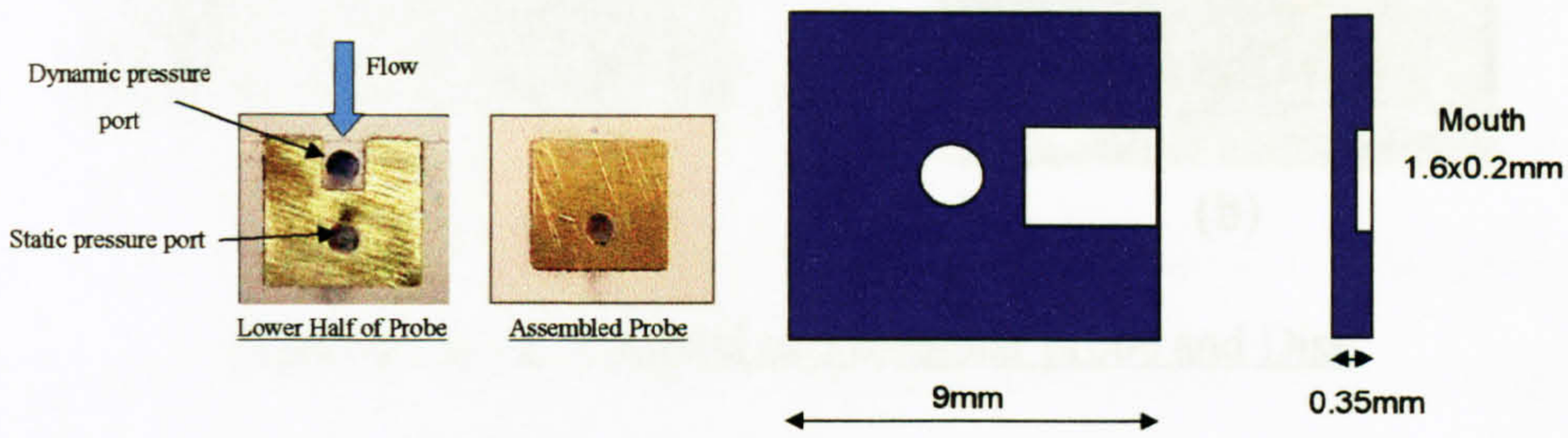

Figure 3.15 – Square shaped probe details

The punch used to produce the probes (both types) was designed with Pro–E and machined by electro–chemical erosion to obtain the necessary accuracy. A series (four) of punches was realised (cost~500US$), one for each probe and one for each probe half or layer. Punch design was iterated several times not only because of difficulties in punching the brass plate without burrs or lips edges but to overcome the complexity of extracting the punched parts.

An attempt at realising the triangular probe was also made with stereolithography technology. The idea was to evaluate the precision of this technology and determine if it could be used to realise a matrix of probes that were originally foreseen for step 3. The experimented model was based on a triangular probe and a thin circular disk similar to the solution used in step 2.

The end result, which was measured with the same LASER non–contact surface finish instrument used to evaluate EMPA roughness (see chapter 6), was surprisingly accurate, just <15% of the total probe height and even less (<5%) for the area (see Fig. 3.16a).

The real drawback turned out to be the warping (see Fig. 3.16b) of the part due to the thickness of the model. However, this design flaw can be overcome by including strengthening ribs and/or increasing the thickness (and cost) of the model. Close–up pictures of this prototype are shown next (see also Fig. 3.33):

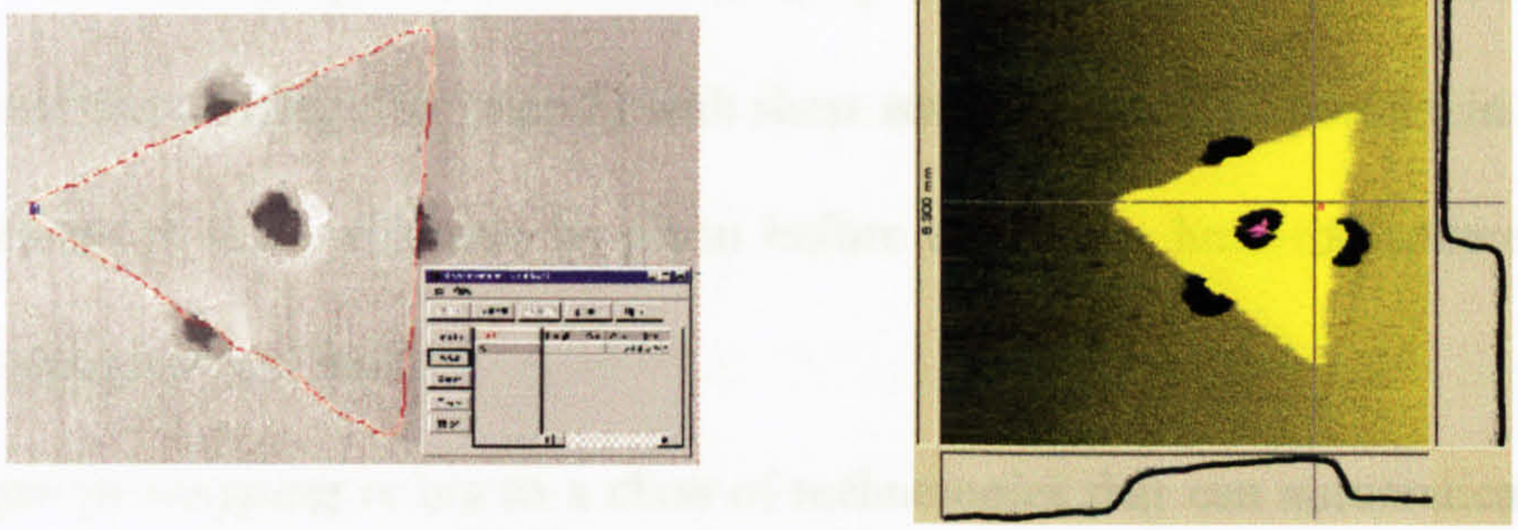

(a) (b)

Figure 3.16 – R.P. model of Triangular probe and Disk

Model Creation and Rapid Prototyping Technologies

In addition to the water tunnel the research also involved the conceptualisation, design and building of other prototypes, especially the weave and sphere models [ref. 3.11]. Both models were made possible thanks to the use of advanced rapid prototyping [ref. 3.12] technologies. Since there was a certain learning curve involved, and this part of the work may be beneficial for future research and researchers, these technologies will now be illustrated.

Overview of Rapid Prototyping

Remarkably although rapid prototyping (R.P.) has been around for well over a decade it is still essentially only used in large industries where it has been applied to the initial part of the product ideation process e.g. preliminary design and small pilot production.

Research activity applications of R.P., like those of the MT project, are apparently thin on the ground even though there is no reason why R.P. cannot be used to build any 3D model.

In fact the weave model to be discussed was made possible thanks to the use of 'Solid Ground Curing', one of six rapid prototyping technologies available today. Moreover, in this specific case the only other alternative would have been traditional machining, with all the known implications of costs, time and limitations.

Another rapid prototyping technology known as 'Stereolithography' was used to build the sphere. Again the only other alternative would have been traditional machining with the same

drawbacks. A further example of the stereolithography technology will be given regarding an attempt to build the rotating disk (step 2) with shear stress probes incorporated in the model.

A brief overview of R.P. will now be given before explaining how the sphere and weave models were designed and built.

The term *rapid prototyping* refers to a class of technologies that can automatically construct physical models from Computer–Aided Design (CAD) data provided by CAD packages such as Pro–E. Rapid prototyping machines are "three dimensional printers" that allow designers to quickly create tangible prototypes of their designs, rather than just two–dimensional pictures. Such models are mainly used to communicate ideas and (increasingly) for product development.

RP techniques can also be used to make tooling, referred to as *rapid tooling* [ref. 3.13] and even *rapid manufacturing* [ref. 3.14]. For small production runs and complicated objects, rapid prototyping is often the best manufacturing process available. Of course, "rapid" is a relative term and most prototypes require from three to seventy–two hours to build, depending on the size and complexity of the object. For example the weave model was made in 12 hours, the sphere in 4 hours and the rotating disk in less than 2hours.

This may seem slow, but it is much faster than the weeks or months required to make a prototype by traditional means i.e. such as machining, a notoriously slow material removal process. Moreover in the case of the weave model this would have meant machining and hand finishing each thread in two halves. Rapid Prototyping is often collectively referred to as *layered manufacturing* because the software that is used effectively "slices" the CAD model into a number of thin (~0.1 mm or less) layers, which are then built up one on top of the other. Rapid prototyping is therefore an "additive" process, combining layers of material e.g. paper, wax, or plastic to create a solid object.

In contrast, most machining processes (milling, drilling, grinding, etc.) are "subtractive" or removal processes that remove material from a solid block. RP's additive nature allows it to create objects with complicated internal features that cannot be manufactured by other means. A very good example is the piping or routing inside each thread of the weave model that was necessary to read the block probe pressure on the thread surface.

Rapid prototyping is still being perfected but a general rule–of–the–thumb for the total volume limit is $0.12m^3$ (a cube of approx. 600mm) or less, depending on the R.P. machine. For larger models it is customary to split the object into smaller parts and then bond them together later. The manufacturer or model maker is also very anxious to fill each run, henceforth it is customary to fit as many parts (models) as possible into the run. This is an area where the R.P. machines software plays an enormous role and shows just how skilled the operator is too. In fact the weave model threads were stacked and made in one single run.

Clearly a full run is also a wise way of keeping costs as low as possible (the weave model cost ~2500US$), although delivery times may vary for this reason.

Another area of notable effort is the rapid prototyping of metal models. For the time being this is proving difficult to achieve, especially on larger models, because the sintered metals (and machines) needed are still being perfected. However, this scenario is changing [ref. 3.15] even though conventional manufacturing techniques are usually more economical when the model has to be metal.

At least six different rapid prototyping techniques are commercially available today, each one with unique strengths and drawbacks. All these techniques follow a basic process that will be outlined and explained.

The Basic Process

All of today's rapid prototyping techniques employ the same basic five (or six) step process [ref. 3.16]. The steps are:

1. Create a CAD model of the design (e.g. weave, sphere etc.).
2. Convert the CAD model to STL format.
3. Slice the STL file into thin cross–sectional layers.
4. Construct the model one layer on top of another.
5. Clean and finish the model.
6. Proceed to moulding e.g. vacuum casting, as required.

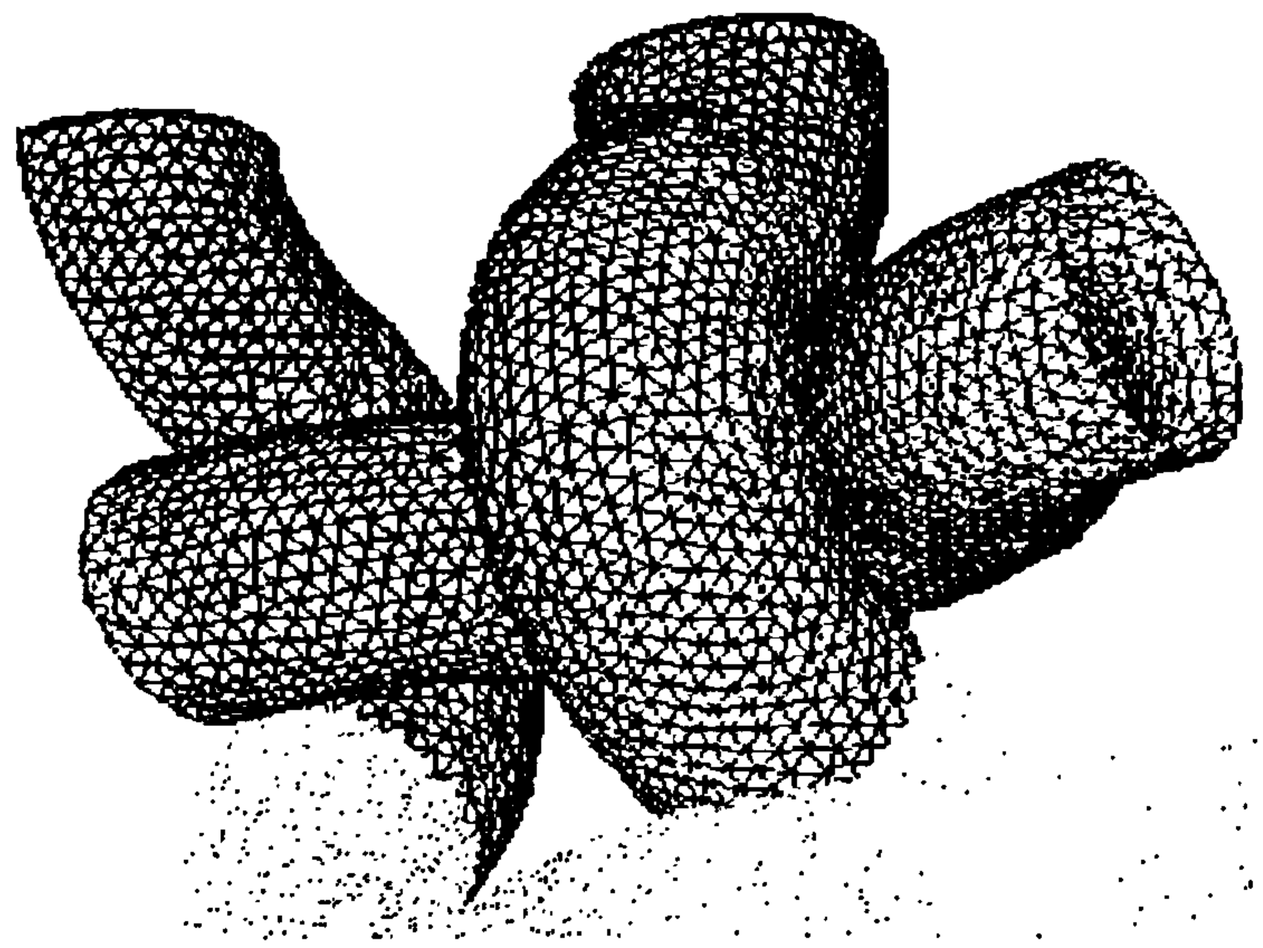

Figure 3.17 – Part of the Weave Model in FLUENT

CAD packages use a number of different algorithms to represent solid objects so as to establish consistency, the STL format (named after stereolithography, the first R.P. technique) has been adopted as the standard protocol.

The second step, therefore, is to convert the CAD file into STL format. This format represents a three–dimensional surface as an assembly of planar triangles, "like the facets of a cut diamond" (see Fig. 3.17). The file contains the coordinates of the vertices and the direction of the outward normal of each triangle. Because STL files use planar elements, they cannot

represent curved surfaces exactly. Increasing the number of triangles improves the approximation, but at the cost of bigger file size. Large, complicated files require more time to pre–process and build, so the designer must balance accuracy with manageablility to produce a useful STL file. Both the weave and sphere models were built to the highest accuracy since the best surface finish was needed to position the block probes.

In the third step, a pre–processing program prepares the STL file to be built. Several programs are available, and most allow the user to adjust the size, location and orientation of the model. Build orientation is important for several reasons. First, properties of rapid prototypes vary from one coordinate direction to another. For example, prototypes are usually weaker and less accurate in the Z (vertical) direction than in the X–Y plane. In addition, part orientation partially determines the amount of time required to build the model. Placing the shortest dimension in the Z direction reduces the number of layers, thereby shortening build time.

This is why the sphere was designed in two halves and the rotating disk was designed "thin". The pre–processing software slices the STL model into a number of layers (0.01-0.7mm thick), depending on the build technique. The program may also generate an auxiliary structure to support the model during the build. Supports are useful for delicate features such as overhangs, internal cavities, and thin–walled sections. Both the weave and sphere models did not require supports and slicing was typically <0.05mm.

The fourth step is the actual construction of the part: using one of six techniques RP machines that will be explained next, the part or model is built one layer at a time either from polymers (resins), paper, or powdered metal. Once completed the part is removed from the machine and the supports detached (simply snapped off). Some types of epoxy need to be fully cured before use, this is done in a curing chamber or box using an UV light source. In addition prototypes may also require minor cleaning and surface treatment such as sanding, sealing, and/or painting to improve the appearance and durability of the model.

Finally the sixth (optional) process is one of preparing a mould so that other prototypes may be generated. This reduces model costs and was indeed used for the sphere model that was subsequently replicated with vacuum casting techniques. This manner allows a certain degree in freedom for the selection of the final resin used in vacuum casting. In fact tests with the sphere were realised both with a soft rubber-like elastomer and a very rigid nylon based resin to demonstrate this flexibility.

Stereolithography

Patented in 1986, stereolithography started the rapid prototyping revolution [ref. 3.18]. The technique builds 3D models from liquid photosensitive polymers that solidify when exposed to ultraviolet light. As shown below the model is built upon a platform situated just below the surface in a vat of liquid epoxy or acrylic resin. A low–power highly focused UV laser traces out the first layer, solidifying the model's cross section while leaving excess areas liquid. Next, an elevator incrementally lowers the platform into the liquid polymer. How precise this translation is clearly determines the accuracy of the process, hence part. A sweeper re–coats the solidified layer with liquid, and the laser traces the second layer on top of the first. This process is repeated until the model or prototype is complete. Afterwards, the solid part is removed from the vat and rinsed clean of excess liquid. In the case of the weave model a further process was required that consisted of removing the semi–liquid epoxy left in each tubing. This was done by using a flexible steel drill–bit like tool prepared especially for this purpose.

After building the prototype supports are broken off and the model is then placed in an ultraviolet oven for complete curing.

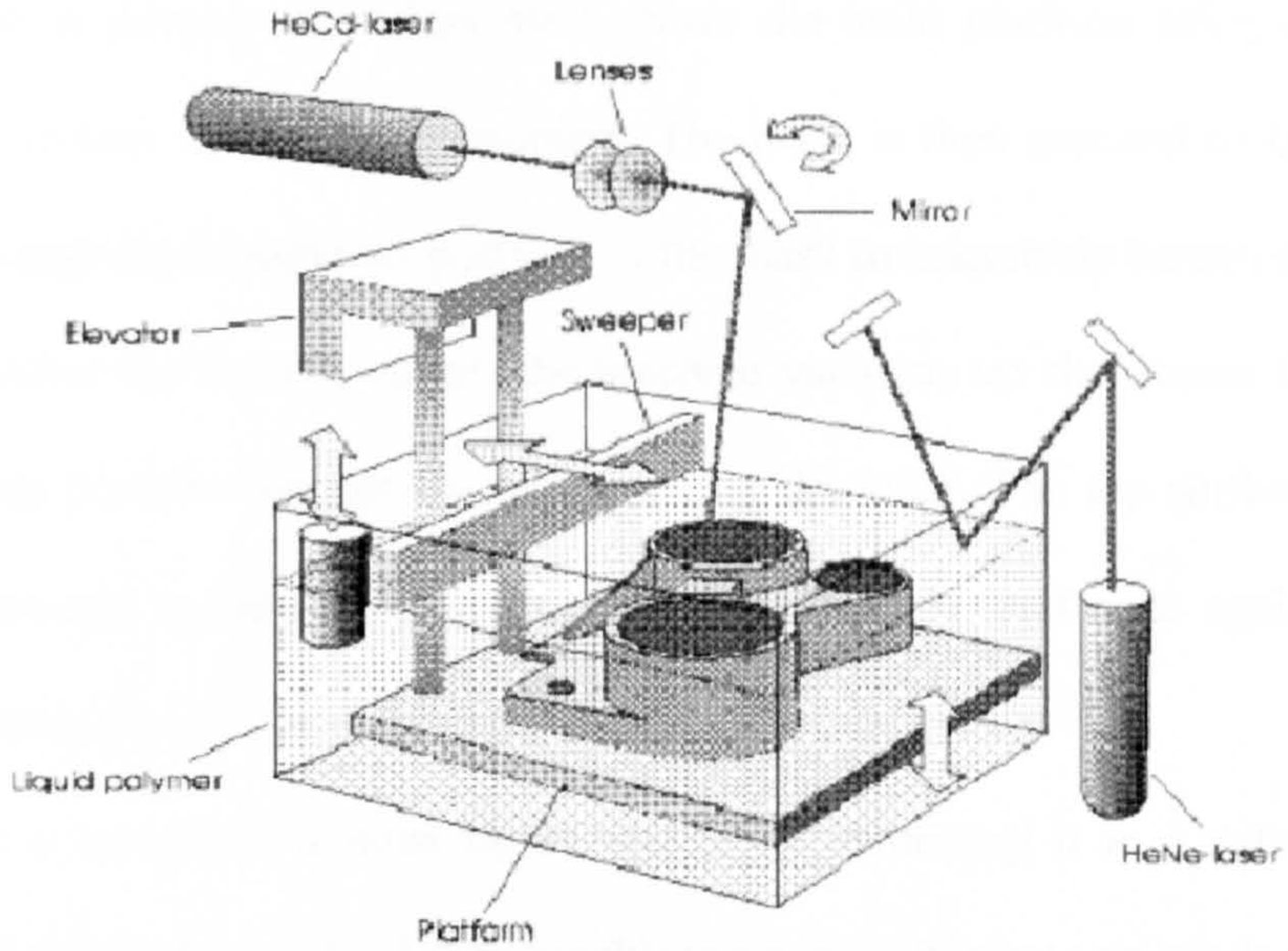

Figure 3.18 – Stereolithography

Stereolithography Apparatus (SLA) machines have been made since 1988 by 3D Systems [ref. 3.19] and it was one of their machines that was used to make the sphere.

This was done by splitting the sphere into two hemispheres to reduce prototyping time. They were then used to make two separate silicone moulds from which all sphere prototypes were made under vacuum. Several different resins, offering different structural properties, were experimented during the vacuum casting process but the final spheres were made of Nylon based resin as this offered the best compromise in terms strength and mass.

As mentioned stereolithography was the first R.P. technique, and is regarded as a benchmark by which other technologies are judged. These will now be briefly discussed:

Solid Ground Curing

Developed by Cubital [ref. 3.20], solid ground curing (SGC) is somewhat similar to stereolithography (SLA) in that both use ultraviolet light to selectively harden photosensitive polymers. Unlike SLA, SGC cures an entire layer at a time. Figure 3.19 depicts solid ground curing, which is also known as the solider process. First, photosensitive resin is sprayed on the build platform. Next, the machine develops a photomask (like a stencil) of the layer to be built.

This photomask is printed on a glass plate above the build platform using an electrostatic process similar to that found in photocopiers. The mask is then exposed to UV light, which only passes through the transparent portions of the mask to selectively harden the shape of the current layer. After the layer is cured, the machine vacuums up the excess liquid resin and sprays wax in its place to support the model during the build. The top surface is milled flat, and then the process repeats to build the next layer. Clearly, and once again, this layering process determines the accuracy of the model.

When the part is complete, it must be de–waxed by immersing it in a solvent bath. SGC machines are distributed by Cubital. The machines are quite big but can produce large models (up to 600x600mm).

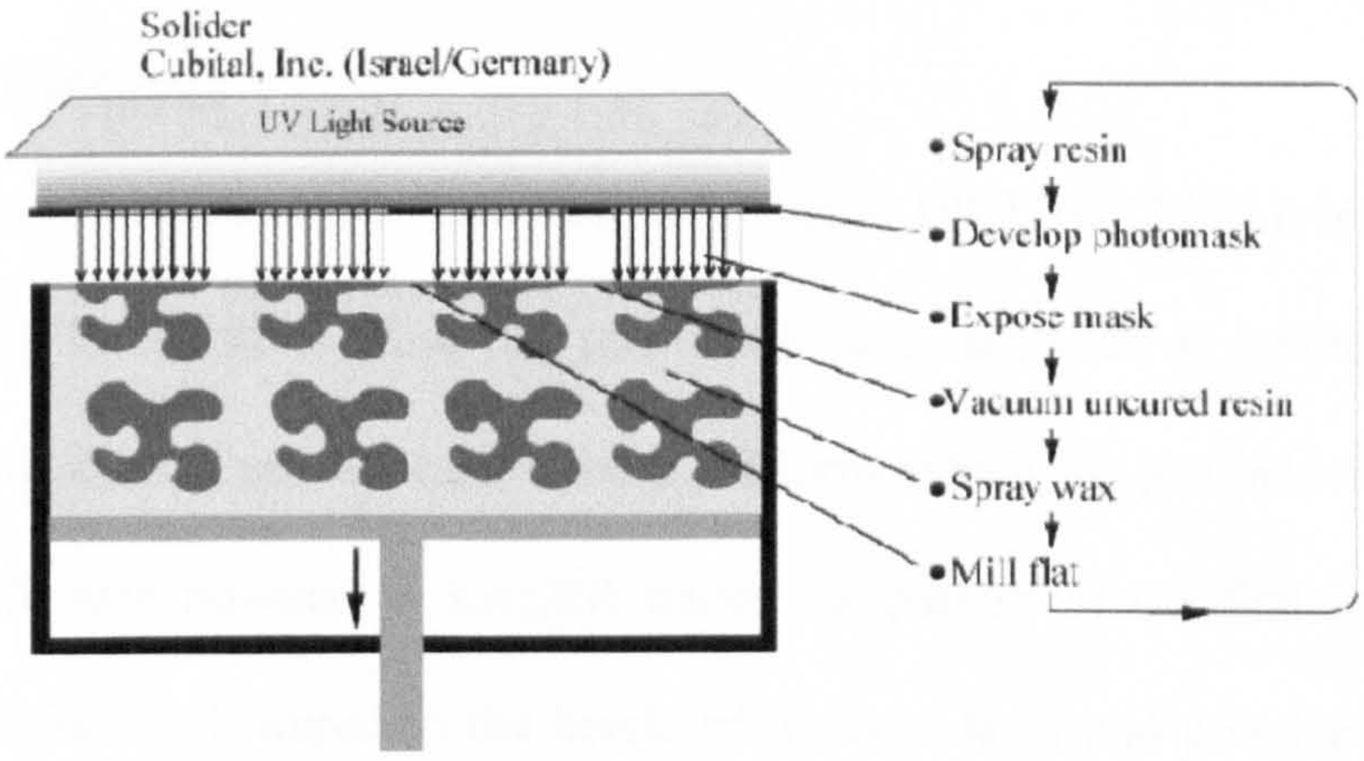

Figure 3.19 – Solid Ground Curing

Laminated Object Manufacturing (LOM)

In this technique, developed by Helisys of Torrance [ref. 3.21], layers of adhesive–coated sheet material are bonded together to form a prototype. The sheet material consists of paper laminated with heat–activated glue and rolled up on spools. This is a very cheap process but is only essentially a communications tool i.e. it is used to convey form, shape or real life image of part size such as in product focus groups.

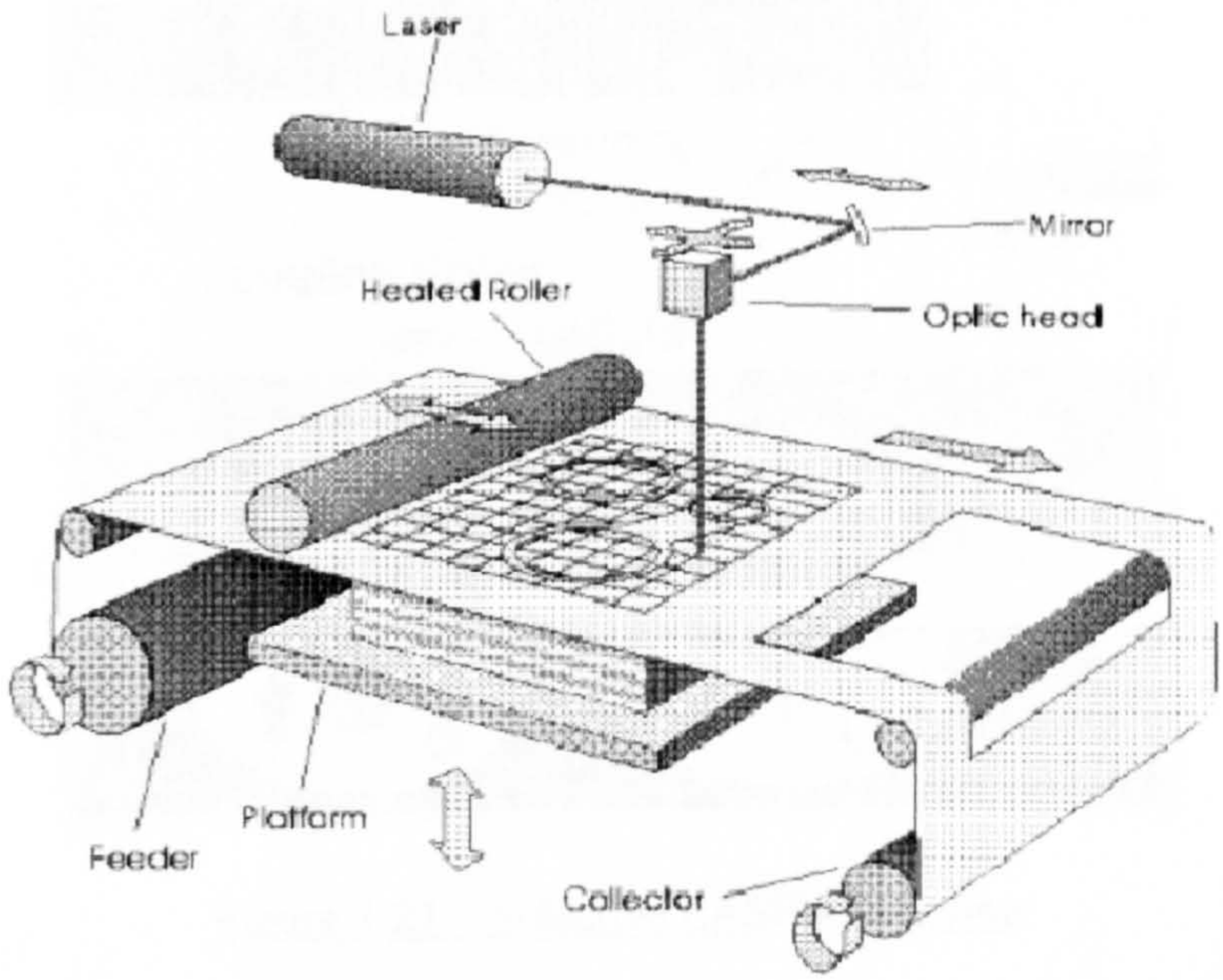

Figure 3.20 – Laminated Object Manufacturing

Selective Laser Sintering

Developed by Carl Deckard at the University of Texas in 1989 [ref. 3.22] it is a technique that uses a laser beam to selectively fuse dry powdered materials, such as nylon, elastomer, and metal, into a solid object. Parts are built upon a platform, which sits just below the surface in a bin of the heat–fusable powder. A LASER traces the pattern of the first layer, sintering it together. The platform is lowered to the height of the next layer and powder is reapplied and process continues until the part is complete. Excess powder in each layer helps to support the part during the build. SLS machines are produced by DTM of Austin, TX.

As a process it is considerably cleaner that stereolithography but heavy models are difficult to produce because their weight tends to compress the powder and thus effect both part precision and finish. In fact this is why parts like the weave model cannot be produced with this technology.

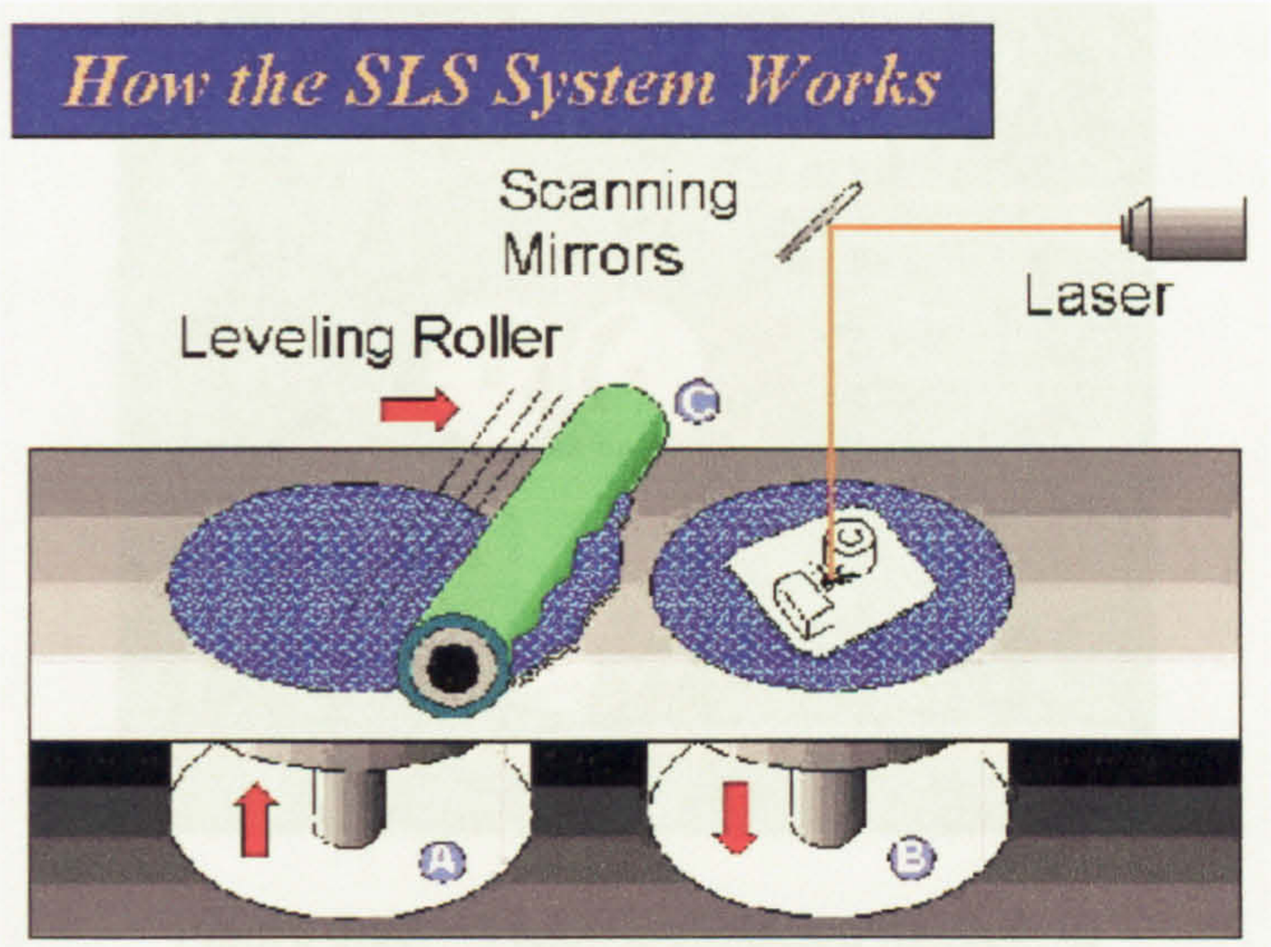

Figure 3.21 – Selective LASER Sintering

Fused Deposition Modelling

In this technique, filaments of heated thermoplastic are extruded from a tip that moves in the X–Y plane [ref. 3.23]. Like a baker decorating a cake, the controlled extrusion head deposits very thin beads of material onto the build platform to form the first layer. The platform is maintained at a lower temperature, so that the thermoplastic quickly hardens. After the platform lowers, the extrusion head deposits a second layer upon the first. Supports are built along the way, fastened to the part either with a second, weaker material or with a perforated junction. Stratasys (USA) makes a variety of FDM machines ranging from fast concept modellers to slower, high–precision machines. Materials include polyester, polypropylene, ABS, elastomers, and investment casting wax.

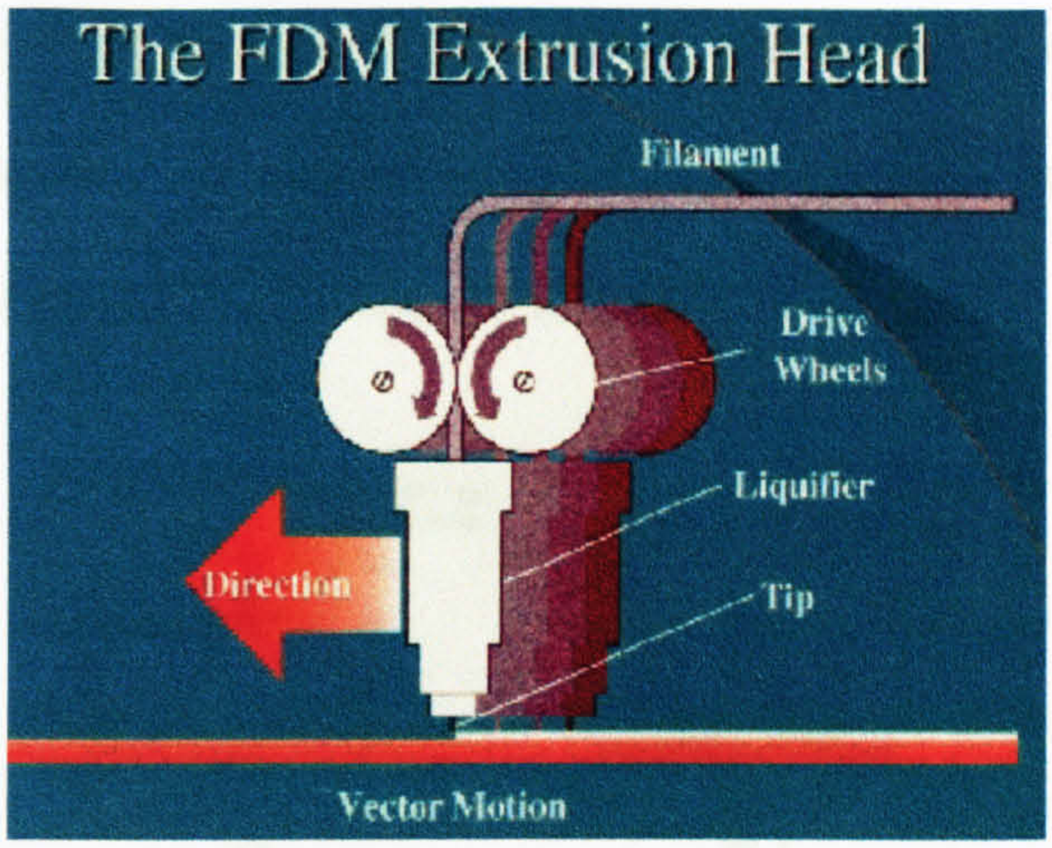

Figure 3.22 – Fused Deposition Modelling

Ink–Jet Printing

Unlike the above techniques, Ink–Jet Printing refers to an entire class of machines that employ ink–jet technology. The first was 3D Printing (3DP), developed at MIT and licensed to Soligen Corp. etc. [ref. 3.24]. As shown in figure 3.23a, parts are built upon a platform situated in a bin full of powder material. An ink–jet printing head selectively "prints" binder to fuse the powder together in the desired areas. Unbound powder remains to support the part. The platform is lowered, more powder added and levelled, and the process repeated. When finished, the green part is sintered and then removed from the unbound powder. Soligen uses 3DP to produce ceramic moulds and cores for investment casting, while Extrude Hone (USA) hopes to make powder metal tools and products. Sanders Prototype of Wilton, NH uses a different ink–jet technique in its Model Maker line of concept modellers. The machines use two ink–jets (see figure 3.23c). One dispenses low–melt thermoplastic to make the model, while the other prints wax to form supports. After each layer, a cutting tool mills the top surface to uniform height. This yields extremely good accuracy, allowing the machines to be used in the jewellery industry. 3D Systems has also developed an ink–jet based system. The Multi–Jet Modelling technique (figure 3.23d) uses an array of 96 separate print heads to

rapidly produce thermoplastic models. If the part is narrow enough, the print head can deposit an entire layer in one pass. Otherwise, the head makes several passes. Ballistic particle manufacturing, depicted in Fig. 3.23b, was developed by BPM Inc.

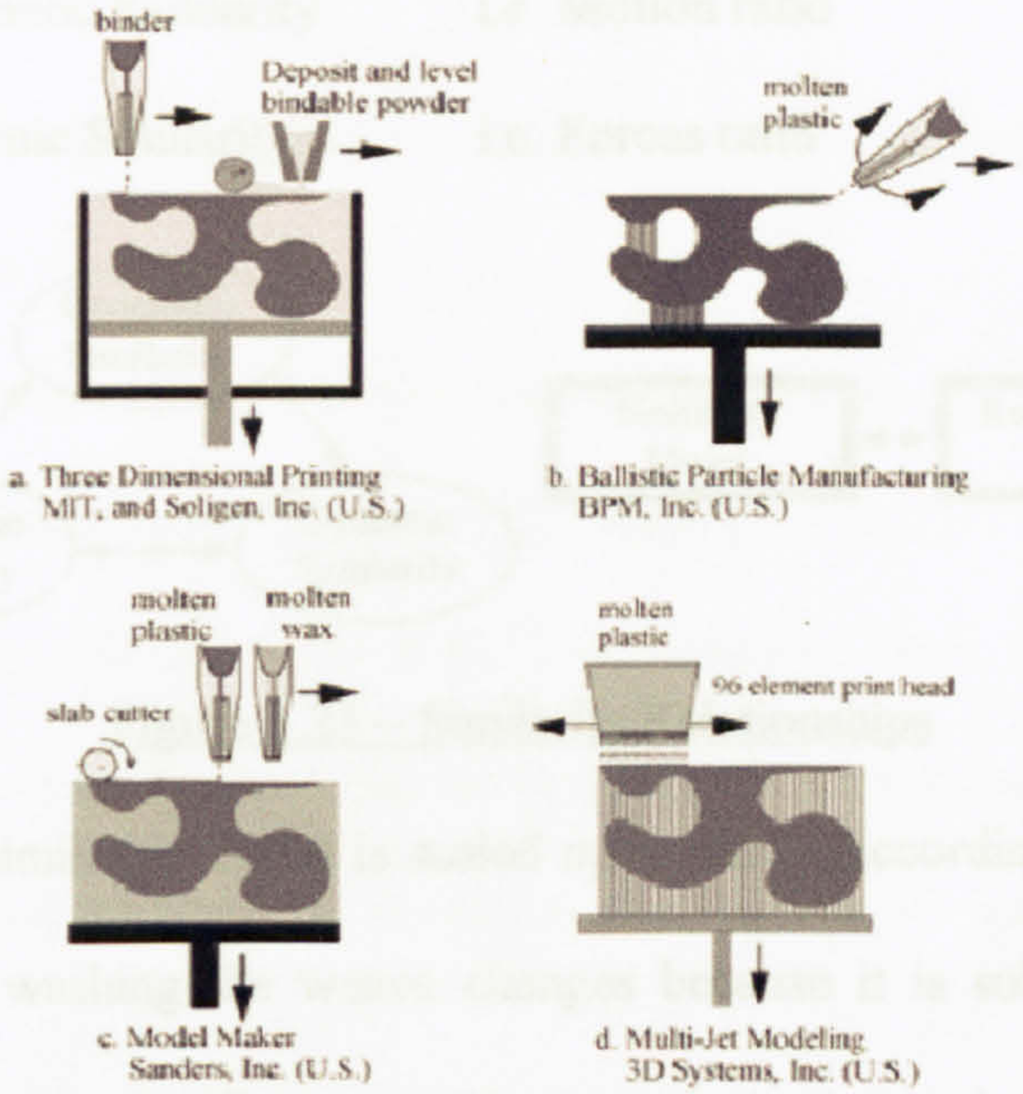

a. Three Dimensional Printing MIT, and Soligen, Inc. (U.S.)

b. Ballistic Particle Manufacturing BPM, Inc. (U.S.)

c. Model Maker Sanders, Inc. (U.S.)

d. Multi-Jet Modeling 3D Systems, Inc. (U.S.)

Figure 3.23 – Ink–Jet Printing

Weave model

The original scope of the weave model was to emulate a plain weave typical of most garments based on cotton fibre [ref. 3.25] and subject this model to hydrodynamic conditions to measure the surface shear stress directly in the tunnel. This is depicted below:

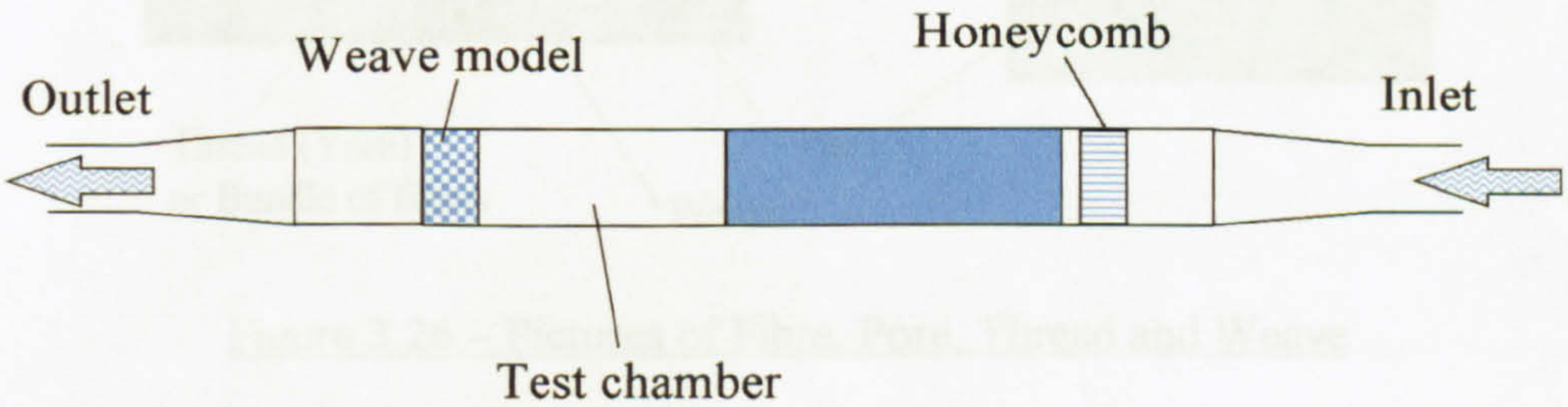

Figure 3.24 – Weave Model in Water Tunnel

Hence originally it was to be a natural extension of steps 1 and 2. However, to design the model implied that the weave could be correctly scaled i.e. the similarity model was reliably

scaled and truthful. However, to ensure this from a fluid dynamics point of view entails satisfying the 3 fundamental similarity principles:

1. Geometric Similarity i.e. Shape ratio
2. Kinematic Similarity i.e. Motion ratio
3. Dynamic Similarity i.e. Forces ratio

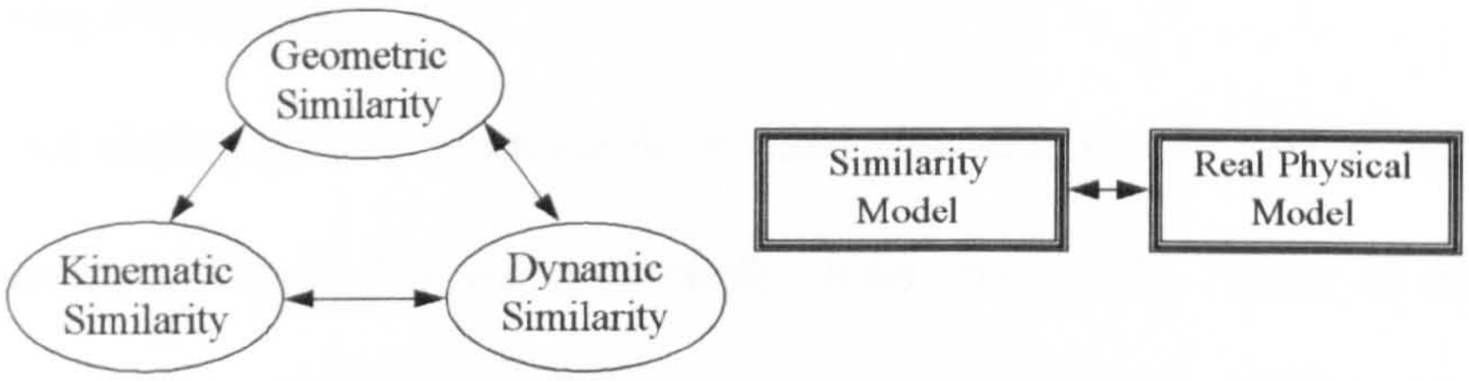

Figure 3.25 – Similarity Relationships

This denotes that the similarity model is scaled up or down according to shape, motion and forces. Clearly during washing the weave changes because it is subjected to many effects including swelling, warping, bending, stretching etc. thus, geometrically speaking, a decision about what scale level should be modelled i.e. pore, fibre, thread, weave and fabric, is compulsory. An example of this complexity is shown below for cotton cloth:

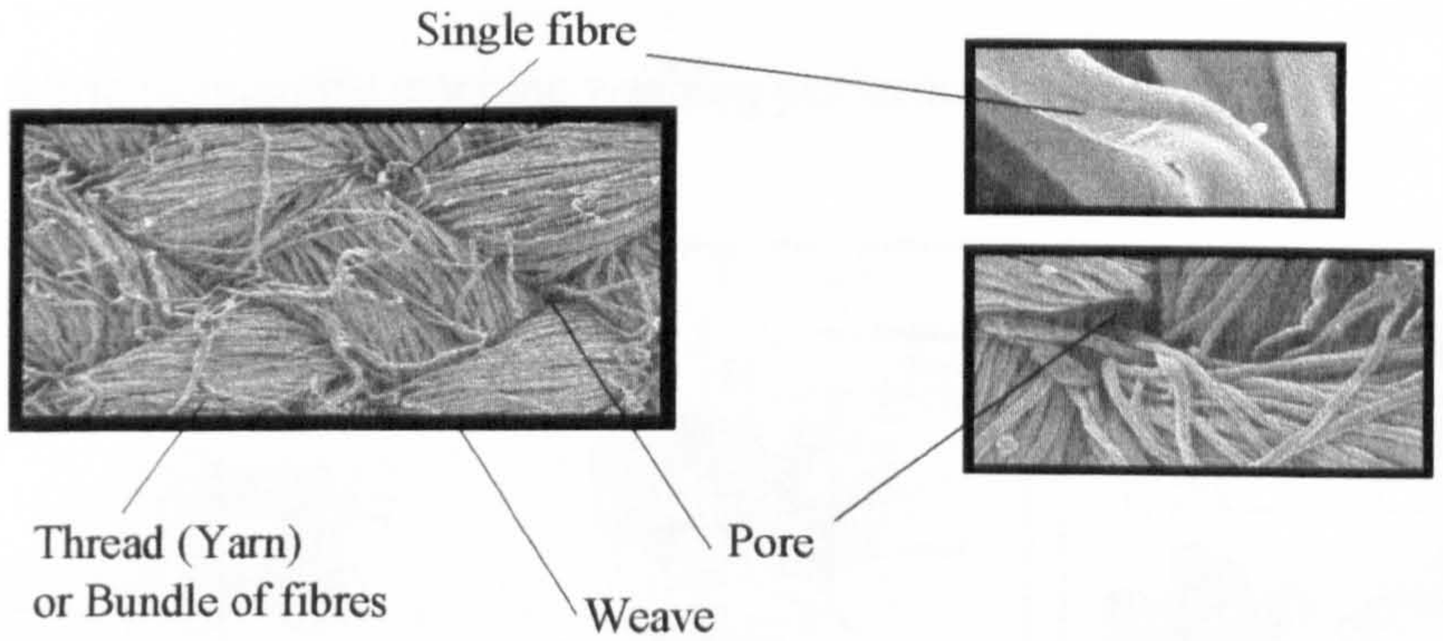

Figure 3.26 – Pictures of Fibre, Pore, Thread and Weave

Extensive literature regarding fibre and thread diameters, pore area etc. [ref. 3.26] is available but to simplify this scenario the thread diameter was used to design the weave model.

However, it was also found that while geometrical factors are reasonably easy to assess, weave motion and dynamics are extremely more complicated. Consequently achieving perfect similarity is unlikely without knowledge of wash load motion and weave dynamics during the washing process.

Indeed the scope of the fabric plug model and high speed filming in step 5 was to attempt to grasp this missing information.

Knowing perfect similarity was improbable implied that the weave model was built not to assess shear stress, although this was eventually done [ref. 3.27], rather to explore R.P. in complex 3D modelling and how this could be integrated with CFD packages such as FLUENT. As there are several weave patterns available including Twill, Satin and Linen (see Fig. 3.27) it was decided to base the model on the plain weave using cotton fibre for the following reasons:

- It offered the greatest complexity, and hence technical challenge.
- It is the most common weave found in garments and apparel.
- Above all, the plain weave is used both for the fabrication of the EMPA samples and the wash load fabric to quantify machine washing performance.

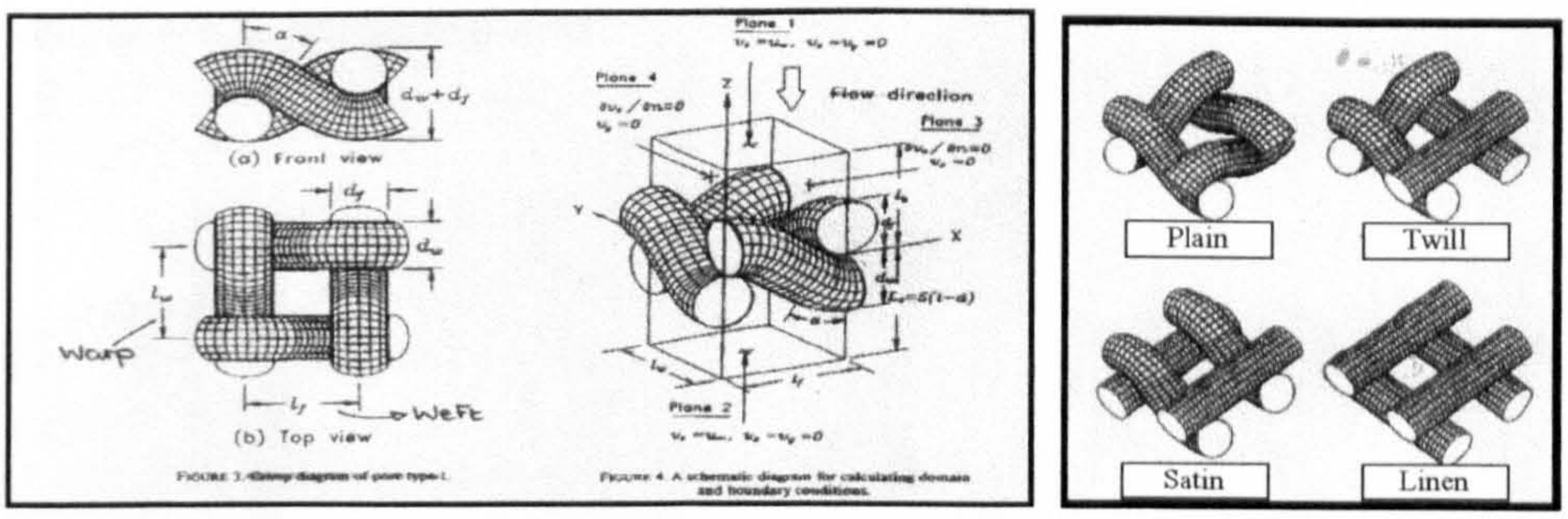

Figure 3.27 – Weave Classification

Consequently the dimensioning of the weave model was based on the average thread diameter (400–450microns) of the EMPA samples [ref. 3.28]. The final diameter of the thread model

was set at approx. 45mm as this was a convenient multiple of the real diameter and this was the largest possible diameter without mechanical interference between the threads. Clearly, the larger model the easier it would be to install the block probes and visualise the flow pattern, especially around the pore.

Next, the overall dimensions were aligned with the tunnel cross–section (300x300mm) which allowed us to install a total of six threads. Hence the weave model was composed of three horizontal or weft threads, and 3 vertical or warp threads (16 pores). These were assembled at right angles to the fluid flow as shown below:

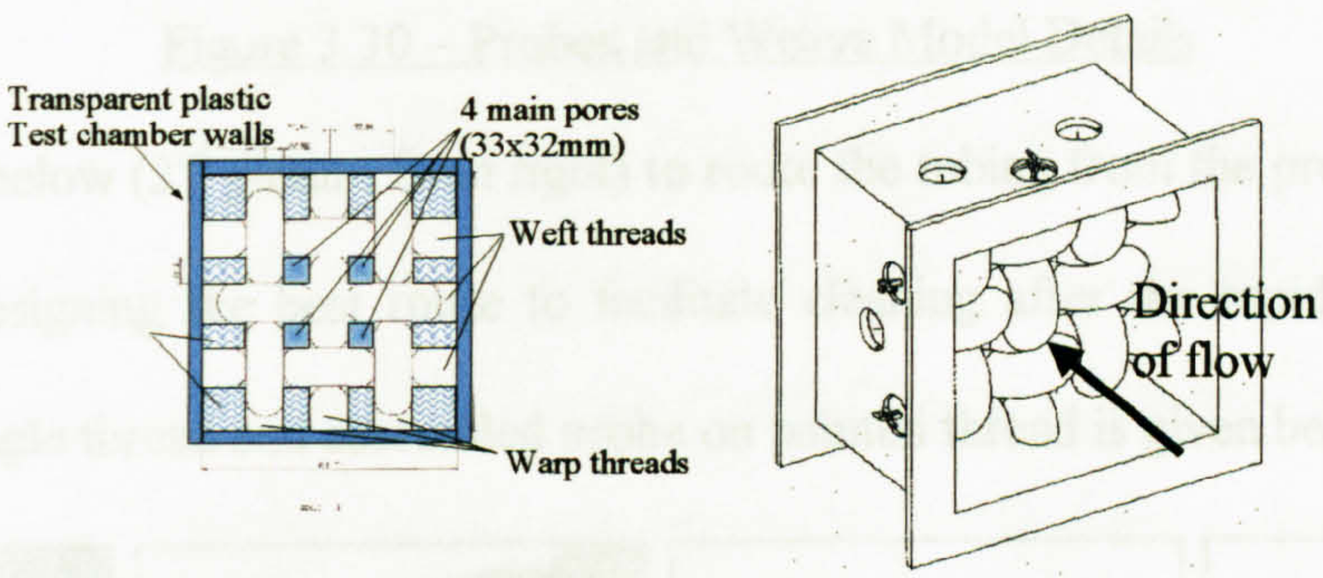

Figure 3.28 – Weave Model and Box

It was also decided to attempt to incorporate in each thread the necessary tubing (1mm dia.) to connect the block probes to outside the model box. The outside connections for each thread and relative tubing are hence shown next.

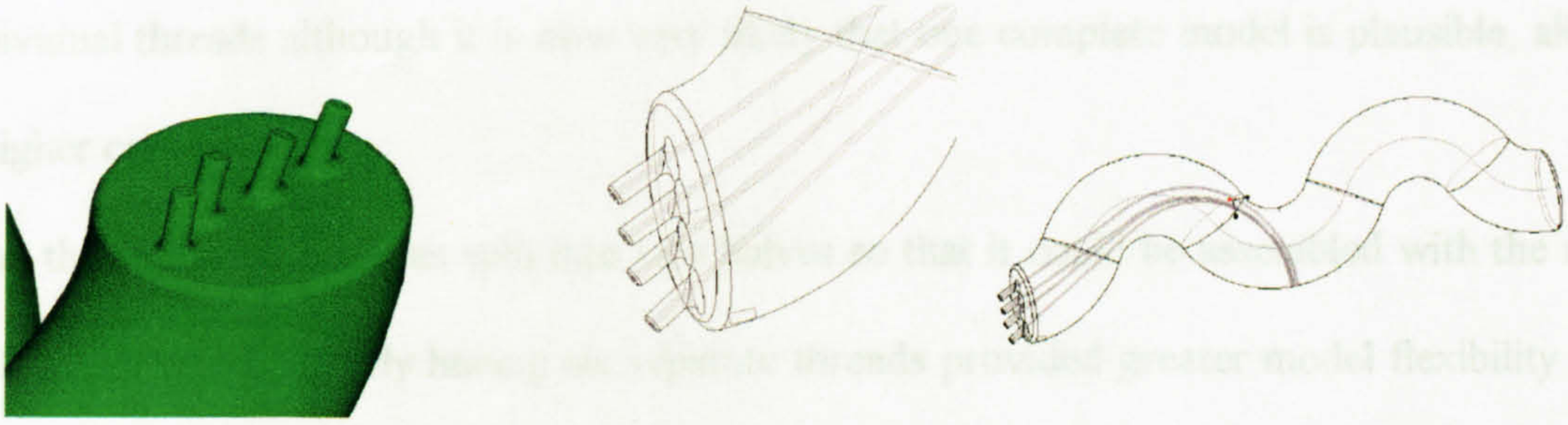

Figure 3.29 – External Connections and Internal Tube Routing

To measure weave model surface stress 9 block probes were fitted, that required a total of 36 individual surface pressure tappings and tubings. This is shown in the central part of the next figure.

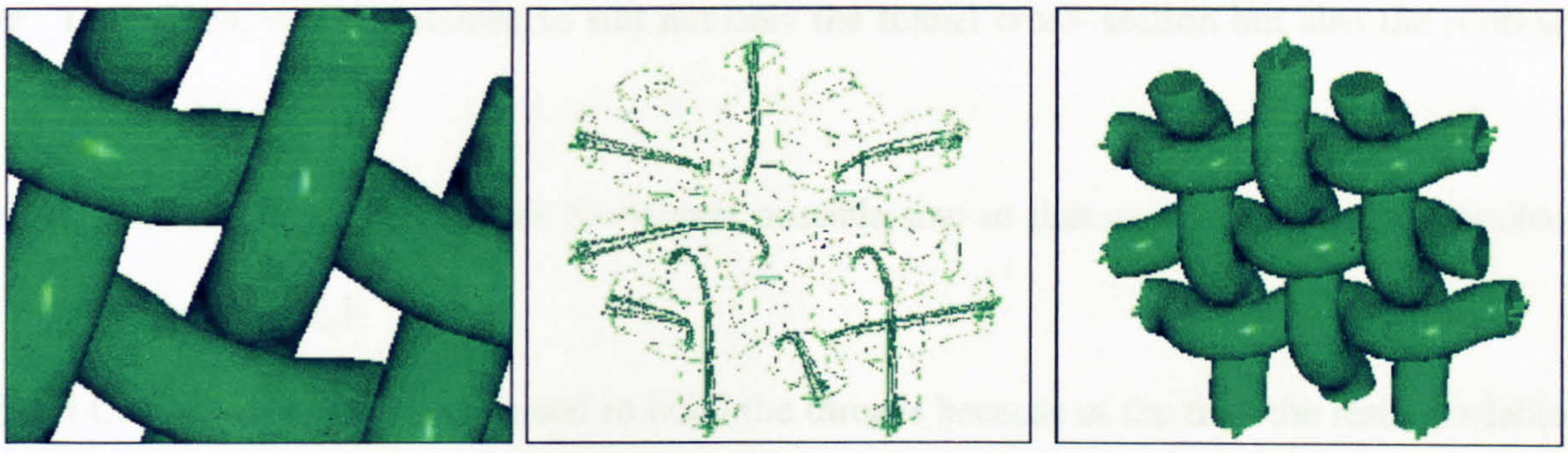

Figure 3.30 – Probes and Weave Model Details

As can be seen below (2nd picture from right) to route the tubing from the probe to outside the box required designing the best route to facilitate cleaning after the rapid prototyping. An example of a single thread and assembled probe on painted thread is given below:

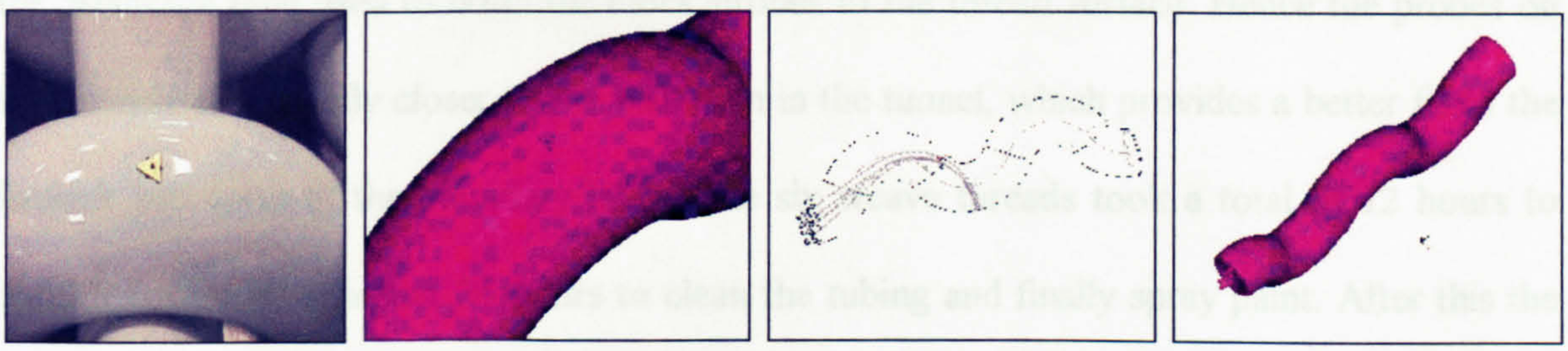

Figure 3.31 – Dexter Probe and Thread Details

It must be said that not knowing the outcome of the R.P. process forced us to design individual threads although it is now very likely that one complete model is plausible, albeit at a higher cost.

Also the central thread was split into two halves so that it could be assembled with the rest of the weave model. Clearly having six separate threads provided greater model flexibility but at the price of making the model more difficult to assemble. In order to facilitate assembly (and disassembly) the threads were sealed in place, i.e. in the box, using silicone sealant.

By building the model this way forced several other fundamental lessons, these being:

- ❖ Block probe tubing was realised so as to render tube cleaning easier, hence the tube routing was as straight as possible. It also turned out to be the shortest path from probe to outside ports.
- ❖ Thread size was determined to suit not only the tunnel cross–section but also the routing of the tubing.
- ❖ Thread size was made to suit the largest possible size so that as many probes as possible could be mounted.

Solid Ground Curing R.P. was used to build the threads because at the time the resin available offered the strongest mechanical solution at the cheapest cost. Today the weave model could also be prepared with stereolithography and then duplicated with a suitable vacuum silicone mould. This approach would be less expensive and stronger (with the latest resins) than SGC.

It was also decided to paint spray the threads after R.P. because this allowed the recovery of the 50micron tape used to bond the block probes to the thread surface. Hence the probes on the threads are actually closer to the wall than in the tunnel, which provides a better fit to the laminar sub–layer of the boundary layer. The six weave threads took a total of 12 hours to build followed by a further 24 hours to clean the tubing and finally spray paint. After this the threads were assembled in the weave box and mounted on the test jig shown below:

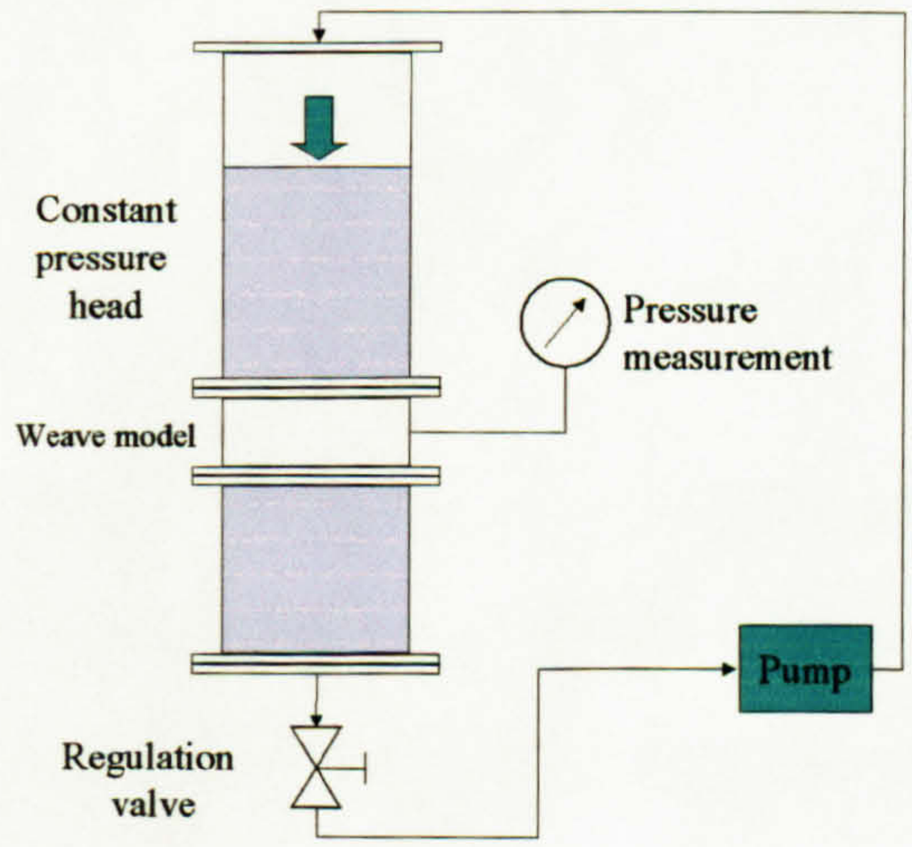

Figure 3.32 – Weave Model Test Rig

Tests were then carried out and simple differential pressure recordings taken [ref. 3.29].

A thin (5mm) disk was also designed using Pro-E and five probes were incorporated in the design. The picture below shows the central probe coloured (figure 3.33a) while the underside of the disk is shown in Fig. 3.33b.

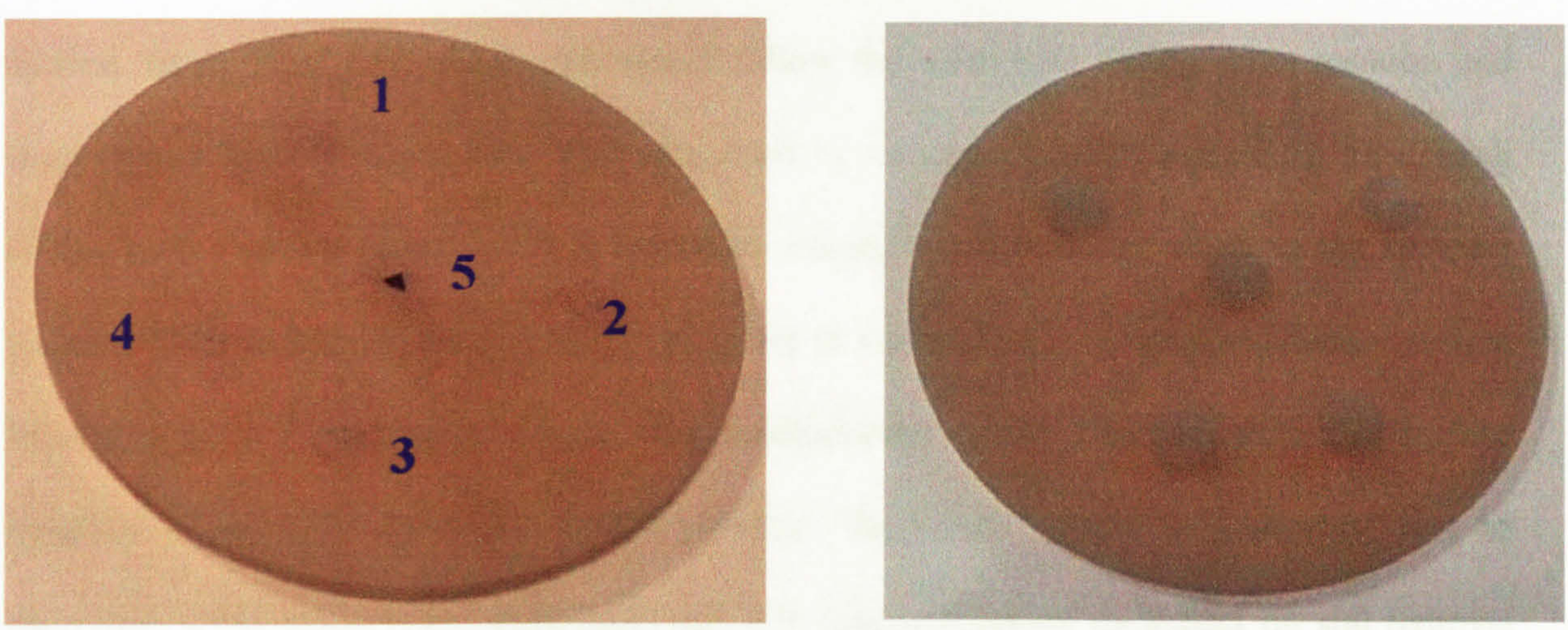

a) b)

Figure 3.33 – Rotating Disk - R.P. Model

Sphere Prototype

The sphere is basically the transmitter side of a remote monitoring system designed to provide essential real time flow data inside the washing machine drum during the wash process.

The notion behind the sphere was to provide a means of representing a mass of fabric, hereon termed 'fabric plug' [ref. 3.30], that would follow the wash load during drum rotation and thus capture local flow velocity. This was done by sensing the surface pressure on a small (100mm dia.) plastic sphere using a triangular shaped block probe attached to the sphere's surface. This surface dynamic pressure detected is transmitted to a data acquisition system located outside the washing machine. The measurement concept was to relate this surface dynamic pressure to the local surface velocity. The scope of the measurement was to determine if the velocity was significant and, if it was, understand its impact on soil removal [ref. 3.31]. Consequently the exact numerical value of the flow velocity was not the prime goal, rather it was to ascertain if it was very low (e.g. mms^{-1}) or high (e.g. ms^{-1}). The sphere, realised in two halves, is shown below:

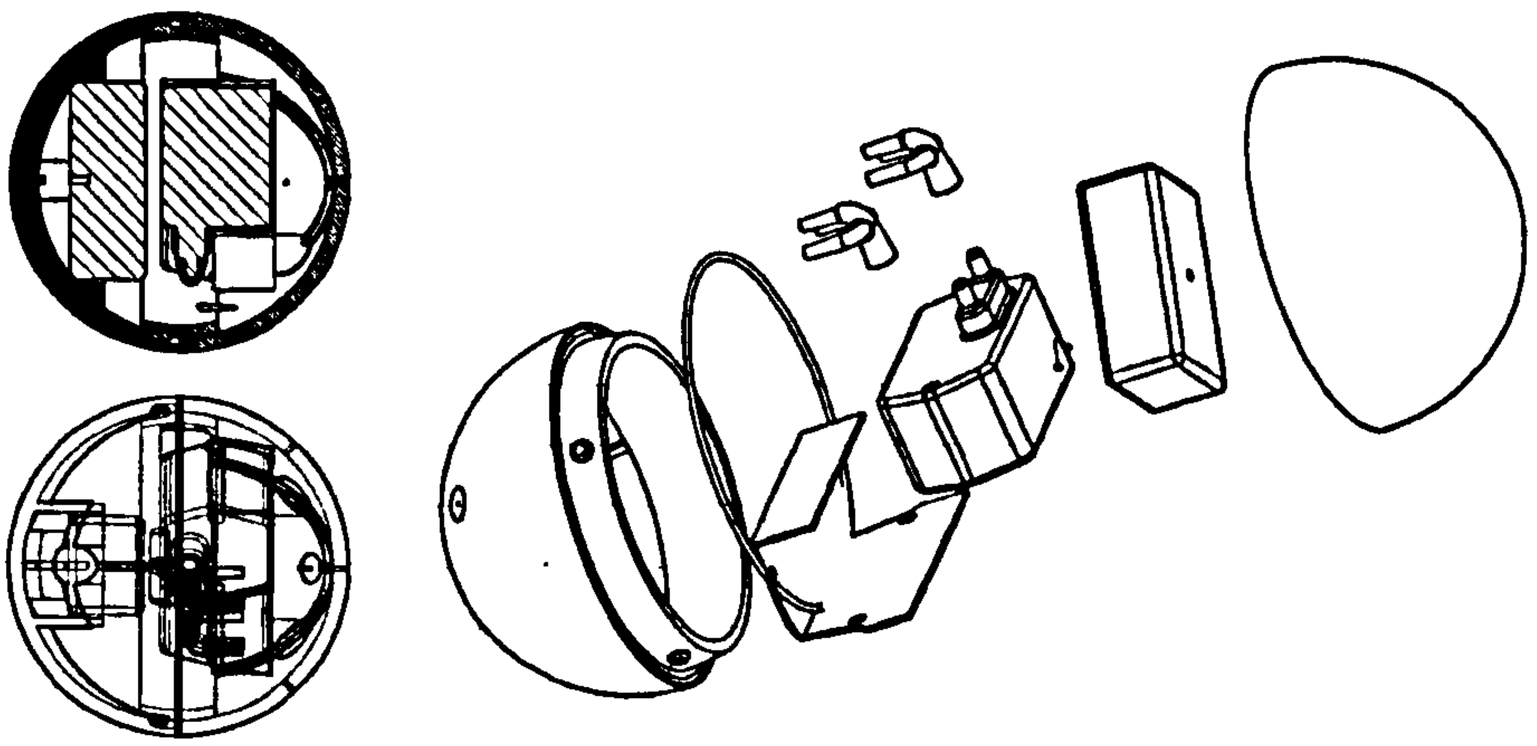

Figure 3.34 – Pro-E drawings of Sphere

The two semi-spheres were designed to house the voltage-to-frequency converter, transmitter, battery and pressure transducer. A picture of the first prototype is shown next.

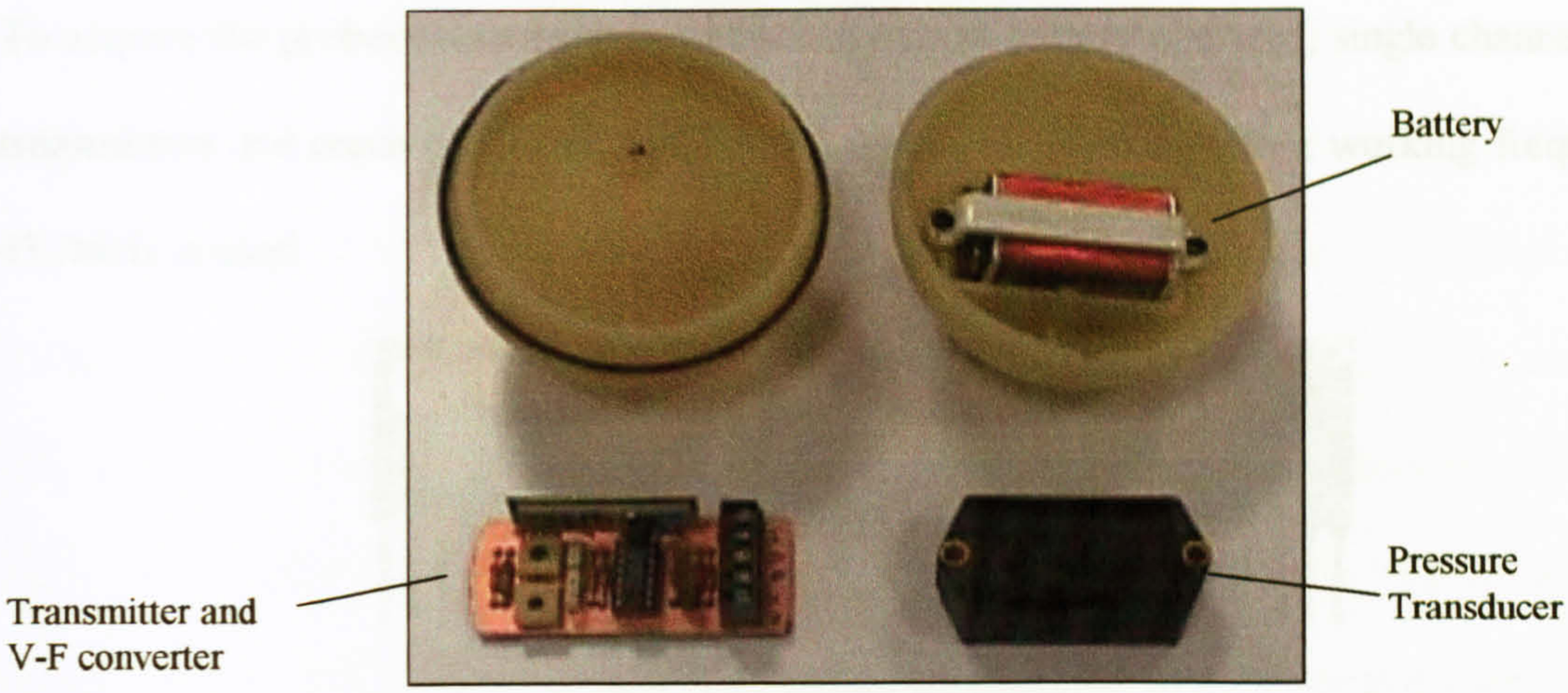

Figure 3.35 – Pictures inside the sphere

(showing battery, transducer, transmitter and V-F converter)

The small piezoresistive pressure transducer (Honeywell mod. 164PC01D76) fitted inside the sphere is directly connected to the small block probe.

As can be seen below most of the transducer size is taken up by the housing and the use of standard IC technology and technology.

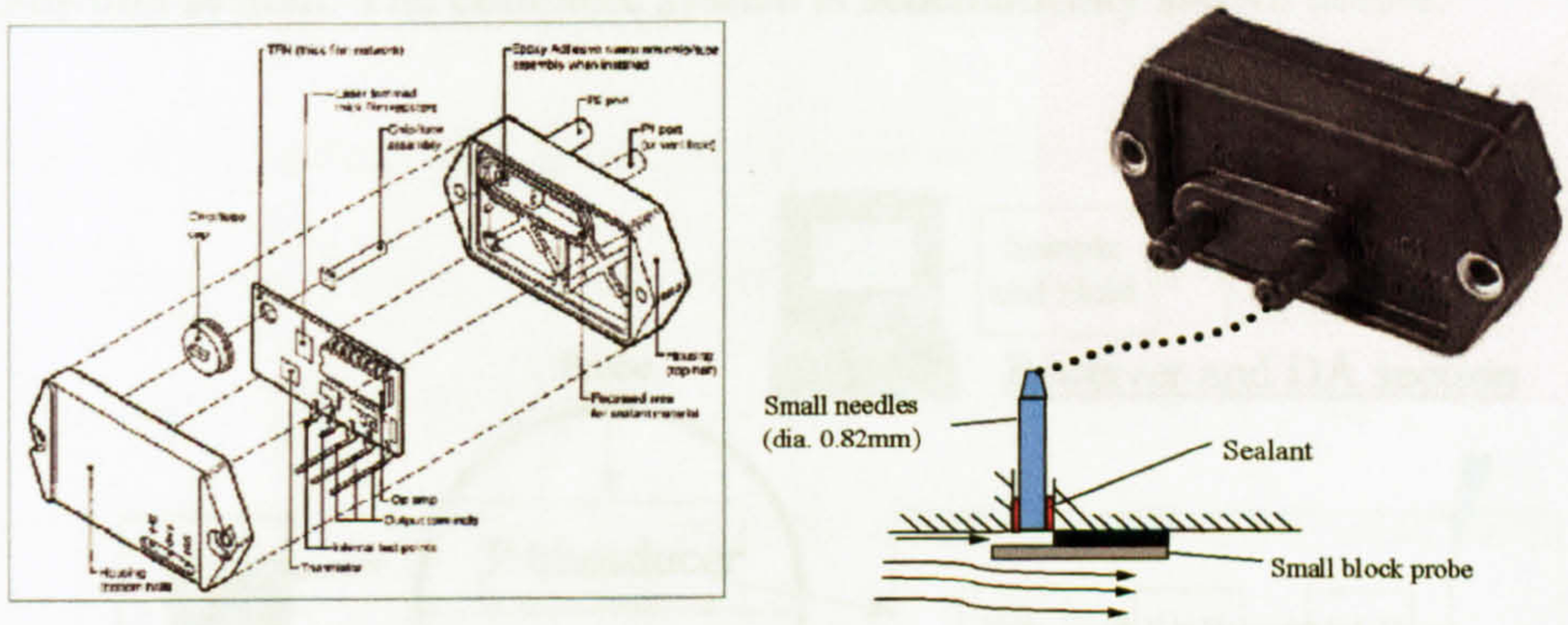

Figure 3.36 – Inside the Piezoresistive Pressure Transducer

In reality the size of the transducer and voltage-to-frequency converter could be considerably reduced by integrating them with the hybrid receiver, alternatively smaller SMD technology could be used. This means that a signal chip or PCB could be used and tagged to a garment to provide not only wash process data but also garment identification [ref. 3.32].

To acquire the probes pressure data a matched pair of battery operated, single channel, hybrid transmitters and receivers (Aurel TX SAW I.A. and RX-290A) with a working frequency of 433MHz is used.

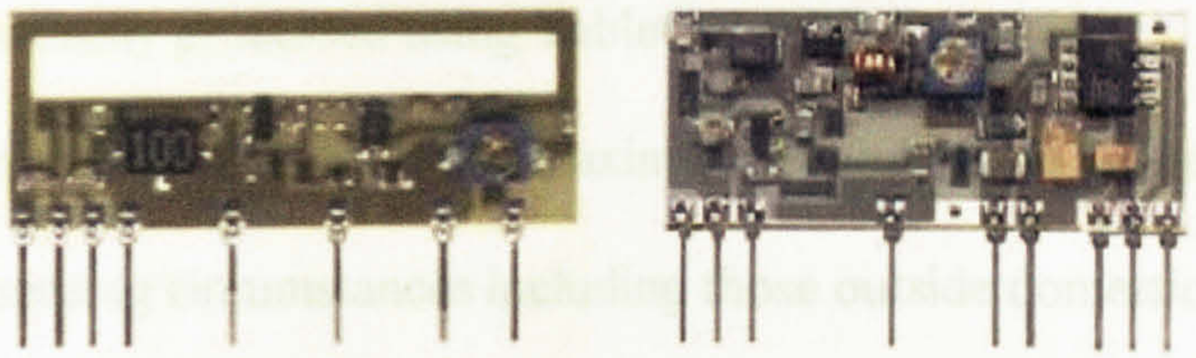

a) b)

Figure 3.37 – a) Transmitter Circuit, b) Receiver Circuit.

Operation of the system is as follows: During drum rotation the probe detects flow across the surface, this is then translated into a voltage by the pressure transducer. The voltage is then converted into a frequency that is then modulated and transmitted via radio. Outside the washing machine the receiver picks up the modulated signal from the transmitter, it then reconverts it from frequency to voltage and stores this information through a dedicated data acquisition system. The complete system is schematically shown below:

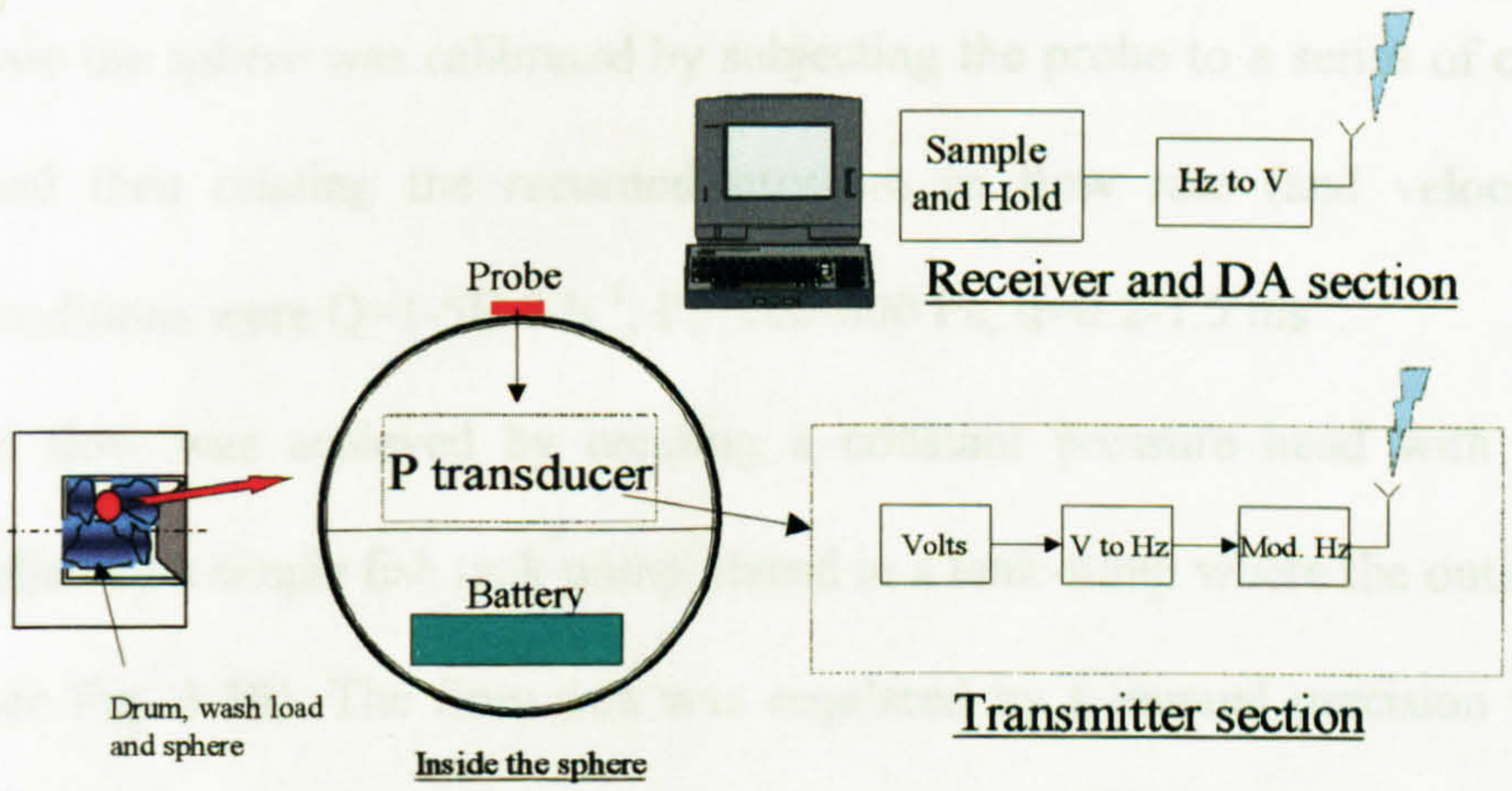

Figure 3.38 – Complete System

The data acquisition system is based on a Pentium 2 laptop, connected to a data acquisition PCMCIA format card (housed in the laptop), a sample-and-hold board (National Instruments SC2040), terminal block and LABVIEW software.

The SW has been specifically prepared for this application and provides the acquisition and display of raw data, basic statistical post processing (MIN, MAX, AVERAGE and StDev) and the storage of test data. The final processing is done in a common spreadsheet package (Excel) and mathematically processed using TableCurve 2D [ref. 3.33].

The system has been designed to offer the maximum flexibility and is therefore applicable to many other remote sensing circumstances including those outside domestic appliances.

The system is also capable of measuring other parameters such as temperature, humidity, resistance etc. simply by changing the transducer and adapting the transmitter side of the electronics.

Sphere Calibration and Test Bench

The construction and calibration of the sphere also involved designing and building a dedicated test bench. The objectives of this test bench was:

- ❖ To calibrate all three dynamic pressure ports of the triangular probe.
- ❖ To characterise the complete system in real flow conditions

In the first case the sphere was calibrated by subjecting the probe to a series of constant flow conditions and then relating the recorded pressure to flow rate (and velocity). Typical calibration conditions were Q=1-5E-3 ls^{-1}, P_d=100-600 Pa, u=0.2-1.5 ms^{-1}.

The constant flow was achieved by creating a constant pressure head with a graduated cylinder supplied by a simple fish tank pump placed in a tank-sump where the outlet water was recovered (see Fig. 3.39). The flow rate was regulated by a manual precision valve placed between cylinder outlet and probe under test. Pressure measurements were recorded manually using a Yokogawa MT120 digital pressure manometer while flow rate was measured simply by the metering flow and recording the time taken to reach a specific volume (usually 30-100ml) in the measuring cylinder. These measurements were taken for all three dynamic

pressure tappings with each pressure tapping placed directly in-line with the flow. These measurements were repeated also by varying the angle between flow and tapping so as to provide an angular calibration for the probe [ref. 3.34]. The sphere was also calibrated using the remote data acquisition system and therefore Honeywell pressure transducer of the sphere.

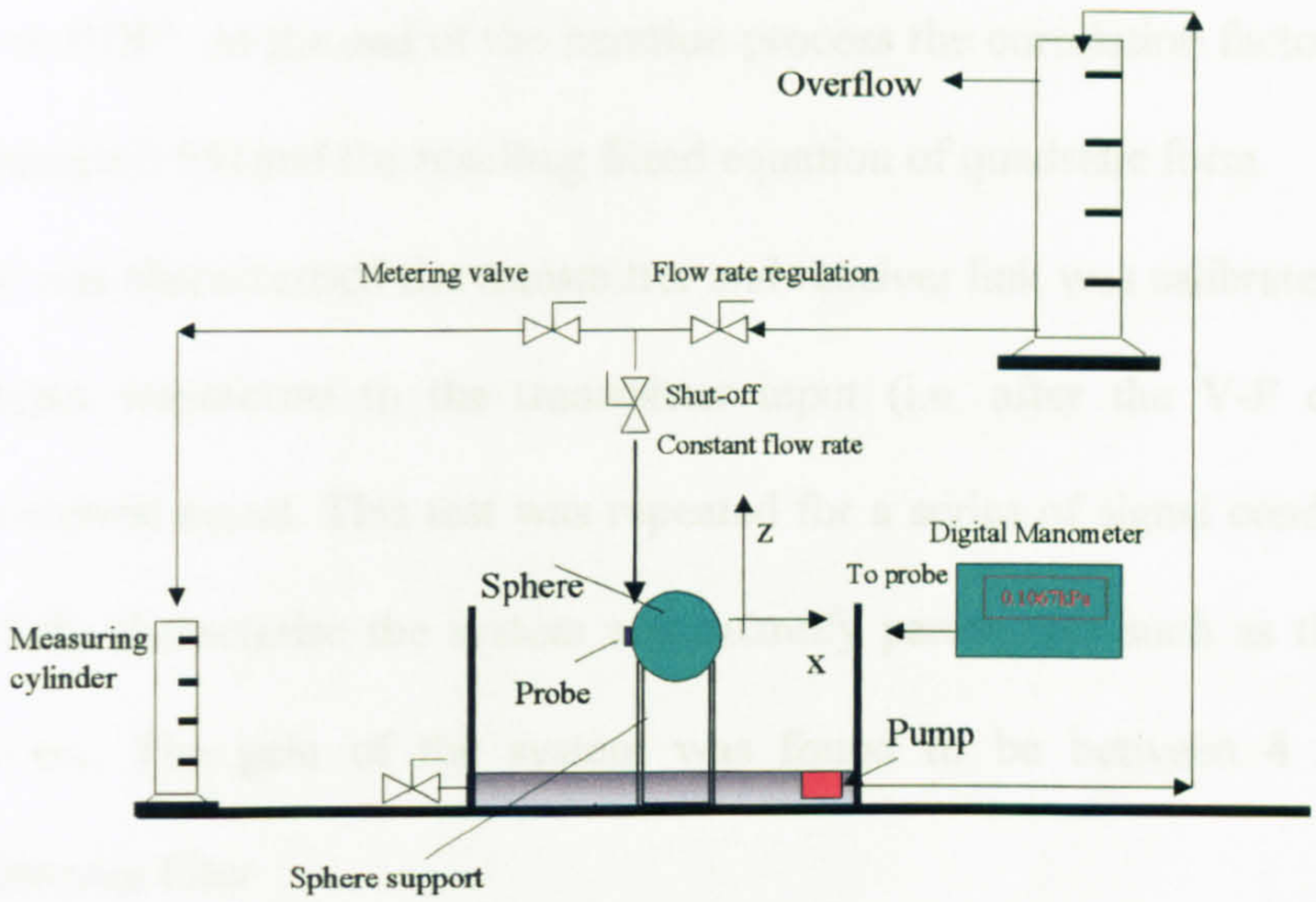

Figure 3.39 – Calibration of Probe and Transducer

In this way it was possible to relate flow rate, local flow velocity and dynamic pressure as shown in the next graph.

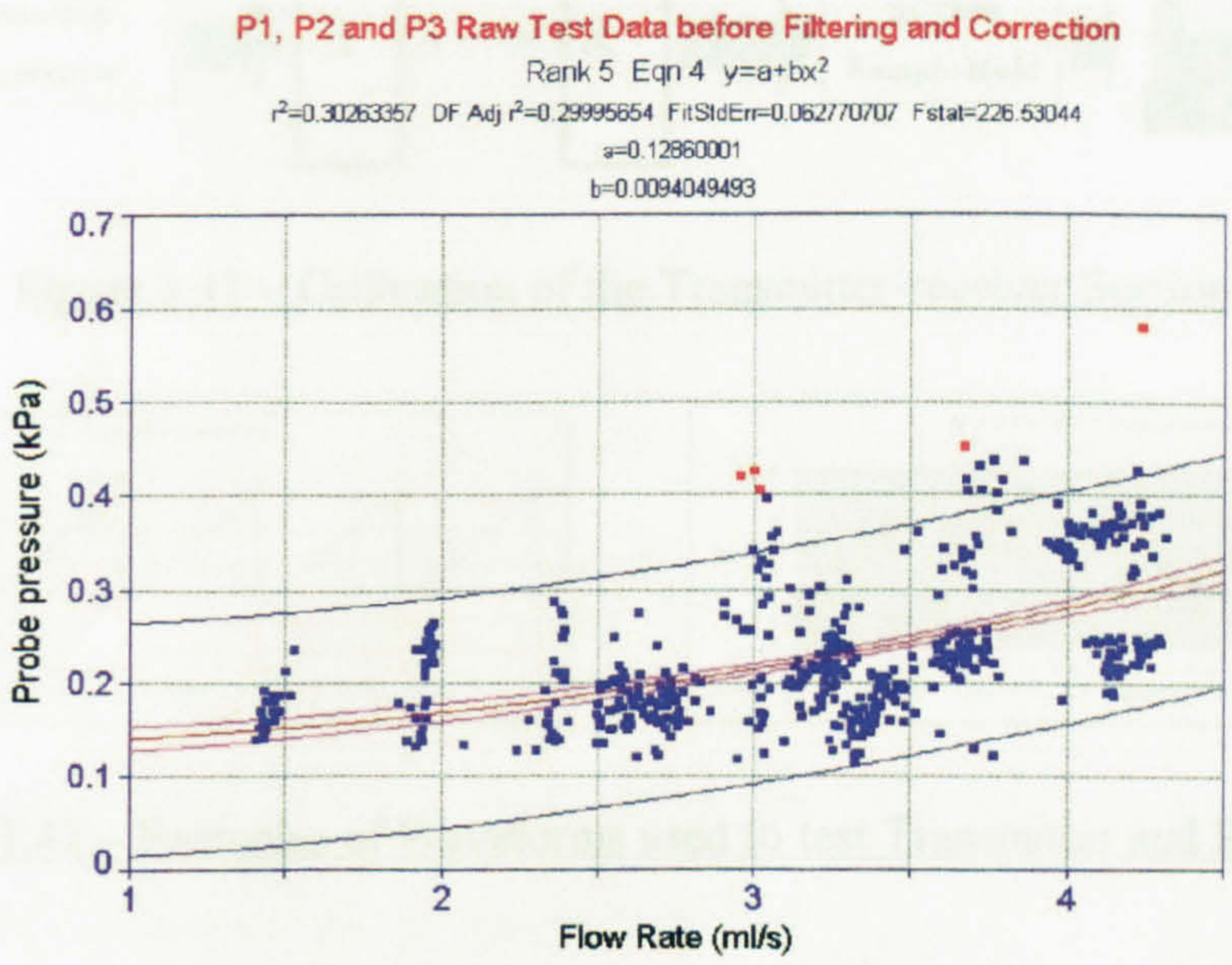

Figure 3.40 - Sphere Probe Pressure Data

In the above graph all non-filtered pressure data (P1, P2 and P3) has been plotted together. This data was then temperature adjusted and then fine tuned by a process of manual iteration based on the confidence value. This consisted of first removing suspect experimental data and then filtering out the raw data that did not fit the initial confidence value of 0.95, which was later increased to 0.99[1]. At the end of the iteration process the correlation factor was typically R^2>0.94 (confidence 0.95) and the resulting fitted equation of quadratic form.

Once the probe was characterised the transmitter and receiver link was calibrated by supplying a several different waveforms to the transmitter input (i.e. after the V-F converter) and recording the received signal. This test was repeated for a series of signal conditions in order to be able to fully characterise the system and quantify parameters such as the gain, noise, signal-to-noise etc. The gain of the system was found to be between 4 and 6 with a Butterworth low-pass filter

The test set-up is illustrated in the figure below followed by a series of traces obtained during this procedure:

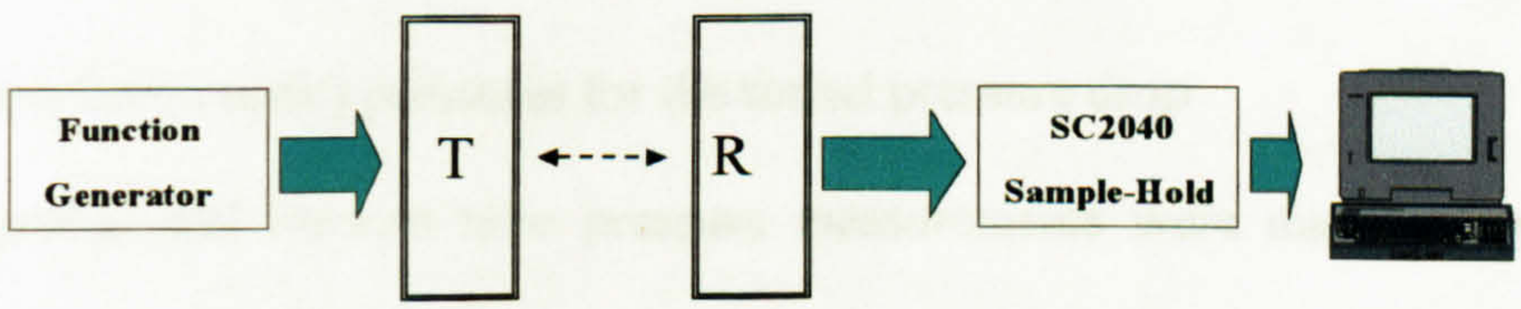

Figure 3.41 – Calibration of the Transmitter-receiver Section

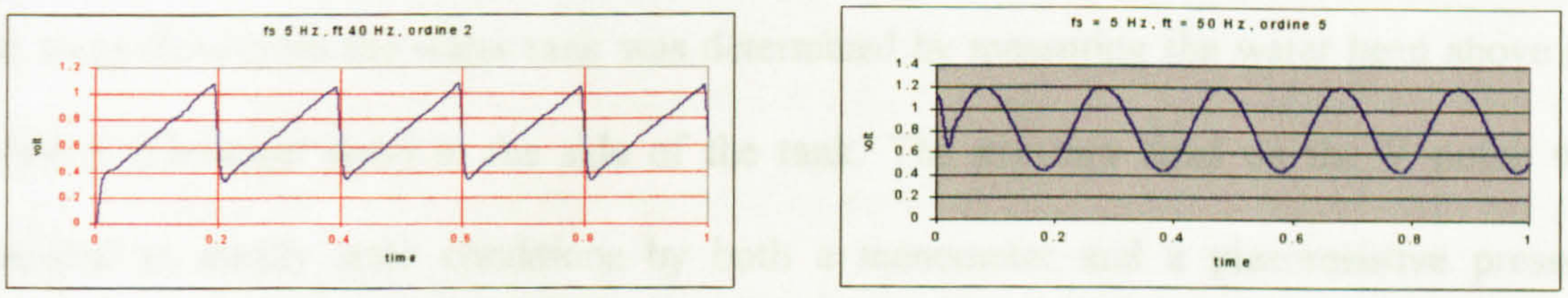

Figure 3.42 – Examples of Waveforms used to test Transmitter and Receiver

[1] The red dots shown in figure 3.40 represent the initial data that was excluded in this iteration process

Pressure Measurements, Data Acquisition and LABVIEW Programs

A fundamental aspect that appears in all five steps of the research is the measurement and management of pressure data. Hence pressure measurements, the relative data acquisition and software programs, were a vital part of the research.

Broadly speaking the pressure measurements for analytical purposes were split between steps 1 and 2 and steps 4 and 5. In step 3, measurements were taken essentially for monitoring purposes only. As will be explained next (see refs. 3.34, 40 to 42) three software programs were developed and three different pressure measuring instruments used.

Pressure Measurement and Acquisition in Steps 1 and 2

In steps 1 and 2 the water tunnel pressure measurements were based on four pressure inputs these being:

- Small block probe pressures (static and dynamic pressures)
- Preston tube pressure (dynamic pressure)
- Thomson weir (V–notch tank) water height or static (head) pressure
- Manometer head (static) pressures for the tunnel pressure drop

The block probes and Preston tube pressure measurements were made using a precision differential pressure transducer (model LPM 9481) supplied by Druck [ref. 3.35] with a range of 0 to 1000Pa.

The water flow from the water tank was determined by measuring the water head above the V–notch (Thomson weir) in the side of the tank. The pressure head on the V–notch was measured in steady state conditions by both a manometer and a piezoresistive pressure transducer (Honeywell mod. 162PC01D), the latter providing the worst accuracy but fastest response time and widest range (±2%, 1ms, 0–7000 Pa).

Test section pressure drop measurements were realised by two manometers positioned, respectively, in the vicinity of the inlet and outlet of the test section. The manometers were chosen because of the large inlet tunnel pressure (up to 10000Pa) and, above all, the accuracy, ease and simplicity of this technique.

The scope of these pressure measurements was to provide a supplementary way of determining shear stress magnitude via pressure drop recordings. This was a convenient way of correlating average shear stress value for the test section to the local shear stress determined by the block probes and Preston tube.

Preston tube measurements required extra caution mainly because of the possible non perfect contact of the tip of the Preston tube to the upper wall or roof of the tunnel.

In all of the above cases the pressure was classified either local, i.e. measured near the area of interest, or remote i.e. in the vicinity of the small block probe. This latter case was classified "reference" or the baseline pressure. The layout of the complete pressure measurement system for the tunnel is shown in the next figure.

Transducer data was recorded automatically through a dedicated, laptop PC based, data acquisition system and post–processed separately on a desktop PC. The manometer pressure data was recorded manually, as was the water temperature.

The data acquisition system was based on a National Instruments 12bit DAQ card with PCMCIA format connected via a flat cable to the terminal board and pressure transducers. To minimise measurement errors e.g. aliasing, the differential measurement method was used with shielding wiring. The DAQ card was managed by purpose designed data acquisition programs based LABVIEW object programming language [ref. 3.36] by National Instruments.

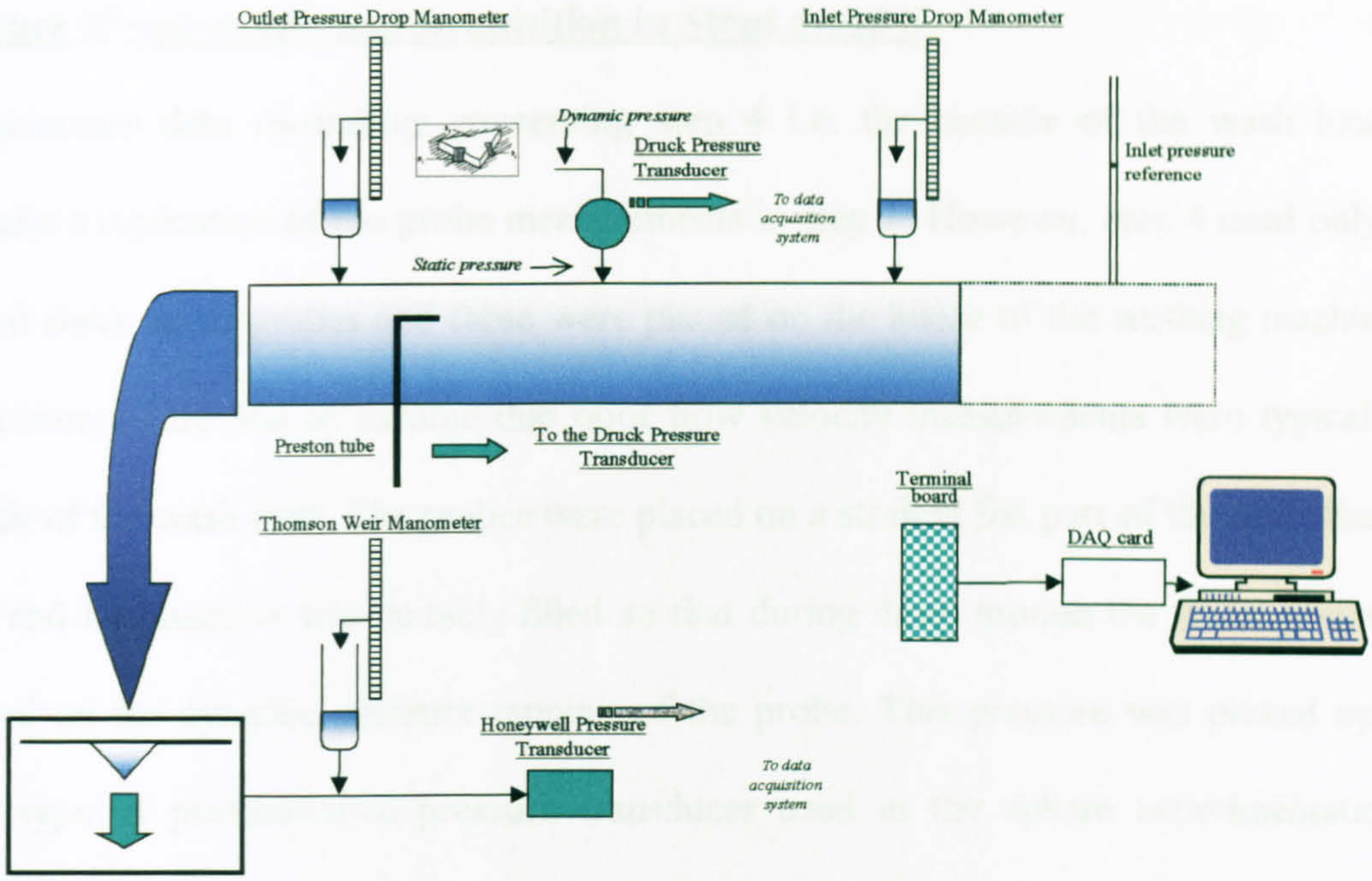

Figure 3.43 – Layout of the Pressure Measurement System

To ensure stable measuring conditions, all pressure transducer power supplies were obtained from precision power supply units (PSU). The complete system is illustrated below:

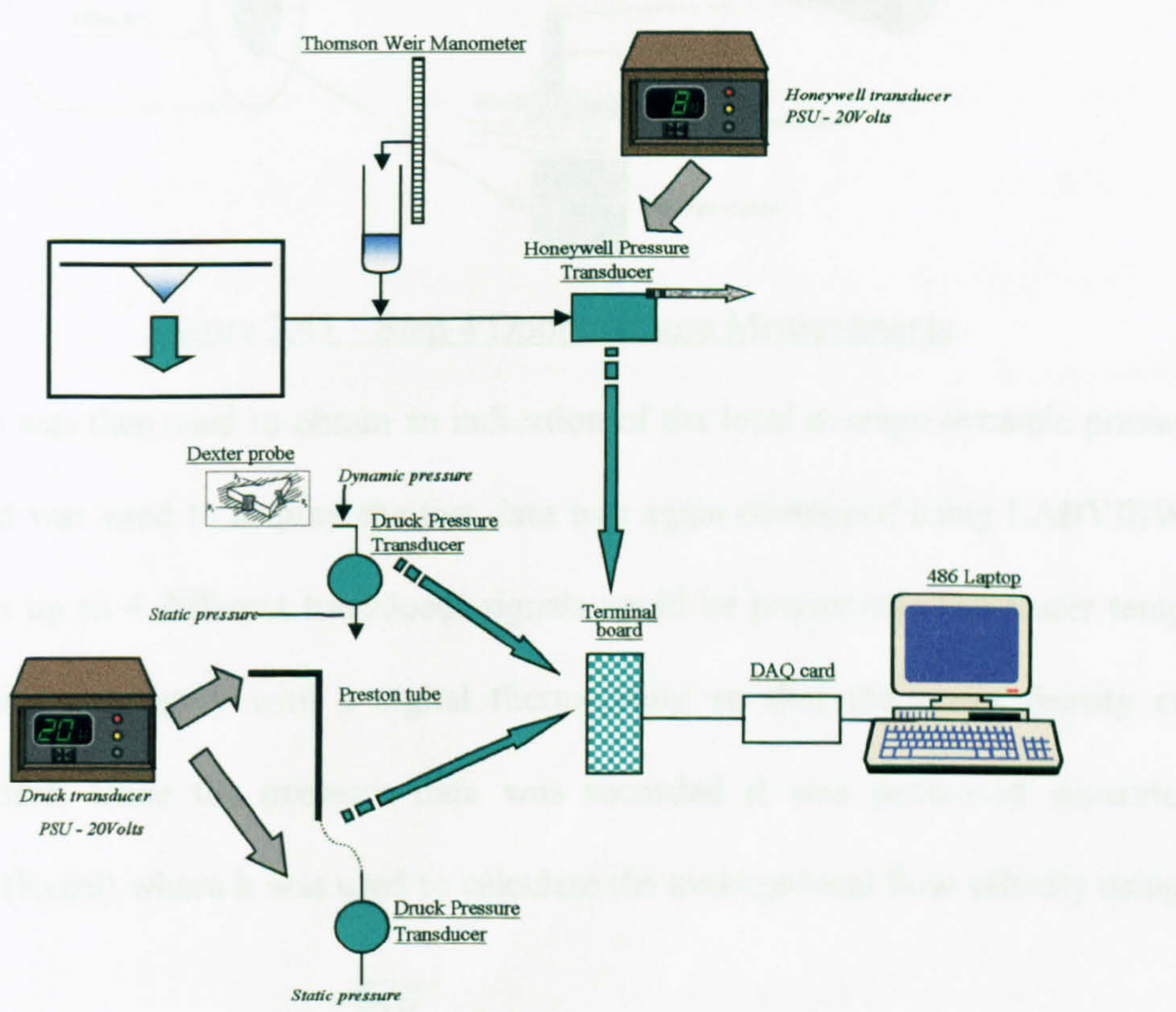

Figure 3.44 – Weir Data Acquisition System Schematic

Pressure Measurement and Acquisition in Steps 4 and 5

The pressure data recordings concerning step 4 i.e. the outside of the wash load, were basically a replication of the probe measurements in step 1. However, step 4 used only square shaped shear stress probes and these were placed on the inside of the washing machine door. The concept here was to assume that door flow velocity measurements were typical for the outside of the wash load. The probes were placed on a straight flat part of the inner face of the door and the machine was suitably filled so that during drum motion the water pressure was exerted on the dynamic pressure tapping of the probe. This pressure was picked up by the same type of piezoresistive pressure transducer used in the sphere experimentation. The transducer voltage output was led to the data acquisition system.

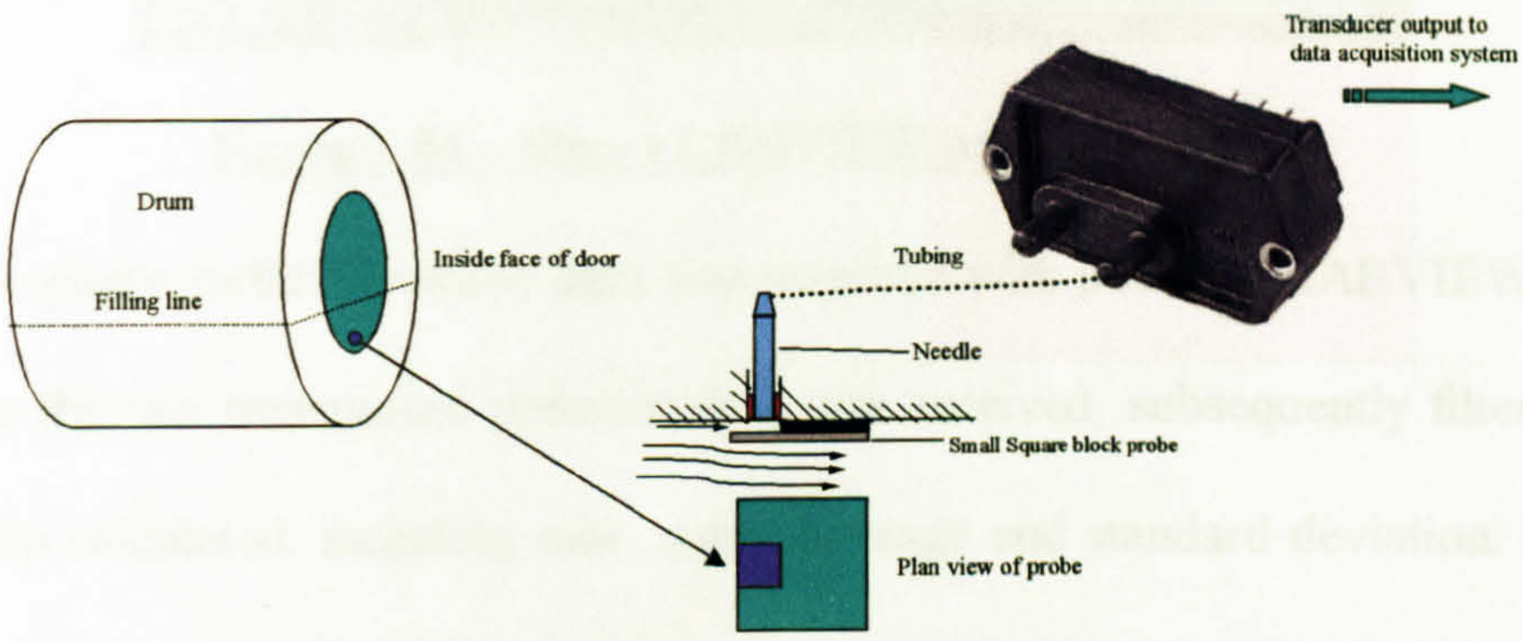

Figure 3.45 – Step 4 Door Pressure Measurements

This voltage was then used to obtain an indication of the local average dynamic pressure. The program that was used to acquire the test data was again developed using LABVIEW and in this program up to 4 different transducer signals could be processed. The water temperature was monitored separately with a digital thermometer so that the water density could be calculated later. Once the pressure data was recorded it was processed separately in a spreadsheet (Excel) where it was used to calculate the average local flow velocity using:

$$\bar{u} = \sqrt{\frac{2\overline{P_D}}{\rho}} \qquad \text{Equation 3.1}$$

In this way it was possible to estimate the typical flow velocity on the outside of the wash load. An example of the program interface (raw and filtered data plotted in upper and lowers charts respectively) is shown below:

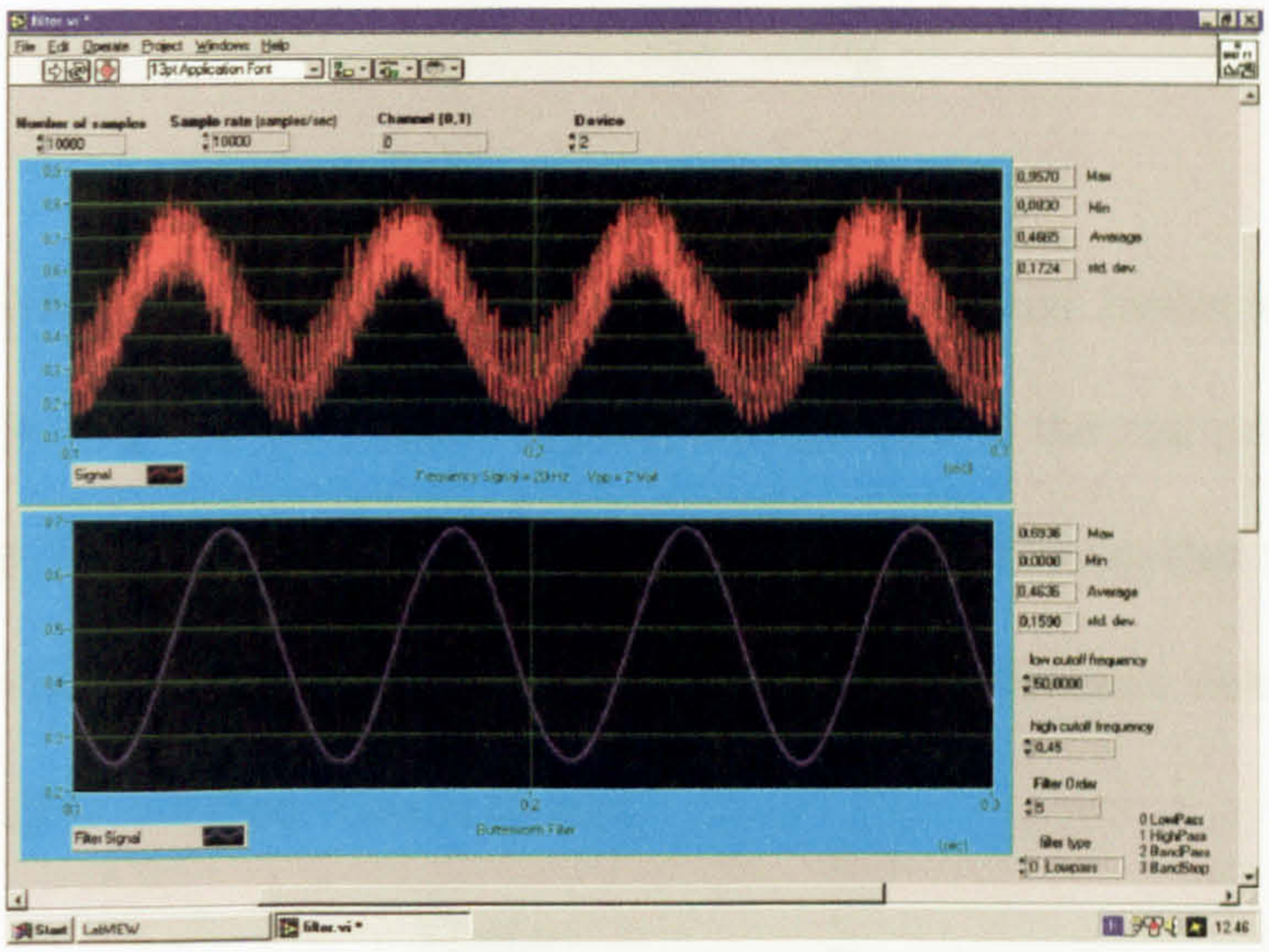

Figure 3.46 – Step 4 LABVIEW program interface

In step 5 the sphere surface pressure data was acquired with a further LABVIEW program. In this program the raw transmitted pressure data was received, subsequently filtered and basic statistical data calculated, including min., max., average and standard deviation. Equation 3.1 was again used to calculate the local flow velocity but in this case the flow was that of the sphere. An example of the program interface and relative block diagram is shown below:

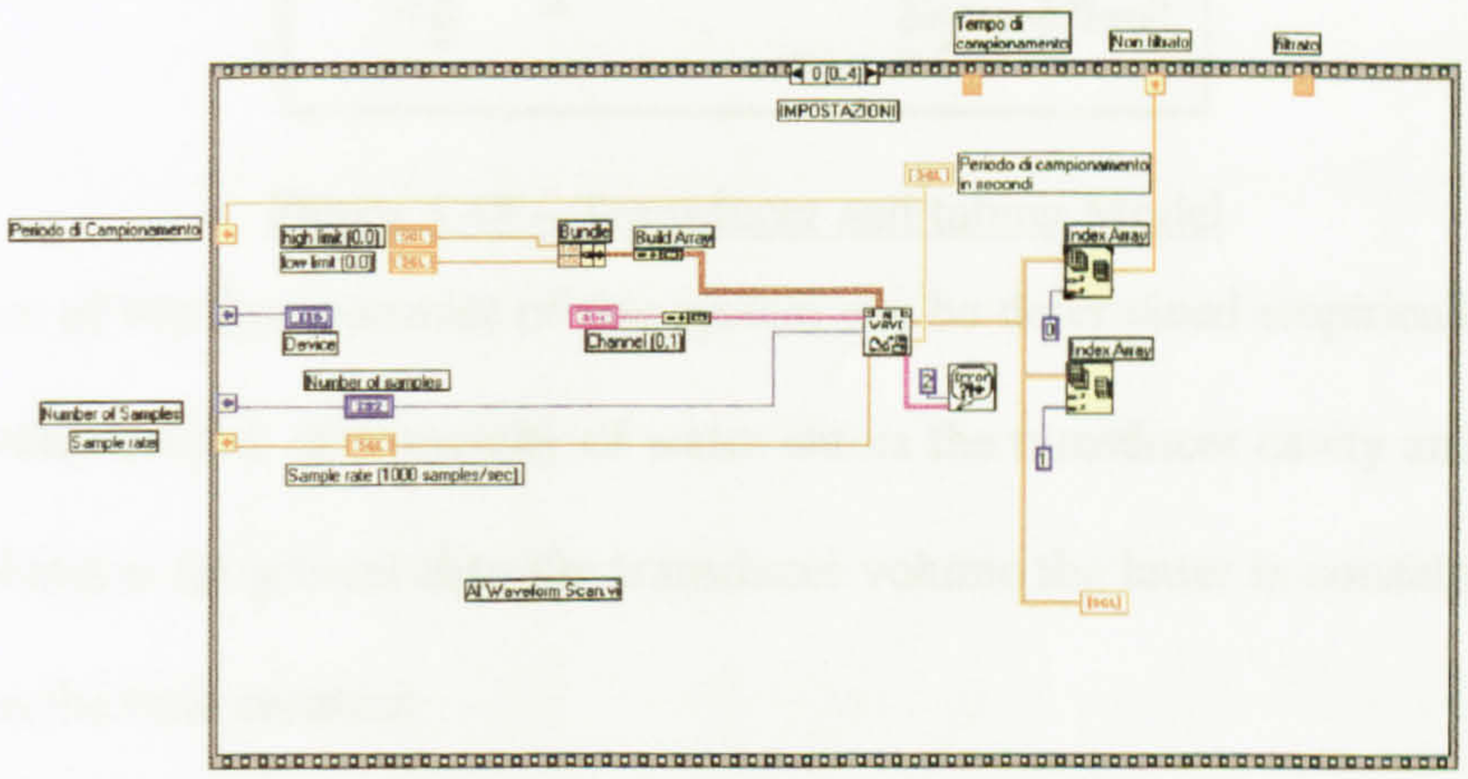

Figure 3.47 – Step 5 LABVIEW program (sampling part only) for Sphere pressure data

Some Modelling Aspects of the Pressure Measurements

The water tunnel pressure measurements provided essentially two models of pressure transducer, these being:

- Highly damped and slow–acting
- Moderately damped and fast–acting

The highly damped case is typical of the Druck transducer and manometer and both are characterised by the fact that the measured pressure lags behind the real pressure and this lag is a first–order lag. These conditions can be approximated by assuming that the pressure in the volume leading to the transducer (including both tubing and transducer volumes) is described by steady laminar flow in a pipe. That is to say:

$$p_i - p_m = \frac{32\mu L u}{d_t^2} \qquad \text{Equation 3.2}$$

where p_i and p_m are the respective real pressure and measured pressures, μ is the fluid dynamic viscosity, u is the average flow velocity, L is tubing length and d_t the diameter of the tubing.

This situation is depicted for the Druck pressure transducer below:

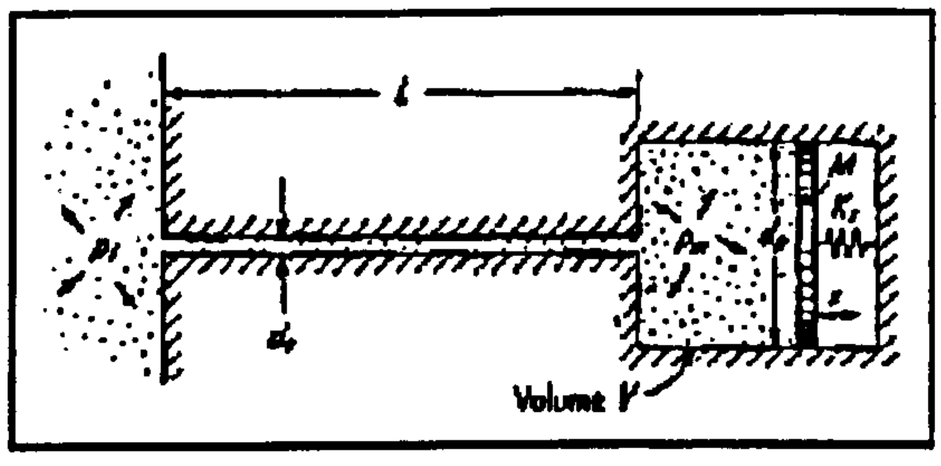

Figure 3.48 – Transducer and tubing Model

The calculation of the time constant of this system can be determined empirically by assuming that during a time interval dt a quantity of water enters the transducer cavity and tubing. Since the tubing volume is far greater than the transducer volume the latter is considered negligible, thus leading to the time constant:

$$\tau \cong \frac{128\mu L C_{vp}}{\pi d_t^4} \qquad \text{Equation 3.3}$$

For example, the tunnel test set–up typical conditions for the Druck transducer were: τ=10msecs (100Hz), L=0.3m, d_t=0.002m, μ=1E–3 Nsm^{-1}, $C_{vp}\approx$1E–11 m^3/bar. Practically speaking though the steady state conditions (after a step change) occurred after $\approx 5\tau$ i.e. >50mseconds (20Hz) hence pressure variations faster than 20Hz were naturally 'clipped' in the tunnel measurements. In general pressure measurements were taken over 10 second period and only when the pressure was sufficiently stable. This condition was judged on the variance of the pressure data recorded over 10 seconds (~1000 samples).

A moderately damped and fast–acting system was typical of the weir pressure head measurements, which simply supplemented the manometer measurements. Here, in parallel with the weir manometer a piezoresistive transducer detected the V–notch water height continuously but with a time constant of only 1ms. Since this is ten times more responsive than the Druck counterpart it provided some insight into what the manometer effectively dampened during tests.

In fact this latter time constant provided $C_{vp}\approx$1E–10 m^3bar^{-1}, which certainly aids data analysis. Unfortunately, the length of the tubing (circa 1.5m) and the disturbance of the weir tended to compensate this advantage. Similar reasoning was applied to the two manometers although measurements here were more stable because of heavier dampening.

Of greater importance than the manometer dynamics was the human error due to the manual reading of the manometers. Foremost, this error was important because the two manometers were used to measure the local static pressures between two different pressure points arbitrarily distanced by 1826mm. This pressure drop was used to relate tunnel skin friction effects (i.e. the pressure drop) to the measurement of the shear stress for specific tunnel hydrodynamic conditions. The static pressure reading error for each manometer was $\approx 0.1 mmH_20$ i.e. $\approx$1Pa.

The tunnel flow rate was determined by using a Thomson weir [ref. 3.37] placed at the outlet of the tunnel in conjunction with the above mentioned weir manometer.

The Thomson weir (shown below) is a special case of the 90° V–notch weir [ref. 3.38], which acts as a variable area orifice upon the water level of the free surface.

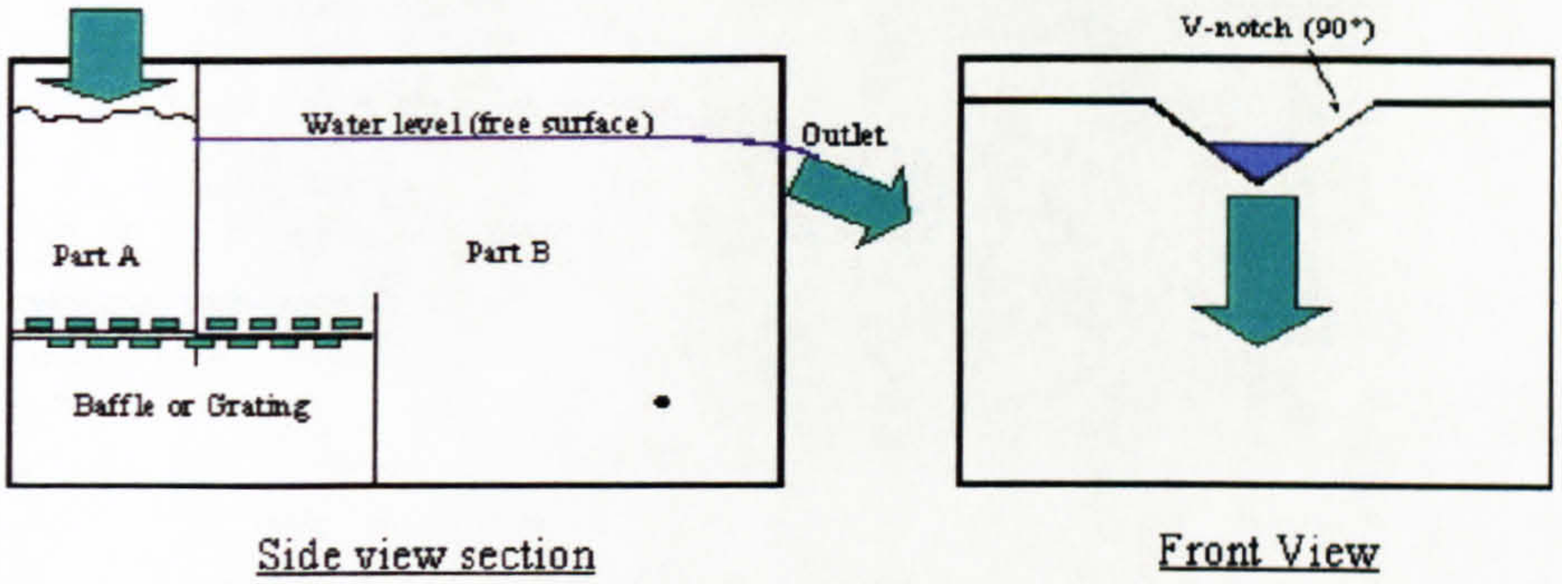

Figure 3.49 – Thomson Weir

The notch water level height (H) was related to a specific flow rate via a discharge coefficient defined as:

$$k = \frac{0.304}{H^{0.03}} \qquad \text{Equation 3.4}$$

For flow rates in the range of $3 \leq Q \leq 30$ ls^{-1} the value of k for the weir used was 0.6 and virtually constant. In practise the range can be safely extended by ~10% without introducing significant error [ref. 3.38].

Since the height of the water level above the apex of the notch was a direct measure of the water flow rate the difficulty was essentially one of measuring this height.

This was done manually with a precision piezometric stick i.e. the manometer, or using the Honeywell pressure transducer.

The piezometric stick consists of a fine precision adjustment screw to which a pointed tip is connected. By lowering or raising this tip and placing it just in contact with the water level meniscus it is possible to read the value of H directly from the graduated scale and thus determine the flow rate with eq. 3.5.

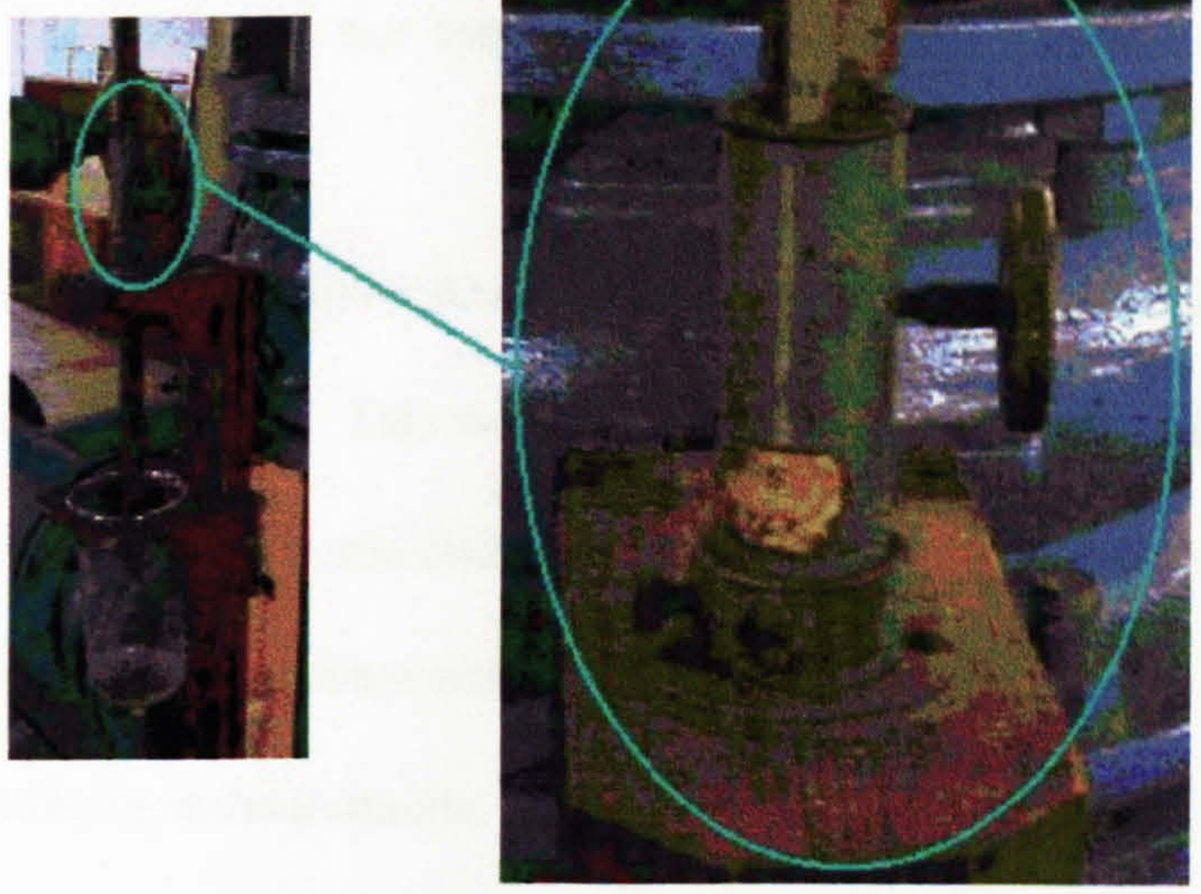

Figure 3.50 – Piezometric Stick and scale close–up

The flow rate through a notch of known angle θ may be written in the form [ref. 3.39]:

$$Q = \frac{8}{15} H^2 \sqrt{(2g)\tan\left(\theta/2\right)H} \qquad \text{Equation 3.5}$$

This equation assumes that the flow velocity in the vicinity of the notch is very small and hence kinetic energy effects are negligible. In practise this is usually not the case and the tank and V–notch need calibrating. For the Thomson weir used in the experimentation this entailed determining a calibration coefficient (discharge coefficient) versus the flow rate, which adjusts eq. 3.4 to match the real flow rate. Figure 3.49 shows that the Thomson weir has a notch angle of 90° hence equation 3.4 becomes:

$$Q = 1.417 H^{\frac{5}{2}} \qquad \text{Equation 3.6}$$

To evaluate the accuracy of the flow rate measurements it is necessary to differentiate eq. 3.6. Thus by applying the maximum flow rate conditions and a manometer reading error of 1mm this amounts to a 0.48% maximum error ($0.13 ls^{-1}$) or <2E–3 ms^{-1} in flow speed variation.

In reality the manometer reading error is less (0.1mm division instead 1mm) thus experimental data error was certainly much less. When the water level height was measured with the

Honeywell transducer the precision was lower (±0.25% of the 737mmH_20 transducer span) i.e. ±1.84mmH_20. The stick was not temperature-compensated as this error was considered negligible.

However, the transducer had a higher sensitivity and response time and provided a continuous reading of the weir water height. This was particularly useful when evaluating transients and establishing when to record the probe and Preston tube data. In general during the experiments both manometer and transducer were used and only when the flow was absolutely stable did we exclude the transducer measurements.

Chapter 4 – Literature Reviews

List of Contents

List of Figures

Literature Reviews

The research discussed in this thesis has encompassed four different areas of expertise that have required searches in different literature backgrounds. Although it is not claimed that the four relevant literature reviews are entirely exhaustive there is sufficient evidence to show that the coverage is broad enough to ensure that the concluding knowledge base is thorough. Rather than list all the papers, texts etc., that appear at the beginning of each chapter anyway, I have summarised each of the four reviews. I have also chosen a selected list of recommended documentation that have moulded both this research and are considered a very good reference or starting point for all future attempts at understanding soil removal from textiles.

A diagram illustrating the reviews is provided below and the reviews are presented in chronological order:

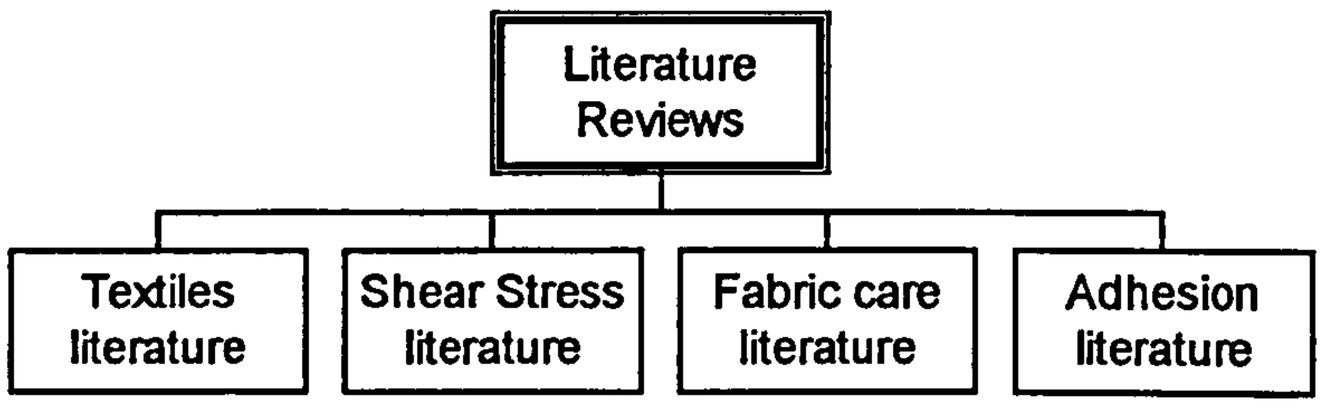

Figure 4.1 - The Four Literature Reviews

Textiles Literature Review

The scope of this review, which was the first of the four reviews, was to understand what work had already been tackled in terms of hydrodynamics in textiles.

The outcome of this literature search was that early research (up to early 1950s) focused initially on macro fluid flow properties and parameters such as pressure drop, Reynolds numbers, drying performance, flow resistance and thermal coefficients (Robertson, Backer, Penner, 1950-51). The principal aim was to improve apparel performance such as water-proofness, wearability etc. in military and heavy-duty equipment (e.g. battle dress, parachutes, tents etc.) and apparel (coats).

After about 1950 and up to late 1960s attention moved towards a smaller scale level especially textile characteristics such as weave and fibre classification, pore size and ultimately pore shape. Here work essentially concentrated on using textiles for the filtration and separation industries (Rushton, 1968). Consequently this work was essentially concerned with flow in steady state conditions with static weaves. Moreover the work was carried out at very low Reynolds numbers (Re<100) where the scope was to 'clean' or filter the fluid via porous media made of textile fibre.

After the mid. 1960s and up to early 1980s research interests were realigned with porous media thus characteristics such as permeability, zeta potential, pore size etc. for a whole series of fluids were studied (Scheidegger, Rushton, Macdonald, Stanek, Dybbs, 1971-84).

More recent research (1980s onwards) has concentrated on a much wider use of textiles including "smart" textiles such as Goretex®, fire fighting apparel, mountaineering and climbing equipment (Adanur, 1996) and industrial processing of fibres.

One could therefore claim that research in textiles-flow phenomena has followed a 20 year cycle and recent research is now concentrating on wider applications ranging from high tech. fashion clothing to advanced materials used in complex engineering structures.

The scope here is to improve textile performance and create niche markets that are traditionally very profitable e.g. sportswear. However, the main fibre type for domestic fabrics remains cotton (80% of total world market) although other natural fibres such as wool, silk and cashmere have gained importance in the eyes of the consumer. Consequently the importance of care and personal appearance means that the consumer mind set has change from simple washing to total fabric care.

On a much lower standing (5-10% of world market), but nonetheless important, are synthetic fibres e.g. rayon, nylon, polyester etc. Here nylon fibre remains the front runner while polyester (mixed with cotton) has the largest share of the mixed fibre (world) market.

Summarising the literature search uncovered no evidence of attempts to understand the link between fluid flow and soil removal (or re-deposition) in washing processes. Although a fine

example of fluid flow through textile weaves is given by Wei-Ming Lu et al. (1996) which, incidentally, was the starting paper for all of my work.

At the end of this literature search it was therefore concluded that research concerning the hydrodynamic effects on soil removal was either at a very infantile stage, involved some other field or had been totally neglected.

The highlights of the literature search and recommended readings are:

- Robertson A. F., Air Porosity of Open-Weave Fabrics Parts 1 and 2: Metallic Meshes, pp.838-845, Textile Research Journal, Dec. 1950.
- Backer S., The Relationship between the Structural Geometry of a Textile Fabric and its Physical Properties - Part 4 - Interstice Geometry and Air Permeability, pp.703-714, Textile Research Journal, Oct. 1951.
- Penner S.E. and Robertson A.F., Flow Through Fabric-Like Structures, pp.775-788, Textile Research Journal, Nov. 1951.
- Lynn J. E. and Press J. J., Advances in Textile Processing, vol. 1, Textile Book Publishers, 1961.
- Rushton A., Green D. J. and Khoo H. E., Flow of Fluids in Filter Cloths, Filtration and Separation, June 1968.
- Rushton A. and Griffiths P., Fluid Flow in Monofilament Filter Media, Vol.49, pp.49-59, Transaction Institution Chemical Engineers, 1971.
- Scheidegger E., The Physics of Flow through Porous Media, University of Toronto Press, 3rd Edition, 1974.
- Macdonald F. et al, Flow through Porous Media – Ergun Equation Revisited, Ing. Eng. Chem. Dund., vol. 18, pp.199-208, 1979.
- Stanek V. and Szekely J., Three-Dimensional Flow of Fluids through Non-uniform Packed Beds, A.I.Che.E. J., vol. 20, pp.974-980, 1974.
- Dybbs S. and Edwards R. V., A New Look at Porous Media Fluid Mechanics – Darcy to Turbulent Flow, Martinus Nijhoff Publications, pp.199-254, 1984.
- Bear J., Dynamics of Fluids in Porous Media, Dover, 1988.
- Dullien F. A. L., Porous Media: Fluid Transport and Pore Structure, Academic Press. 2nd Edition, 1992.
- Morton W.E. and Hearle J. W. S., Physical Properties of Textile Fibres, The Textile Institute, Manchester, UK, 1993.
- Johnston P. R., A Survey in Test Methods in Fluid Filtration, Gulf Publishing Co., USA, 1995.

- Adanur, S., Wellington Sears Handbook of Industrial Textiles, Technomic Publishing Co., USA, 1996.
- Wei-Ming Lu, Kuo-Lun Tung and Kuo-Jen Hwang, "Fluid Flow Through Basic Weaves of Mono-filament Filter Cloth", Textile Research Journal, May 1996.
- Tortora P. G. and Collier B. J., Understanding Textiles, Prentice-Hall, 1996.

Shear Stress Measurement Literature Review

Reviewing shear stress measurement research was probably the most convenient of the four reviews because most of the original work has been realised in one field, aeronautics (Prandtl, 1934), although other fields such as environmental engineering, micro-electronics and medicine are becoming increasingly common.

Boundary layer research in aeronautics dates back to the early part of the last century and has gradually received increasing attention because of the quest for better wing and aircraft efficiency through the reduction of skin friction and drag. The period of 1930 to 1970 seems to have provided the largest amount of basic shear stress research material but recent (last 10 to 20 years) advances in smart materials and the advent of nano-technology is providing a new impetus, especially in terms of actuators and sensors.

Environmental engineering has taken an active interest in shear stress research because of the impact it has on river beds, water flows, and civil engineering in general. For example the erosion of river beds (Pilotti, 1997) and flow around bridge pillars (Monti, 1994).

On a more esoteric footing, and more recently (early 1980's onwards), is the study of shear stress in blood flows. This area deals with the effects of shear on the removal and/or prevention of accumulation of debris on artery walls, with special attention on vascular and cardiac issues (Bardelli, 1995).

Overall whatever the field of interest it was found that the measurement of wall shear stress is generally divided into two macro-categories (Goldstein, 1996) i.e. Direct and Indirect, the latter category providing the majority of methods and devices.

Direct methods have been successfully used to measure shear force in high-speed flows. The basic concept is to connect a force sensor to a free moving surface or element on which the shear stress acts, for this reason these devices are often termed balances (Mabey and Gaudet, 1975, Schmidt 1988, Tcheng, 1996). In this way the sensor directly measures either the displacement or the deformation of the surface (head) or element. Unfortunately direct measurement balances are prone to numerous errors ranging from simple (but critical) misalignment to being simply too bulky (Winter, 1977).

Indirect shear stress measurements range from using simple coloured dyes to sophisticated velocity profile reconstruction using LASERs and chemical dispersion using mass transfer probes (Beversdoff, 1997). The approach is always the same, that is one or more parameters are correlated to shear stress through analytical or empirical expressions. Methods available fall under one of seven categories, these being:

1. Visualisation and reconstruction of the boundary layer velocity profile using Optical methods
2. Image Velocimetry
3. Bubbles, Traces, Dyes, Smoke, Tufts, Clay etc.
4. Oil-Film Gauges
5. Heat Transfer
6. Mass Transfer
7. Pressure

Research has also delivered numerous derived, sophisticated, techniques, for example image velocimetry may include Vortex shedding (Poisson-Quinton, 1967), PTV (Particle Tracking Velocimetry), LDV (LASER Doppler Velocimetry) etc. Ultrasonics have also proved successful to measure flow conditions in industry (Doebelin, 1990) and again this technique is based on reconstructing the velocity profile near the pipe wall (Chiuch, 1999). Particular interest has been

centred around the correlation of pressure and shear stress (Preston, 1953, Welsh, 1989) using some form of small sampling pipe or probe. This technique has inspired many researchers because of its simplicity, cheapness yet remarkable accuracy (Rechenberg, 1963). One technique using a triangular shaped probe (Dexter, 1973) has also lead to the development of a yawmeter (Gaudet et al. 1994) which was the starting point of the authors work in the water tunnel.

More recently (early 90s onwards) work in the fields of micro machines and fluidics has resulted in attempts to bring direct and indirect methods together under one roof. This has been made possible through the use of Micro-machined Wall Shear Stress Sensors (Kälveston, 1996, Lee & Sung, 1999). These sensors have the benefit of being small, self-calibrating and ideal for turbulence studies.

On a concluding note a useful way of connecting soil removal and hydrodynamics has been provided by Soltani and Ahmadi (1993) who examined particle removal in turbulent flow. The authors also wanted to determine if removal occurred via rolling, sliding, or lifting in turbulent flow. They concluded that rolling of the particle was the dominant mechanism for removal and that hydrodynamic torque acting on the particle was significant.

The highlights of the shear stress literature search and recommended readings are:

- Prandtl L. and Tietjens O. G., Fundamentals of Hydro and Aeromechanics, Dover, 1934.
- Preston J. H., The Determination of Turbulent Skin Friction by Means of Pitot Tubes, J. R. Aeronaut. Soc., vol. 58, pp.109-121, 1953.
- Schlichting H., Boundary Layer Theory, 4th edition, McGraw Hill, 1960.
- Rechenberg I., The Measurement of Turbulent Wall Shear Stress, A.R.A. Translation No.11, Bedford, UK, 1963.
- Poisson-Quinton P. and Werlé H., Water Tunnel Visualisation of Vortex Flows, Astronaut. Aeronaut., June 1967.
- Welch N. E. and Hines R. H., The Practical Application of the LASER Anemometer for Fluid Flow Measurements, presented at the ISA Electro-Optical Systems Conf., New York, N.Y. Sept. 1969

- Dexter P., Evaluation of a Skin-friction Vector Measuring Instrument for use in 3-D Turbulent Incompressible Flow, Project Report, Univ. of Southampton, Dept. of Astronautics and Aeronautics, UK, 1974.
- Mabey D. G. and Gaudet L., Performance of Small Skin Friction Balances at Supersonic Speeds, J. Aircraft, vol. 12, pp.819-825, 1975.
- Winter K. G., An Outline of the Techniques Available for the Measurement of Skin Friction, Progr. Aerospace Sci., vol. 18, pp.1-57, 1977.
- Gerhart P. and Gross R., Fundamentals of Fluid Mechanics, Addison Wesley, 1985.
- Schmidt M. A., Howe R. T., Senturia S. D. and Hanitondis J. H., Design and Calibration of a Micro-machined Floating-element Shear Stress Sensor, IEEE Trans. Electron. Devices, vol. 35, pp.750-757, 1988.
- Welsh B. L. and Ashill P. R., Pressure Measurement Techniques in use at the Royal Aerospace Establishment, Measurement Techniques in Aerodynamics, Von Karman Institute for Fluid Dynamics, Lectures Series, 1989.
- Young A. D., Boundary Layers, BSP Professional Books, UK, 1989
- Doebelin E. O., Measurement Systems – Application and Design, McGraw-Hill, 1990.
- Sherman F., Viscous Flow, McGraw Hill, 1990.
- White F. M., Viscous Fluid Flow, McGraw-Hill, 1991.
- Gaudet L. et al., Calibration and Use of a Triangular Yawmeter for Surface Shear Stress and Flow Direction Measurement, Proc. 2nd Intern. Conf. On Experimental Fluid Mechanics, Torino, Italy, 1994.
- Monti R., Indagine sperimentale delle caratteristiche fluido dinamiche del campo di moto intorno ad una pila circolare, *(Experimental Investigation concerning the Fluid-dynamics Properties of a Velocity Field around a Cylindrical Pillar)*, Engineering degree thesis, Politecnico di Milano, Italy, 1994.
- Bardelli M. et al., Misura della Sensibilità spaziale di Sonde Ecografiche per la valutazione dello Shear Stress in Arteria, *(Spatial sensitivity measurements of ecograph probes for the evaluation of shear stress in arteries)*, (International Symposium on Acoustical Imaging, pp.79-80, 3-6 Sept., Firenze, Italy, 1995.
- Goldstein R. J., Fluid Mechanics Measurements, 2nd Ed. Taylor and Francis, 1996.
- Tcheng Ping, Skin Friction Balance Development, Experimental Testing Div., NASA, 1996
- Kälveston E., Pressure and Wall Shear Stress Sensors for Turbulence Measurements, PhD Thesis, KTH, Sweden, 1996.
- Chiang C. and Eaton J. K., An Experimental Study of the Effects of Three-Dimensionality on the Near Wall Turbulence Structure Using Flow Visualisation, Experiments in Fluids, vol. 20, pp.266-273, 1996.

- Pilotti M., Menduni G. and Castelli E., Monitoring the Inception of Sediment Transport by Image Processing Techniques, Experiments in Fluids, vol. 23, pp.202-208, Springer-Velag, 1997.
- Fincham M. and Spedding G. R., Low Cost High Resolution DPIV for Measurement of Turbulent Fluid Flow, Experiments in Fluids, vol. 23, pp.449-462, 1997.
- Zang J. et al., Turbulent Flow Measurement in a Square Duct with Hybrid Holographic PIV, Experiments in Fluids, vol.23, pp.373-381, 1997.
- Beversdoff H. W., Gyr A., Hoyer K., Sobolik V., Simultaneous Wall Shear Rate Measurements by a Three Segmented Electro-diffusion Probe and Laser-Doppler -Anemometry, Experiments in Fluids, vol. 22, pp.281-285, 1997.
- Bocchiola D., Una Metodologia per la Misura Puntuale dell'Attritto di Parete in Correnti Cilindriche, *(A Method for Measuring Localised Skin Friction in Cylindrical flows),* Engineering degree thesis, Mat. No. 611090, Politecnico di Milano, Italy, 1998.
- Lee I. And Sung H. J., Development of an Array of Pressure Sensors with PVDF film, Vol.27, pp.27-35, 1999.
- Viterbo M., Sonde di Strato Limite per la misura dello Sforzo d'attritto – Studio Sperimentale ed Analisi Teorica, *(Boundary Layer Probes used for the Measurement of Wall Shear Stress and Skin Friction – Experimental investigation and Theoretical analysis),* Engineering degree thesis, Mat. No. 599289, Politecnico di Milano, Italy, 1999.
- Chiuch D., Misure del Campo fluididinamico all'interno di un Condotto Circolare mediante Velocimetro Doppler ad Ultrasuoni, *(Measurement of the Fluid-dynamic field in a Circular-section Duct using Ultrasonic Doppler Velocimetry),* Engineering degree thesis, Mat. No. 608486, Politecnico di Milano, Italy, 1999.
- Isaacs L. T., Boundary Shear Stress Measurement in Open Channels, 1999.
- Ward D., 2nd Boundary Layer Report, Ch. 4, pp.79-119, Whirlpool internal report, 1999.

Washing Literature Review

A great deal of the research into washing fundamentals has focused on the field of detergency because this has been the most convincing way of improving washing performance, fabric care and leveraging consumers. The majority of this work spans across the last 50 years although one of the most complete works (with 5 volumes) was published in 1972 by Cutler and Davis. This work also has the added advantage of being written by experts in washing machine design and, in my opinion,

still remains probably the best starting point in understanding the washing process.

One major stumbling block in the washing literature review was that it was difficult to separate washing phenomena because the soil removal mechanism is complex, cannot be broken down to single events and is still largely unexplained. Attempts at understanding washing have either branched off into other fields such as adhesion and detergency or taken on a typical (empirical) machine design approach. Elementary adhesion models have all started from very basic considerations and ideal conditions such as glass spheres on smooth, rigid and flat surfaces (Ghosh and Ryszytiwskyj, 1995) while detergency models consider washing as a chemical process (Tuzson and Short, 1960).

On the other hand basic washing research has essentially considered the washing process as a blend of heat and mass transfer (Ganguli and van Eendenburg, 1980) with elements of hydrodynamics and machine-wash load dynamics (Van den Brekel, 1986). The washing machine has also been considered a sort of mixing vessel in which the clothes and detergent are mixed in a soil-detergent transporting medium (Schmidt, 1959).

Some effort has gone into designing the washing machine better (Panilov, 1987) and using parametric modelling in the design process (Ward, 2000). But the fundamental difficulty lies in the actual assessment of washing machine performance, which is done optically through specific reflectance measurements (IEC 60456, 1998). The approach is typically empirical with a certain degree of uncertainty because of variability of the washing process, wash load and measurement technique. The technique consists of subjecting specific soiled (cotton) textile samples to a washing cycle and then measuring the reflectance of the soil (EMPA, 1998). Indeed the fate of many washing machine innovations is determined by this test methodology and even a standard (reference) washing machine has been introduced to reduce variability even further (Electrolux Wascator, 1999). An interesting paper by Saito (1985) established a method for measuring both

washability and soilability in a washing machine but unfortunately it looks only at the mechanisms for removing oily soils.

Summarising, the washing literature review could be viewed as being the most unfruitful of the four but did confirm that the scope of the Mass Transfer project was correct i.e. to start assembling soil removal fundamentals for textiles is essential if a quantum leap in washing is to be achieved.

The highlights of the literature search and recommended readings are:

- Monsanto Chemical Co., Wash-and-Wear Evaluation Method, Textile Technical Bulletin, No. 2299, 1956.
- Schmidt H., Washebewegung in Trommelwashmachinen, Washereitechnik unde chemie, vol.10, pp.500-504, 1957, vol.11, pp.224-232, 1958 and vol.12, pp.549-554, 1959.
- Tuzson J. and Short B. A., Mass Transfer and the Washing Process, Journal of Textile Institute, Dec. 1960.
- Cutler W. G. and Davis R. C., Detergency Theory and Test Methods part 1, vol. 5, Marcel Decker, N. York, 1972.
- Slater K., Textile Mechanics, The Textile Institute, UK, 1977.
- Ganguli K.L. and Van Eendenburg J., Mass Transfer in a laboratory washing machine, Textile Research Journal., pp.428-432, vol. 50, 1980.
- Panilov N., Design methods for household cylinder-type washing machines, Elektrotekhnika, vol.56, No.6, pp. 33-36, 1985.
- Van den Brekel L. D. M., Hydrodynamics and Mass Transfer in Domestic Drum-type Fabric Washing Machines, PhD thesis, Delft University of Technology, 1987.
- Rosen M. J., Surfactants and Interfacial Phenomena, Wiley & Sons, 1989.
- Washing Machine Performance Evaluation, International Standard IEC 60456, 1994.
- Das S. K., Sharma M. M. and Schechter R. S., Adhesion and Hydrodynamic Removal of Colloidal particles from Surfaces, Particulate Science and Technology, Vol. 13, pp. 227-247, 1995.
- Kovich M. B. Solid Contaminant Removal from Hydrophylic Surface, M.Sc thesis, Notre Dame University, 1998.
- EMPA materials specification, Swiss Federal Laboratories for Materials Testing and Research, St Gall, CH-9014, www.empa.ch., 1998
- Electrolux Wascator washing machine operation and installation manual, model FOM71MP LAB, Electrolux,

Sweden, 1999.

- Ward D., High Speed Filming of Clothes and Fabric Plug Motion, Whirlpool Internal Report, Sept. 1999.
- Ward D., Modelling of a Horizontal-Axis Domestic Washing Machine, J. Text. Inst., Vol. 91, Part 1, No. 2, 2000.
- Journal of Surfactants and Detergents, AOCS Press.
- Ash M., Handbook of Industrial Surfactants, Synapse Information Resources Inc, March, 2000.
- Surfactants website: http://surfactants.net/s-acad.htm

Adhesion Literature Review

In this final review the focus has been on understanding how soil particles adhere to a surface, rigid or compliant, with particular attention paid to this latter case. There is more information provided here because adhesion is not treated elsewhere in the thesis.

Adhesion research covers basically two major areas i.e. the removal of contaminants from rigid surfaces such as wafers in the micro-electronics industry and from compliant surfaces as for the washing industry. One must also not forget the filtration and separation industries where the scope is to purify fluids and therefore capture contaminants.

Although the forces present between the particle (soil) and surface (rigid or compliant) are well characterised qualitatively, a quantitative description is still lacking (Kovich, 1998).

Investigating the de-contamination of rigid surfaces has involved understanding the influence of factors such as particle size, surface characteristics, medium composition with several methodologies including wiping, high pressure spray cleaning, ultrasonic, scrubbing, and centrifugal cleaning. Unfortunately there is still no single technique for cleaning rigid surfaces. For example, large particles are best removed with ultrasonics while high-pressure spray and or surfactant methods dislodge smaller particles better.

The washing industry offers the greatest challenge because the contaminants are in the form of soils that range from stains to particulate oily soils and also the soiled surfaces are compliant. Although

mechanical effort is useful the major weapon for soil removal today is still detergency and in particular the surfactants they contain.

The goal is unique i.e. the breaking down of the bond between fibre and soil by reducing the surface tension between the contaminant and the substrate thus enabling spontaneous removal of (film) soils.

In the washing machine environment the predominant adhesion force is that due to Van der Waals force the other forces are capillary and electro-static forces but these are virtually negligible. Particle adhesion is the result of intermolecular activity between small particles and any surface. These intermolecular forces may present an attractive or repulsive force between the particle and the surface and the direction of the forces depends on the chemical and physical characteristics of the two surfaces involved.

The comprehension of adhesion phenomena started in the 1940s when two teams of scientists – Derjaguin and Landau and Verwey and Overbeek, published a theory (the DLVO theory) concerning colloidal stability and adhesion. This theory considers two types of adhesion forces: A) a long-range Van der Waals force operating independent of the chemical nature of the particles or the medium, B) a double layer repulsive force that is a result from either a surface charge or ion adsorption on the particle surface from the medium. Depending on the magnitude of the attractive and repulsive forces an interaction potential versus distance curve develops. The DLVO theory provided the first insight into the interactions between small particles and various substrates. Hamaker (1937) made a further step forward by proposing a theory that connected the Van der Waals forces and surface energies. This was soon followed by another important discovery by Liftshitz who related the Van der Waal's interactions with the dielectric properties of the material (Visser, 1995).

When the three theories were combined, Derjaguin determined that the contact radius depends on the particle size, the separation distance between particle and surface, and the interaction energies.

Derjaguin also began studying the effect of deformation and its influence on contact area.

This brought about the JKR (deformation) theory that assumes that at the point of separation there remains a finite contact point between the particle and surface. The JKR theory incorporates surface energy and deformation effects to develop a representative contact model. The JKR theory predicts adhesion forces for systems with a high Young's modulus, low surface energy, and a small particle radius. Research also indicates that the JKR theory is valid for soft surfaces and indicates discrepancies when predicting hard surface phenomena (Soltani, 1993).

A second deformation theory exists predicting the force of adhesion on a deformable load. This so called DMT theory (named after Derjaguin, Muller, and Toporov, 1975) states that the point of contact at the moment of separation is reduced to zero. The DMT theory also predicts that the force required to remove a particle from the surface is 4/3 times larger than the JKR value. The DMT model is valid for low Young's modulus, high surface energy, and large particle diameters. It is also valid for hard surfaces and shows deviations with soft surfaces.

All of the studies discussed above evaluate particle removal from a hard surface. In clothes washing, the textile surface is a compliant surface that does not lend itself to ultrasonic or impinging jet approaches. Compliant textile surfaces can also be damaged easily. Tuzson and Short (1960) completed early work on mass transfer in the wash process and suggest that the mass transfer processes in a washing machine dominate the soil removal efficacy. They also believe that in the case of smaller particles the detachment of soil from the fibre surfaces takes place mainly by chemical action. It is hypothesised that small particle removal occurs due to the adsorption of a surfactant mono-layer creating a repulsion force allowing for removal.

Loeb et al (1970) studied the effect water and detergent had on the frictional coefficient and soil removal. They concluded that the frictional force increased as you increased the normal load and cotton-to-cotton contact produced the highest frictional forces.

Ganguli and van Eendenburg (1980) studied mass transfer in a laboratory washing machine. They provided insight into the wash process by developing a model using diffusion length as a characteristic parameter. They believed that the length of each region depended on agitation, cloth-to-water ratio, textile porosity, and temperature. Their final conclusion stated that distance uniquely characterises the impact of mechanical agitation as a function of cloth to water ratio, textile porosity, and temperature.

Van Hoorst Vader and van Eedenburg (1981) found that rubbing and folding were beneficial to particulate soil removal. They attempted to model clothes motion as it relates to soil removal performance. Beneficial deformation effects were only reached at high folding frequencies and high folding angles. The folding frequencies fell between 30 to 60 fold/min and angles between 100-300 degrees. Krussman et al. (1984) stated that relative motion between the fabric and wash water was essential in achieving wash performance. Krussman believed this movement was a dominant force in removal of particulate in washing. He calculated an optimal tumble speed using a horizontal axis washer to determine cloth to water ratio and agitation patterns. This work along with van Hoorst Vader et al. attempted to understand the role of impact, in a horizontal-axis tumble washer, on soil removal.

Van den Brekel (1986) used hydrodynamic and mass transfer models to predict rinse efficiencies and soil removal relative to deformation in a (European) horizontal axis washer. Van den Brekel found that poor performance was found when swatches were attached to the garment themselves and attributed this reduction to the decrease in tangential flow across the EMPA stripe surfaces. Van den Brekel also found through additional experiments that tangential flow across the surface provided a considerable effect on soil removal and went on to say that flow along and within the fabrics is of more importance than the rubbing action of contacting fabrics and the folding of cloth.

Montalvo (1987) looked at aerodynamic removal of dust from cotton. His hypothesis is that if dust particles cannot be removed below the fibre break point then particle removal is not practical with

this cleaning method: the study showed that the velocity required for aerodynamic removal ranged from $25ms^{-1}$ to $60m^{-1}$. Montalvo goes onto to state that if a dust particle is present on the fibre in the concave valley, it will be shielded from the drag force and, consequently, more difficult to detach than if it were on the fibre outside the concave valley. Any particle present on the backside of the fibre with respect to the direction of airflow will likewise be subjected to the shielding effect. Montalvo (1989) also used fibre frictional force to remove particles from a sample of ginned cotton and developed two models in the process.

It was stated earlier that the predominant adhesion force encountered between a dirt particle and a textile surface immersed in a detergent solution is the Van der Waals force. Van der Waals forces are intermolecular forces of electrostatic nature. London (1944) later quantified these molecular interactions and these forces are now commonly referred to as London - Van der Waals forces (Visser, 1995).

Hamaker applied London's findings in attempt to quantify the attractive and repulsive forces between a particle and a surface. The expression for determining the adhesion force contains Hamaker's constant, which represents the properties of the particle, fluid medium, and the surface. Van der Waal's force of adhesion may be expressed as a negative or positive quantity depending on the distance of separation between the particle and surface (Birdi, 1997). The separation distance, z, is of the magnitude of 4 to 7 nm and was determined through atomic force microscope measurements (Israelachvili, 1991).

Calculation of the Hamaker constant for a textile remains very difficult due to the lack of detailed optical data and material property data. Van Oss (1993) developed a method for approximating Hamakers constant utilising surface tension and contact angle between the liquid and surface of interest. The advantage in this approach is that one can characterise materials not commonly found in the literature. While Hamaker constants are usually positive, resulting in attractive Van der

Waals, the theoretical expressions allow for the existence of negative values that imply repulsive Van der Waal's forces (Donovan, 1993).

So far little has been said about deformation and surface roughness although it has been stated that the adhesion and removal of particles from a substrate depend on both the interaction energy and the mechanical properties of the surface. Depending on the stresses created by the surface force, deformations can be elastic, plastic or viscoelastic (Rimai 1995).

Textile surfaces have irregularities that change the area of contact between particles and surfaces, the separation distance between the continuous bodies, and the adhesion interaction. Very few surfaces are perfectly smooth or flat and depending on the geometry or roughness the ability to remove a contaminant becomes quite difficult. The term rough is a qualitative term and depends on the length scale being studied. The surface may feel smooth but on a microscopic scale the surface can be very rough. With rough surfaces there are competing effects between compressive forces exerted by higher asperities and attractive forces from lower asperities (Bhushan, 1995). The fact that the surface is rough results in a reduction of the contact area between the two surfaces and translates to a lower adhesion force. However, in washing and in general for fluid flow across the weave surface the roughness will not only affect the flow above the surface but will shield the soil from tangential shear force should it not be located on the crest of the fibre or thread (Ward, 1999).

As can be appreciated from this brief account adhesion phenomena has still plenty to offer especially in terms of compliant surfaces and no doubt developments will occur that may completely overturn some of the afore mentioned theories.

The highlights of the literature search and recommended readings are:

- Hamaker H. C., The London-Van der Waals Attraction Between Spherical Particles, *Physica*, vol. 4, No. 10, pp. 1058-1072, 1937.

- O'Neil M. E., A Sphere in contact with a Plane Wall in a Slow Linear Shear Flow, Chemical Engineering Science, Vol. 23, pp. 1293-1298, 1968.
- Derjaguin B. V., Muller V. M. and Toporov Y.P., Effect of Contact Deformations on the Adhesion of Particles, Journal of Colloid and Interface Science, Vol. 53, No. 2, pp. 314-326, 1975.
- Ganguli K. L. and Van Eendenburg J., Mass Transfer in a Laboratory Washing Machine, Textile Research Journal, Vol. 80, pp.428-432, 1980.
- Soltani M., Ahmadi G., Bayer R. and Gaynes M., "Particle detachment from rough surfaces under substrate acceleration", Journal of Adhesion Science Technology, Vol. 9, No. 4, pp. 453-473.Krussman et al, 1984.
- Ranade M. B., Adhesion and Removal of Fine Particles on Surfaces, *Aerosol Science and Technology*, Vol. 7, No. 2, pp. 161-176, 1987.
- Montalvo J. G., Aerodynamic Removal of Native Dust from Cotton, Textile Research Journal, vol. 57, No. 3, pp. 133-141, 1987.
- Musselman R. P. and Yarbrough T. W., Shear Stress Cleaning for Surface Deparliculation, Journal of Environmental Sciences, vol. 30, pp. 51-56, 1987.
- Ranade M. B., Menon V. B., Mullins M. E. and Debler V. L., Adhesion and Removal of Particles: Effect of Medium", in Particles on Surfaces I: Detection, Adhesion and Removal, Marcel Dekker, New York, pp.179-191, 1988.
- Bardini J., Methods for Surface Particle Removal: Comparative Study in Particles on Surfaces: Detection, Adhesion and Removal, pp. 329-338, Marcel Dekker, N. York, 1988.
- Van Voorst Vader F. and Van Eendenburg J., 1988, Influence of Agitation on Composite Soil Removal, Unilever internal report, pp. 129-139, 1988.
- Montalvo J. G., Kinetics of Dust Removal from Cotton by Repetitive Mechanical Cleaning Part I: Theory, Textile Research Journal, vol. 59, No 1, pp. 33-45, 1989.
- Wang H. C., Effects of Inceptive Motion on Particle Detachment from Surfaces, Aerosol Science and Technology, Vol. 13, pp. 193-203, 1990.
- Lieng-Huang Lee, Fundamentals of Adhesion, Plenum Pub., 1991.
- Israelachvili J., Intermolecular and Surface Forces, 2nd Ed., Academic Press, New York, 1992.

- Sharma M. M., Chamoun H., Sita Rama Sarma D. S. H. and Schechter R. S., Factors Controlling the Hydrodynamic Detachment of Particles from Surfaces, Journal of Colloid and Interface Science, vol. 149, No. 1, pp. 121-134. 1992.
- Soltani M., Ahmadi G., Bayer R. G., and Gaynes M. A., Particle Detachment Mechanisms from Rough Surfaces under Substrate Acceleration, *Journal of Adhesion Science and Technology*, Vol. 9, No. 4, pp. 453-473, 1993.
- Donovan R. P., Yamamoto T. and Periasamy R., "Particle Deposition, Adhesion, and Removal", Material Research Society, Vol. 315, pp. 3-22, 1993.
- Yamamoto T., Periasamy R., Donovan R. P., and Ensor D. S., Flow Cell for Real Time Observation of Single Particle Adhesion and Detachment, Journal of Adhesion Science and Technology, Vol. 8, No.5, pp. 543-552, 1994.
- Soltani M. and Ahmadi G., On Particle Adhesion and Removal Mechanisms in Turbulent Flows, Journal of Adhesion Science and Technology, vol. 8, No. 7, pp. 763-785, 1994.
- Evans D. W. and Wennerstrom H., The Colloidal Domain: Where Physics, Chemistry, Biology and Technology Meet, VCH Publishing, New York, 1994.
- Rimai D. S. and Busnaina A. A., The Adhesion and Removal of Particles from Surfaces, *Particulate Science and Technology*, Vol. 13, pp. 249-270, 1995.
- Bhushan B., Handbook of Micro-Nano Tribology, CRC Press, New York, 1995.
- Visser J, Particle Adhesion and Removal: A Review, Particulate Science and Technology, Vol. 13, pp. 169-196. 1995.
- Ghosh, A. and Ryszytiwskyj, W.P., Removal of Glass Particles from Glass Surfaces: A Review, K.L.Mittal, ed., Marcel Dekker, N. York, 1995.
- Mollinger M. and Nieuwstadt F. T. M., Measurement of the Lift Force on A Particle Fixed to the Wall of a fully Developed Turbulent Boundary Layer, Journal of Fluid Mechanics, pp.285-306, 1996.
- Kovich M. B. Solid Contaminant Removal from Hydrophylic Surface, M.Sc thesis, Notre Dame University, 1998.
- Demejo L. P., Rimai D. S. and Sharpe L. H., Fundamentals of Adhesion and Interfaces, G & B Science Pub., USA, 1999.
- Ward D., EMPA Soil Roughness Measurements, Whirlpool internal report, Dec. 1999.

Other Recommended Journals and Readings

Fluid Abstracts - Civil Engineering

- Ceylan K., Herdem S. and Abbasov T., A theoretical model for the estimation of drag force in the flow of non-newtonian fluids around spherical solid particles, Powder Technology, vol.103/3, pp.286-291, Technology, 1999.
- Pironneau O, Numerical models for turbulent flows in complex geometries (in french), Comptes Rendus de l'Academie de Sciences - serie 3b, vol. 327/4,pp.325-331, 1999.

Fluid Abstracts - Process Engineering

- Wu R. M. and Lee D. J., Highly porous sphere moving through centreline of a circular tube filled with a Newtonian fluid, Chemical Engineering Science, vol. 54/23, pp.5717-5722, 1999.

Experiments in Fluids

- Lawson N. J., Rudman M., Guerra A., Liow J.L., Experimental and Numerical Comparisons of the break-up of a Large Bubble, Vol.26, pp.524-534, 1999.
- Lee I. And Sung H. J., Development of an Array of Pressure Sensors with PVDF film, Vol.27, pp.27-35, 1999.
- Buttsworth D. R., Elston S. J. and Jones T. V., Skin friction measurements on reflective surfaces using liquid crystals, vol. 28, pp.64-73, 2000.

Meccanica - Int. Journal of the Italian Assoc. of Theoretical and Applied Mechanics

- Lewis R. W. and Schrefler B. A., The Finite Element Method in the Static and Dynamic Deformation and Consolidation of Porous Media, J. Wiley, 1998.

Transport in Porous Media

- Bartley J. T. and Ruth D. W., Relative Permeability Analysis of Tube Bundle Models, vol. 36, No.2, pp.161-187, 1999.

Numerical Methods in Fluids

- Hwang C. B. and Lin C. A., Low-Reynolds k-□ Modelling of Flows with Transpiration, vol. 32, No.5, 495-514, J. Wiley, 2000.

Journal of Fluid Mechanics

Fluid Flow Measurements - Abstracts -BHRA, Cranfield, UK